



**PROGRAMA DE PÓS-GRADUAÇÃO EM BIOTECNOLOGIA  
UNIVERSIDADE FEDERAL DO MARANHÃO**

**Ilmar Alves Lopes**

**ELABORAÇÃO E CARACTERIZAÇÃO DE COMPÓSITOS  
POLIMÉRICOS COM O USO DE *Attalea speciosa Mart. ex  
Spreng* E OUTRAS MATRIZES NATURAIS**

**São Luís – MA**

**2019**

**Ilmar Alves Lopes**

**ELABORAÇÃO E CARACTERIZAÇÃO DE COMPÓSITOS  
POLIMÉRICOS COM O USO DE *Attalea speciosa Mart. ex  
Spreng* E OUTRAS MATRIZES NATURAIS**

Tese apresentada como parte dos requisitos para obtenção do título de Doutor em Biotecnologia, junto ao Programa de Pós-Graduação em Biotecnologia da Rede Nordeste de Biotecnologia (RENORBIO), da Universidade Federal do Maranhão, Campus de São Luís.

**Orientador:** Prof. Dr. Allan Kardec Duailibe Barros Filho

**Co-orientadora:** Prof<sup>a</sup>. Dr<sup>a</sup>. Audirene Amorim Santana

**Área de concentração:** Biotecnologia em Recursos Naturais

**São Luís – MA**

**2019**

# ELABORAÇÃO E CARACTERIZAÇÃO DE COMPÓSITOS POLIMÉRICOS COM O USO DE *Attalea speciosa Mart. ex Spreng* E OUTRAS MATRIZES NATURAIS

Ficha gerada por meio do SIGAA/Biblioteca com dados fornecidos pelo(a) autor(a).  
Núcleo Integrado de Bibliotecas/UFMA

Lopes, Ilmar Alves.

Elaboração e caracterização de compósitos poliméricos com o uso de *Attalea speciosa Mart. ex Spreng* e outras matrizes naturais / Ilmar Alves Lopes. - 2019.  
117 p.

Coorientador(a): Audirene Amorim Santana.

Orientador(a): Allan Kardec Duailibe Barros Filho.

Tese (Doutorado) - Programa de Pós-graduação em Biotecnologia - Renorbio/ccbs, Universidade Federal do Maranhão, São Luís - MA, 2019.

1. *Attalea speciosa*. 2. Biopolímeros. 3. Degradação. 4. Mesocarpo de coco babaçu. 5. Sustentabilidade. I. Barros Filho, Allan Kardec Duailibe. II. Santana, Audirene Amorim. III. Título.

**BANCA EXAMINADORA:**

---

Prof. Dr. Allan Kardec D. Barros Filho  
Orientador – RENORBIO/UFMA

---

Prof. Dr. Antônio Carlos Romão Borges  
RENORBIO/UFMA

---

Prof. Dr. Rafael Augustus de Oliveira  
FEAGRI/UNICAMP

---

Prof.Dr. Denilson Moreira Santos  
DEDET/UFMA

---

Prof. Dr. Victor Elias Mouchrek Filho  
DETEQI/CCET/UFMA

**10 de dezembro de 2019**

Dedico primeiramente ao DEUS, criador do Universo e de todas as Coisas nele existentes, pela oportunidade em vida de realizar este trabalho que me foi sempre motivo de desejo e aspiração e aos meus pais João Francisco Lopes e Teresinha de Jesus Alves Lopes pela proteção na minha infância e orientação para a vida adulta.

## AGRADECIMENTOS

Agradeço antes de tudo a DEUS JEová, Criador do Universo e de todas as coisas nele existentes, por permitir realizar este passo, pois ele representa o passo maior nas Ciências dos homens e um pouco de minha contribuição para a casa onde habitamos (planeta Terra).

À minha co-orientadora a Prof<sup>a</sup>. Dr<sup>a</sup>. Audirene Amorim Santana, pelo importante apoio, dedicação, disposição e orientação em todo momento na realização deste trabalho, pelos conhecimentos transmitidos e por abrir as portas do Laboratório de Engenharia de Produtos e Processos em Biorrecursos (LEPPBio) do Curso de Engenharia Química (DEEQ/CCET/UFMA);

Aos alunos pesquisadores do LEPPbio, Jonas Santos Junior, Dennys Correia da Silva, Layrton José Souza da Silva, Adones Almeida Rocha, Gustavo Augusto Silva Santos pelo convívio e ajuda na realização dos experimentos;

A todos os membros da banca examinadora da qualificação e defesa, pelas correções e sugestões que muito contribuíram para a redação e finalização desta tese;

A minha querida Mãe Teresinha de Jesus Porto Alves, pelo apoio e pelo carinho especial a mim depositado;

Ao Departamento de Engenharia Química da UFMA, do qual faço parte, pela oportunidade de realização dessa etapa marcante em minha vida;

A todas as pessoas que me apoiaram e/ou contribuíram de alguma forma para a realização deste trabalho e por estarem sempre presentes ao meu lado nos momentos de tomada de decisões no decorrer desta pesquisa;

Aos laboratórios: Central Analítica de Química (DEQUI/CCET/UFMA), Central de Energia e Ambiente (CEA/DEEE/CCET/UFMA); Central de Materiais-CEMAT (DEFIS/CCET/UFMA); Núcleo de Combustíveis, Catálise e Ambiente-NCCA (DEQUI/CCET/UFMA); Laboratório de Materiais do Departamento de Odontologia I (CCBS/UFMA), pelas análises realizadas.

***Muito obrigado a todos!***

## *Pensamento Contemporâneo*

*O indivíduo deveria se tornar cidadão cosmopolita para perceber a importância do Planeta Terra presente maior de Deus, Criador do universo. Se se interessar pelas causas dele e então perceberia que não vale a pena viver focado como patriota defendendo causas e interesses locais. Entender que tudo é de natureza global e que todos os efeitos advindos serão também de natureza global. Então, deveria pensar em atitudes desvinculadas de culturas e soberanias locais para numa visão mais holística enxergar o mundo como um todo. Qualquer esforço não será suficiente para garantir a sobrevivência humana no planeta se não prevalecer o espírito global através de comprometimentos e atitudes locais quebrando paradigmas de consumo e de padrões capitalistas de qualidade de vida preconizado pela Sociedade Contemporânea.*

Ilmar Alves Lopes

“Minha palavra é como as estrelas, elas não empalidecem. Como pode-se comprar ou vender o céu, o calor da terra? Tal ideia é estranha. Nós não somos donos da pureza do ar ou do brilho da água. Como pode então comprá-los de nós? Decidimos apenas sobre as coisas do nosso tempo”....

(Resposta do Cacique Seattle ao homem branco Estadunidense ao fazer proposta de compras de suas terras).

## RESUMO

A Sociedade Contemporânea convive com a persistência dos plásticos sintéticos no seu pós-uso nos compartimentos ambientais, gerando impactos negativos à biota e aos seres humanos. Iniciativas têm surgido com o intuito de solucionar o problema. Uma delas é a introdução dos biopolímeros ou plásticos naturais, provenientes de fontes renováveis. Pesquisas buscam conciliar baixo custo, degradabilidade e tentam se aproximar das propriedades mecânicas dos plásticos sintéticos. O estudo aqui apresentado faz uso de matrizes com estas características, com a utilização do fruto da palmeira babaçu (*Attalea speciosa* Mart. ex Spreng), de vasta ocorrência no Estado do Maranhão. No primeiro artigo fez-se a incorporação do mesocarpo do fruto (MCB) com matrizes de fontes vegetal e animal. Testes foram realizados com uso de pectina (P) e concentrado proteico do soro de leite (CPS) com formulações fazendo uso do glicerol como plastificante e o cloreto de cálcio dihidratado como reticulante. Os filmes produzidos ficaram consistentes, homogêneos e flexíveis com baixa tendência a lixiviação e solubilização nos testes realizados. No segundo artigo foram elaborados biopolímeros com o uso de MCB, pectina e glicerol utilizando um Delineamento Composto Central Rotacional - DCCR. Os filmes apresentaram boas propriedades mecânicas, principalmente após a segunda reticulação. Os testes mostraram que o MCB contribui de forma positiva para o fechamento das cadeias poliméricas, tornando os filmes menos hidrofílicos. No terceiro artigo foi estudada a elaboração de biopolímeros a base de MCB e alginato. Estes filmes mostraram-se promissores na produção de bio-termoplásticos. Das combinações destas matrizes naturais, selecionou-se formulações tendo-se em vista a interpretação analítica da morfologia por microscopias, análises do comportamento térmico, análises de arranjos moleculares e ensaios de desempenho mecânico. Os resultados mostraram que os produtos gerados apresentaram características semelhantes, com possibilidade de aplicação, ainda que com algumas limitações comparadas aos polímeros sintéticos. Os testes realizados mostraram boas propriedades mecânicas (filmes com tensão de ruptura de 226,673 MPa) e baixa solubilidade (filmes com solubilidade de 4,170%). Ficou evidente a eficácia das metodologias de *crosslinking* na compactação e aperfeiçoamento das propriedades de solubilidade, umidade e resistência à lixiviação em geral. Estes resultados mostraram a possibilidade de uso do mesocarpo de babaçu como matéria-prima para obtenção de biopolímeros. O uso do mesocarpo do coco babaçu também pode contribuir para agregar maior valor à cadeia produtiva do babaçu, impactando positivamente o desenvolvimento social e a preservação ambiental por se tratar de produtos com tempo de degradação de poucas semanas quando dispostos ao meio ambiente.

**Palavras chave:** *Attalea speciosa*; Mesocarpo de coco babaçu; Biopolímeros; Degradação; Sustentabilidade.



## ABSTRACT

The Contemporary Society lives with the persistence of synthetic plastics in its post environmental compartments, causing negative impacts on biota and humans. Initiatives have emerged in order to solve the problem. One is the introduction of biopolymers or natural plastics from renewable sources. Research seeks to reconcile low cost, degradability and try to get closer to mechanical properties of synthetic plastics. The study presented here makes use of matrices with these characteristics, by using the fruit of the babassu palm *Attalea Speciosa* Mart. ex Spreng), of wide occurrence in the State of Maranhão. In the first article the incorporation of the fruit mesocarp (BCM) with matrices from plant and animal sources. Tests were performed using pectin (P) and whey protein concentrate (WPC) formulations making use of glycerol as plasticizer and calcium chloride dihydrate as crosslinker. The selected films remain consistent, homogeneous and flexible with a low tendency to leach and solubilize in the tests performed. In the second article, the production of biopolymers using BCM, pectin and glycerol using a Rotational Central Compound-DCCR. The films showed good properties mainly after the second crosslinking. Tests have shown that BCM contributes positively to the closure of polymer chains, making films less hydrophilic. In the third article was studying the elaboration of biopolymers based of BCM and alginate. These films have shown promise in producing bio thermoplastics. With the combinations of these natural matrices, formulations with a view the analytical interpretation of morphology by microscopy, thermal analysis, analysis of molecular arrangements and mechanical testing. The results showed that the products generated had similar characteristics, with the possibility of although with some limitations compared to synthetic polymers. The tests performed showed good mechanical properties (films with tensile strength of 226.673MPa) and low solubility (films with solubility of 4.170%). The effectiveness of crosslinking methodologies in the compaction and improvement of solubility, moisture and leaching properties in general. These results showed the possibility of using babassu mesocarp as a raw material for obtaining biopolymers. The use of babassu coconut mesocarp can also contribute to adding more value to the babassu production chain, positively impacting social development and environmental preservation because it is of products with degradation time of a few weeks when disposed in the environment.

**Keywords:** *Attalea Speciosa*; Babassu coconut mesocarp; Biopolymers; Degradation; Sustainability.

# SUMÁRIO

<b>RESUMO</b> .....	viii
<b>ABSTRACT</b> .....	ix
<b>INTRODUÇÃO GERAL</b> .....	1
<b>ORGANIZAÇÃO DO TRABALHO EM CAPÍTULOS</b> .....	3
<b>REFERÊNCIAS</b> .....	4
<b>CAPÍTULO 1:REVISÃO BIBLIOGRÁFICA</b> .....	6
<b>1.1 POLÍMEROS SINTÉTICOS</b> .....	6
<b>1.2 BIOPOLÍMEROS</b> .....	8
1.2.1 Blendas e misturas poliméricas .....	10
1.2.1.1 Isolado e Concentrado Proteico do Soro de Leite (IPS).....	10
1.2.1.2 Pectina .....	12
1.2.1.3Alginato .....	13
1.2.1.4 Amido .....	16
<b>1.3 O BABAÇU</b> .....	18
1.3.1 A Palmeira .....	18
1.3.2 O Fruto e o Mesocarpo de Coco Babaçu .....	20
<b>1.4 REFERÊNCIAS</b> .....	23
<b>CAPÍTULO 2: CHARACTERIZATION OF PECTIN BIOFILMS WITH THE ADDITION OF BABASSU MESOCARP AND WHEY PROTEIN CONCENTRATE</b> .....	29
<b>1. Introduction</b> .....	30
<b>2. Material and Methods</b> .....	32
2.1. Raw Materials and Sample Preparation.....	32
2.3. Characterization of the Biofilms Film thickness .....	32

2.4. Morphology .....	34
2.5. Fourier-transform Infrared Spectroscopy (FTIR).....	34
2.6. Statistical Analysis .....	35
<b>3. Results and Discussion .....</b>	<b>35</b>
3.1. Biofilm Characterizations.....	35
3.2. Morphology Results .....	39
3.3. Fourier-transform Infrared Spectroscopy (FTIR).....	41
<b>4. Conclusions.....</b>	<b>42</b>
<b>REFERENCES .....</b>	<b>43</b>
<b>CAPÍTULO 3: PHYSICAL PROPERTIES OF FILMS BASED ON PECTIN AND BABASSU COCONUT MESOCARP .....</b>	<b>47</b>
<b>1. Introduction .....</b>	<b>48</b>
<b>2. Material and methods .....</b>	<b>50</b>
2.1. Raw materials .....	50
2.2. Film preparation and experimental design .....	50
2.3. Characterization of the biofilms .....	50
<b>3. Results and discussion .....</b>	<b>56</b>
3.1. Physical properties of the films formulated using an experimental design .....	56
3.2. Reformulated films .....	60
3.2.6. Thermal analyses .....	71
<b>4. Conclusions.....</b>	<b>72</b>
<b>5. Acknowledgements .....</b>	<b>72</b>
<b>6. References.....</b>	<b>72</b>
<b>CAPÍTULO 4:ELABORATION AND CHARACTERIZATION OF BIOPOLYMER FILMS WITH ALGINATE AND BABASSU COCONUT MESOCARP .....</b>	<b>78</b>
<b>1. Introduction .....</b>	<b>80</b>
<b>2. Material and methods .....</b>	<b>82</b>
2.1 Materials .....	82

2.2 Elaboration of Composites .....	82
2.3 Physical characterization of composites .....	83
2.3.2 Thickness ( $\delta$ ) .....	83
2.3.3 Moisture content ( $\omega$ ).....	83
2.3.4 Water soluble mass (S).....	84
2.3.5 Water vapor permeability (WVP).....	84
2.4 Analysis of selected films.....	84
2.5 Statistical Analysis .....	86
<b>3. RESULTS AND DISCUSSION</b> .....	<b>86</b>
3.1 Analysis of the visual aspect .....	86
3.2 Physicochemical characterization.....	86
3.3 Selected Films.....	88
<b>4. Conclusions</b> .....	<b>95</b>
<b>Acknowledgments</b> .....	<b>96</b>
<b>REFERENCES</b> .....	<b>96</b>
<b>CONCLUSÃO GERAIS</b> .....	<b>100</b>

# ÍNDICE DE FIGURAS

## Capítulo 1 – REVISÃO BIBLIOGRÁFICA

Figura 1 - Pectina com alto teor de metoxilação. ....	13
Figura 2 - Pectina com baixo teor de metoxilação. ....	13
Figura 3 - Estrutura do: (a) ácido $\beta$ -D-manurônico, (b) $\alpha$ -L-gulurônico e (c) alginato.....	14
Figura 4 - Estrutura da amilose e respectiva conformação helicoidal (a) e da amilopectina e sua forma ramificada (b).....	17
Figura 5 - Palmeira de babaçu. ....	19
Figura 6 - Composição do coco babaçu.....	21
Figura 7 - Descascamento manual para a obtenção do mesocarpo de coco babaçu: a) descascamento com uso de facão e b) coco descascado.....	21

## Capítulo 2 - CHARACTERIZATION OF PECTIN BIOFILMS WITH THE ADDITION OF BABASSU MESOCARP AND WHEY PROTEIN CONCENTRATE

Figura 1 - Biodegradation analysis: (a) Biofilm packaging composed of 100%P (F1), 50%P+50%WPC (F2), 50%P+50%BM (F3) and 50%P+25%BM+25%WPC (F4) and, (b) biofilms in the natural environment.....	37
Figura 2 - Visual aspects of the four pectin biofilms with added babassu mesocarp and whey protein concentrate. (a) 100%P, (b), 50%P+50%WPC, (c) 50%P+50%BM (F3) and (d) 50%P+25%BM+25%WPC.....	39
Figura 3 - shows the SEM images for the formulations 100%P, 50%P+50%WPC, 50%P+50%BM and 50%P+25%BM+25%WPC, respectively. ....	40
Figura 4 - FTIR-ATR spectra of the four biofilm formulations. (a) 100%P, (b), 50%P+50%WPC, (c) 50%P+50%BM (F3) and (d) 50%P+25%BM+25%WPC.....	42

## Capítulo 3 - PHYSICAL PROPERTIES OF FILMS BASED ON PECTIN AND BABASSU COCONUT MESOCARP

Figura 1 - Experimental values for the sorption isotherms (●) of the films A (a) and B (b) and simulated using the GAB model (□). The figure on the right indicates the residuals between the experimental values and those predicted by the model. ....	63
--	----

Figura 2 - Experimental values for the drying kinetics (●) of the films A (a) and B (b) and simulated using the Midilli model (mesh, □). The figure on the right indicates the residuals between the experimental values and those predicted by the model.....	66
Figura 3 - Surface micrographs of films A and B at different magnifications.....	69
Figura 4 - FTIR-ATR spectra of the films A (black –) and B (blue –).....	70
Figura 5 - TGA (blue –) and DTA (green –) curves of the reformulated films.....	71

**Capítulo 4 - ELABORATION AND CHARACTERIZATION OF BIOPOLYMER FILMS WITH ALGINATE AND BABASSU COCONUT MESOCARP**

Figura 1 -Photographs of the film prepared with babassu coconut mesocarp, alginate, glycerol and cross-linked with CaCl <sub>2</sub> .2H <sub>2</sub> O: (a) formulation F6, first stage on left, second stage on right; (b) formulation F7, first stage on left, second stage on right.....	86
Figura 2 -Infrared spectra of alginate and babassu coconut mesocarp powder.....	88
Figura 3 -Overlapping infrared spectra of selected polymer composites of alginate and babassu coconut mesocarp.....	89
Figura 4 -TG (a) and DSC (b) curves of selected polymer composites from alginate and babassu coconut mesocarp.....	90
Figura 5 -Micrograph of the polymer composites of babassu coconut mesocarp and alginate in the first stage (left), and second stage (right), of the surface: (a,b), (c,d), (e,f), formulations films 1, 6 and 7, respectively.....	92
Figura 6 -Micrograph of the polymer composites of babassu coconut mesocarp and alginate in the first stage (left), and second stage (right), of the cross-section: (a,b), (c,d), (e,f), formulations films 1, 6 and 7, respectively.....	93
Figura 7 - Graphs of swelling tests of the films from second stage, samples F1, F6 and F7.....	95

# ÍNDICE DE TABELAS

## Capítulo 1 – REVISÃO BIBLIOGRÁFICA

**Tabela 1** - Propriedades químicas (XG e XM) e físicas ( $\mu$ , Mn e dp) do alginato. .... 15

## Capítulo 2 - CHARACTERIZATION OF PECTIN BIOFILMS WITH THE ADDITION OF BABASSU MESOCARP AND WHEY PROTEIN CONCENTRATE

**Table 1** - Characterization of the biofilms made from the four formulations composed of citric pectin (P), babassu mesocarp (BM) and whey protein concentrate (WPC). .... 38

## Capítulo 3 - PHYSICAL PROPERTIES OF FILMS BASED ON PECTIN AND BABASSU COCONUT MESOCARP

**Table 1** -Experimental results obtained for the physical characterizations of the different filmformulations..... 57

**Table 2** - Simulation of the physical properties using the stepwise-fit method..... 59

**Table 3** - Results obtained for the physical properties of the reformulated films..... 61

**Table 4** - Results of themodelling and simulation of the sorption isotherms of films A and B at 25 °C..... 64

**Table 5** - Results of the modelling and simulation of the drying kinetics of films A and B. .... 67

## Capítulo 4 - ELABORATION AND CHARACTERIZATION OF BIOPOLYMER FILMS WITH ALGINATE AND BABASSU COCONUT MESOCARP

**Table 1** - Planning for the elaboration of polymeric composites formulations.....83

**Table 2** - Moisture content ( $\omega$ ) and water solubility (S), thickness ( $\delta$ ) and water vapor permeability (WVP) of the babassu coconut mesocarp and alginate polymer composites in the first and second stages.....94

**Table 3** - Tensile Strength (TS), elongation at break (e), Young's Modulus (E), and degradability (D) of the babassu coconut mesocarp and alginate polymer composites in formulations F1, F6 and F7..... 94



# INTRODUÇÃO GERAL

A sociedade contemporânea no último século desenvolveu-se e experimentou um padrão de consumo acerbado de produtos obtidos de materiais sintéticos através da indústria petroquímica. Uma vasta modalidade de produtos que advieram deste modelo influenciou o seu uso na rotina doméstica, com utilização de utensílios descartáveis na forma de copos, pratos, talheres, depósitos de mantimentos, assim como, o uso de embalagens para transporte em supermercados e no comércio em geral.

Os polímeros revolucionaram todos os segmentos e, em particular, a indústria alimentícia, pois possibilitou reduzir o peso e o preço das embalagens. Além disso, melhorou a segurança alimentar e reduziu o desperdício.

No primeiro momento, foi uma ideia inovadora e uma fonte de progresso, contudo as embalagens de plástico sintético se tornaram forte alvo de ataques por causa de seus efeitos ambientais. As embalagens plásticas representam atualmente 26% do volume total de resíduos plásticos produzidos no mundo, sendo que apenas 14% dessas são coletadas para reciclagem (GRÉGOIRE e CHAUVELOT, 2019).

Uma das saídas imediatas encontradas foi a reciclagem, com a devolução para a cadeia produtiva do polímero, tendo como vantagem a redução de matérias primas virgens, gastos de energia e grande economia financeira ao setor produtivo. Contudo, a produção mundial muito alta faz com que o esforço da reciclagem nunca atinja o desejado de “reciclar cem por cento do que era produzido” e o descompasso entre o produzido e o reciclado continua a oferecer prejuízos ambientais pela persistência deles aos ecossistemas, especialmente a biota.

Os esforços em pesquisar outras alternativas para artefatos descartáveis conduziram a busca de materiais biodegradáveis que permitissem facilitar e manter a rotina da sociedade, mas que tivesse pouco tempo de residência nos compartimentos ambientais. Também se mostrava necessário que estes materiais tivessem características mecânicas próximos daqueles de origem fóssil (polímeros sintéticos) e sua produção e uso pudesse ser sustentável. Neste contexto, surgiu a ideia de agregar componentes biodegradáveis ao polímero sintético para que pudessem ser fragmentados pelo calor e por microrganismos em estrutura menores, os chamados plásticos oxibiodegradáveis, mas esta estratégia só reduz o volume e os acidentes com animais que ingerem ou se emboscam nos componentes

na forma inteira e eles permanecem na forma de fragmentos (micro plásticos) no seu pós uso por longas décadas de acordo com o tipo de material (CRITCHELL et al., 2019).

Outro esforço com esse objetivo em andamento no qual se enquadra esta pesquisa é a produção de polímeros naturais que tenham sua degradação mais rápida sem deixar resíduos no ambiente e que num futuro próximo possam substituir os produtos derivados de petróleo em sua totalidade. Nesse contexto, destacam-se os biopolímeros, os quais possuem funções de conservação, melhoria das características dos produtos e podem dar suporte nutricional e sensorial, entre outros (MALI et al., 2010; FARIAS et al., 2012; SANTANA e KIECKBUSCH, 2013).

Os biopolímeros são películas preparadas a partir de polímeros naturais de origem vegetal ou animal, tais como polissacarídeos, lipídios e proteínas. Eles têm uma vasta aplicabilidade e sua utilização depende de vários parâmetros. Eles são confeccionados geralmente segundo a técnica *casting*, que consiste em espalhar uma solução filmogênica sobre uma placa, com espessura controlada pela quantidade de massa vertida. Essa técnica tem mostrado bons resultados quando se refere à escala laboratorial, já para escala industrial recomenda-se a utilização do processo de extrusão (MALI et al., 2010; SEIXAS et al., 2013).

Dentre os diversos materiais pesquisados para a produção de biopolímeros, o alginato se destaca dos demais, devido a sua natureza termoestável e característica reológica ajustável. O alginato de sódio é um polissacarídeo linear obtido a partir de algas marinhas ou bactérias, sendo composto por ácidos  $\beta$ -D- manurônico (M) e do ácido  $\alpha$ -L-gulurônico (G), distribuídos ao longo da cadeia. O alginato de sódio detém inúmeras aplicações nas indústrias alimentícias, farmacêuticas, biomédicas e têxteis, por apresentar características de biodegradabilidade, ausência de toxicidade e ação gelificante e espessante (SANTANA; KIECKBUSCH, 2013).

Entre outros materiais pesquisados para a produção de biopolímeros, tem-se a pectina e novos produtos como o isolado proteico de soro de leite, que é a principal fonte de proteínas globulares, usadas na indústria alimentar, por apresentar propriedades de emulsão e de formação de espuma (DICKINSON, 2001).

Um aditivo que pode ser utilizado na produção dos biopolímeros é o mesocarpo de coco babaçu (*Attalea Speciosa* Mart.). Este coco é constituído por quatro partes aproveitáveis, sendo elas a casca, formada pelo epicarpo (11%), mesocarpo (23%) e endocarpo (59%), e amêndoas (7%) (SANTANA et al., 2017). O mesocarpo é, geralmente, transformado em farinha e aplicado na alimentação humana. Para obtenção desta farinha,

são necessárias várias etapas de processamento, que se inicia com a coleta do coco e finaliza com o armazenamento do produto final, passando pelos processos de seleção, lavagem, descascamento, retirada, secagem, moagem e peneiramento.

Na sua composição química está presente, principalmente, 66,51% de amido, 6,8% de fibra alimentar, 1,19% de proteínas, 0,29% de extrato etéreo (CARRAZZA et al., 2012), dentre outros elementos. O amido é formado pela amilopectina e amilose, esta última possui propriedade física, química e funcional para formar géis e filmes (MALI et al., 2010). Portanto, levando em consideração a alta concentração de amido no mesocarpo, investigamos a viabilidade de sua aplicação na produção de biopolímeros.

Com base nas considerações anteriores, pretendeu-se, com desenvolvimento da presente tese, atingir ao seguinte objetivo geral:

- Produzir biopolímeros de carboidratos e proteínas adicionados de mesocarpo de coco babaçu.

Para cumprir com o objetivo geral, foram propostos os seguintes objetivos específicos:

- Avaliar a influência da mistura de mesocarpo de coco babaçu na formação dos biopolímeros e analisar as propriedades químicas, mecânicas, de barreira e de biodegradabilidade dos biopolímeros.

- Determinar a influência das matrizes de mesocarpo de coco babaçu e pectina na produção de biopolímeros e caracterizar suas propriedades físico-químicas, mecânicas e calorimétricas.

- Elaborar formulações de compósitos poliméricos naturais à base de mesocarpo de coco babaçu, alginato e glicerol e avaliar a reticulação com cloreto de cálcio (1º e 2º estágio) sob as propriedades físico-químicas, mecânicas e térmicas.

## **ORGANIZAÇÃO DO TRABALHO EM CAPÍTULOS**

O presente trabalho encontra-se estruturado da seguinte forma:

**Capítulo 1:** Revisão bibliográfica: são apresentados os principais fundamentos teóricos que abrangem este estudo, incluindo informações referentes às definições de polímeros sintéticos, biopolímeros (Blendas e misturas poliméricas; Isolado Proteico do

Soro de Leite (IPS); Pectina; Alginato e Amido), o babaçu (a Palmeira, o Fruto e o Mesocarpo).

**Capítulo 2:** *Characterization of pectin biofilms with the addition of babassu mesocarp and whey protein concentrate.* Nesse capítulo foram descritas as técnicas de produção do mesocarpo de coco babaçu e dos biopolímeros formados com pectina, concentrado proteico de soro de leite e mesocarpo de coco babaçu. Caracterizações como espessura, permeabilidade ao vapor de água, conteúdo de umidade, solubilidade em água, microscopia, espectroscopia no infravermelho e teste de biodegradabilidade foram descritos.

**Capítulo 3:** *Physical properties of films based on pectin and babassu coconut mesocarp.* Neste capítulo foram descritos a produção dos biopolímeros de mesocarpo de coco babaçu e pectina através da utilização de planejamentos experimentais. Caracterização dos biopolímeros por testes físico-químicos, morfologia, propriedades térmicas e mecânicas.

**Capítulo 4:** *Elaboration and characterization of biopolymer films with alginate and babassu coconut mesocarp.* Neste capítulo fez-se a incorporação do mesocarpo de coco babaçu com a matriz alginato de sódio e a caracterização dos biopolímeros obtidos quanto a morfologia, ensaios mecânicos, propriedades térmicas.

## REFERÊNCIAS

CARRAZZA, L. R.; ÁVILA, J. C. C. e; SILVA, M. L. da. Manual tecnológico de aproveitamento integral do fruto e da folha do babaçu. 2. ed. Brasília: ISPN, 2012.

CRITCHELL, K.; BAUER-CIVIELLO, A.; BENHAM, C.; BERRY, K.; EAGLE, L.; HAMANN, M.; HUSSEY, K.; RIDGWAY. Chapter 34 - Plastic Pollution in the Coastal Environment: Current Challenges and Future Solutions. *Coasts and Estuaries*, p. 595-609, 2019.

DICKINSON, E. Milk protein interfacial layers and the relationship to emulsion stability and rheology, *Colloids and Surf. B: Biointerfaces*, v.20 (3), 197p, 2001.

FARIAS, M. G. *et al.* O efeito da permeabilidade ao vapor de água, atividade de água, molhabilidade e solubilidade em água em filmes de amido e polpa de acerola. Embrapa Agroindústria Tropical. 2012.

GRÉGOIRE, N.; CHAUVELOT, I. Accelerating transition to a circular economy in plastics. *Field Actions Science Reports*, v. 19, p. 44-53, 2019.

MALI, S.; GROSSMANN, M. V.; YAMASHITA, F. Filmes de amido: produção, propriedades e potencial de utilização. *Semina: ciências agrárias*, v. 31, n.1, p.137-156, 2010.

SANTANA, A.A.; MARTIN, L.G.P.; OLIVEIRA, R.A.; KUROZAWA, L.E.; PARK, K.J. Spray drying of babassu coconut milk using different carrier agents. *Drying Technology*, v. 35, p. 76-87, 2017.

SANTANA, A. A.; KIECKBUSCH, T. G. Physical evaluation of biodegradable films of calcium alginate plasticized with polyols. *Brazilian Journal of Chemical Engineering*, v. 30, n°. 4, p. 835-845, 2013.

SEIXAS, F. L. *et al.* Biofilms composed of alginate and pectin: effect of concentration of crosslinker and plasticizer agentes. *Chemical engineering transactions*, v. 32, p. 1693-1698, 2013.

# CAPÍTULO 1: REVISÃO BIBLIOGRÁFICA

## 1.1 POLÍMEROS SINTÉTICOS

Os materiais poliméricos são substâncias macromoleculares, de origem orgânica, formados pela repetição dos meros. Atualmente, a variedade de polímeros existente é muito grande. Para facilitar o estudo destes materiais, os polímeros foram classificados de acordo com sua estrutura química. Em relação à forma da cadeia polimérica, os polímeros podem ser classificados em lineares (quando a cadeia não possuir ramificações), ramificados (quando a cadeia apresenta pequenas cadeias laterais) e reticuladas (quando as cadeias estão unidas por ligações químicas cruzadas) (DEMARQUETE, 2010; CALLISTER e RETHWISCH, 2016).

As moléculas dos polímeros de cadeia linear estão mais soltas quando comparadas às de cadeia ramificada e, mais ainda, quando comparadas as que apresentam ligações cruzadas e, desta forma, quanto mais solta uma cadeia, menor é sua elasticidade e, quanto mais ramificada ou cruzada uma cadeia, maior será sua elasticidade. Por exemplo, o nylon (material muito utilizado em meias calças femininas) apresenta grande elasticidade, uma vez que suas estruturas moleculares se apresentam de forma cruzada. Em relação à sua moldagem ao calor, os polímeros podem ser classificados em termorrígidos e termoplásticos. Polímeros termorrígidos são aqueles formados por cadeias cruzadas e não podem ser remodelados, pois o reaquecimento leva a sua decomposição, ou seja, eles não retornam ao seu formato original. Por isso, eles não podem ser reciclados como, por exemplo, o silicone. Termoplásticos são formados por cadeias lineares ou ramificadas e podem ser remodelados, pois o reaquecimento degrada parcialmente o polímero. Na indústria, são aplicados na produção de embalagens, eletrodomésticos, brinquedos, tubulações, entre outros produtos (CALLISTER e RETHWISCH, 2016).

Além dessas classificações, existem outras que estão relacionadas às características físico-químicas ou ao seu desempenho, conforme mostrado a seguir pela classificação técnico-econômica (DEMARQUETE, 2010; CALLISTER e RETHWISCH, 2016):

- Polímeros Comuns (*commodities*) - grupo de maior abrangência; alta produção e baixo custo, tais como Polipropileno-PP, poliestireno-PS e Policloreto de vinila - PVC;
- Polímeros (pseudo-commodities) - grupo de polímeros de uso específico, produção relativa à demanda, médio custo, tais como: Policarbonato-PC, Poliamida-PA, Polimetacrilato de metila-PMMA, Polioximetileno-POM, entre outros;
- Polímeros (*specialties*) grupo de polímeros de alto desempenho, apresentando baixa produção e alto custo, tais como: Poliéster-cetona-PEK, Poli-imida-PI, entre outros.

De acordo com a estrutura do polímero ele poderá apresentar comportamento mecânico plástico, elástico ou em fibra.

- Elastômeros: popularmente conhecidos como borrachas, são polímeros de alta elasticidade, que podem, em condições naturais, deformarem-se e voltar ao seu estado inicial.
- Fibras: são materiais constituídos geralmente por macromoléculas lineares, estirados em filamento, por isso a elevada razão entre comprimento e as dimensões laterais. Possuem alta resistência mecânica, pois resistem a uma variação de temperatura de -50° a 150°C.
- Plásticos: são materiais poliméricos encontrados, na sua composição final, no estado sólido à temperatura ambiente. Atualmente, conhecem-se mais de 60 mil plásticos diferentes, e, dentre os cinquenta produtos químicos mais utilizados, vinte são plásticos (CALLISTER e RETHWISCH, 2016).

Os polímeros provenientes do petróleo são os materiais mais utilizados atualmente para produção de componentes plásticos, mas, recentemente surgiu uma nova tecnologia que está substituindo os plásticos convencionais, denominada de biopolímeros. Os biopolímeros são largamente utilizados na produção de embalagens e produtos plásticos, e podem ser classificados em biopolímeros recicláveis e biodegradáveis. Steinhoff et al. (2009) afirmaram que a produção de resinas plásticas produzidas a partir de materiais biodegradáveis, como as proteínas, conquista uma importância crescente nas indústrias alimentícia e farmacêuticas (FONTOURA e CALIL, 2016).

## 1.2 BIOPOLÍMEROS

Apesar dos plásticos não biodegradáveis possuírem excelentes propriedades funcionais, estes são considerados poluentes e estão envolvidos em problemas ambientais, pois levam muito tempo para se degradarem, permanecendo praticamente intactos ao longo dos anos (LAFTAH, 2017). A biodegradação consiste na degradação dos materiais poliméricos a partir da ação de organismos vivos. Segundo a *American Standard for Testing and Methods* (ASTM-D-883), polímeros biodegradáveis são polímeros degradáveis, nos quais a degradação resulta primariamente da ação de microrganismos, tais como bactérias, fungos e algas, de ocorrência natural, originando o dióxido de carbono, gás metano, componentes celulares microbianos e outros produtos (ASTM, 1999).

Com a intenção de substituir, parcialmente, os plásticos sintéticos, estudos vêm sendo realizados com intuito de encontrar materiais com durabilidade em uso e degradabilidade após o descarte. Há um interesse crescente na produção de plásticos biodegradáveis, a partir de polímeros biodegradáveis naturais como os polissacarídeos e as proteínas, como a proteína do soro de leite, por exemplo, os quais apresentam algumas vantagens, pois são provenientes de fontes renováveis e são capazes de formar uma matriz contínua e coesa (SILVA et al., 2012).

As proteínas possuem uma estrutura com 20 monômeros diferentes, o que confere uma ampla gama de propriedades funcionais, especialmente um potencial para ligações intermoleculares. Assim, os filmes à base de proteínas podem formar ligações em posições diferentes e oferecem grande potencial para a formação de numerosas ligações (RHIM e NG, 2007). No entanto, os biopolímeros não são somente destinados a substituir totalmente embalagens sintéticas tradicionais (eles têm o potencial de reduzir a sua utilização), também têm a função de atuar como sistemas de liberação controlada de substâncias ativas, limitando o passo de umidade, aroma, e migração de lipídios e componentes nos alimentos.

Segundo Santana e Kieckbusch (2013), os filmes biodegradáveis são aqueles obtidos a partir de polímeros de origem animal ou vegetal, como polissacarídeos, lipídios e proteínas e quando descartados não agredem o ecossistema, pois são convertidos em compostos simples, mineralizados e redistribuídos através dos ciclos de carbono, nitrogênio e enxofre. Em síntese, a biodegradação de um polímero é um processo



intrínseco pelo qual os microrganismos e suas enzimas consomem este polímero como fonte de nutrientes, em condições normais de umidade e temperatura.

Os polímeros mais bem adaptados à biodegradação completa são os naturais, aqueles hidrolisáveis a  $\text{CO}_2$  e  $\text{H}_2\text{O}$ , ou a  $\text{CH}_4$  e os polímeros sintéticos que possuem estruturas próximas aos naturais. Com respeito a formulação dos biopolímeros, é preciso selecionar tanto os materiais, bem como as tecnologias de produção. Atualmente, tende-se ao desenvolvimento de materiais que interagem com a embalagem de alimentos, desempenhando um papel ativo na preservação. Uma alternativa, é a incorporação de substâncias ativas ao material de embalagem, como antioxidantes ou moléculas de baixo peso molecular (KECHICHIAN et al., 2010; VARTIAINEN et al., 2014).

O desenvolvimento de biopolímeros para a proteção dos alimentos apresenta bons resultados como barreiras aos gases, mas não ao vapor de água, devido a utilização de polissacarídeos e proteínas para o seu desenvolvimento. No entanto, podem ser obtidos filmes compostos a partir de fibras de origem vegetal, como frutas puras ou celulose (ENCALADA et al., 2016), considerando propriedades funcionais, tais como: barreira a umidade, gases e solutos; solubilidade em água ou lipídeo; propriedades óticas; características mecânicas e reológicas e propriedades térmicas, pois essas podem determinar o processamento, a aplicação, o condicionamento e a espessura do filme (VICENTINI, 1999; TAN et al., 2016).

Segundo Villadiego et al. (2005) a classificação de biofilmes e revestimentos comestíveis pode ser dividida em três grupos:

- Hidrocoloidais - são filmes à base de polissacarídeos ou proteínas. Devido à natureza hidrofílica, são permeáveis ao vapor de água, baixa permeabilidade ao oxigênio, dióxido de carbono e lipídeos;
- Lipídicos - são compostos de lipídeos, os quais por sua natureza hidrofóbica, apresentam baixa permeabilidade ao vapor de água e aos gases;
- Compostos - são combinações de proteínas e lipídeos ou polissacarídeos e lipídeos. Podem existir em camadas separadas, ou associados, em que ambos os componentes são adicionados ao filme. Por isso, têm sido o alvo na pesquisa de biofilmes para o uso em embalagens compostas, devido à combinação das vantagens de cada um dos componentes, reduzindo assim suas desvantagens.

### **1.2.1 Blendas e misturas poliméricas**

Blendas poliméricas são misturas físicas de dois ou mais polímeros, resultando em uma mistura miscível ou imiscível. A mistura de polímeros é uma técnica que tem como objetivo a obtenção de materiais com propriedades diferentes às dos polímeros puros, sendo que essa mistura frequentemente exhibe propriedades superiores quando comparadas às propriedades de cada componente polimérico individualmente. A principal vantagem das blendas é a simplicidade da preparação e o fácil controle das propriedades físicas com a mudança das concentrações dos componentes (CALLISTER e RETHWISCH, 2016).

Além da mistura entre materiais poliméricos, alguns aditivos podem ser incorporados aos polímeros puros ou a essas misturas. A introdução de aditivos à matriz polimérica tem o intuito de melhorar determinadas características dos biopolímeros uma vez que estes podem modificar propriedades físicas ou mecânicas, gerando também a possibilidade de produção de embalagens ativas se o aditivo apresentar alguma propriedade específica (MORAES, 2012; PEREIRA et al., 2013; BIJI et al., 2015, DOMÍNGUEZ et al., 2018).

#### **1.2.1.1 Isolado e Concentrado Proteico do Soro de Leite (IPS)**

O soro lácteo, também conhecido como soro de leite, soro de queijo ou lacto-soro, é um subproduto da indústria de laticínios, representa a porção aquosa do leite que se separa do coágulo durante a fabricação do queijo ou na produção de caseína. É composto basicamente de 94 a 95% de água, 3,8 a 4,2% de lactose, 0,8 a 1,0% proteínas e 0,7 a 0,8% de minerais. É um subproduto de relevante importância na indústria de laticínios, tendo em vista o volume produzido e sua composição nutricional. O interesse na utilização desse material como biopolímero estrutural teve início a partir da década de 70, onde pesquisadores passaram a estudar suas propriedades nestas aplicações (BRANS et al., 2004).

O componente mais valioso do soro são as proteínas, mas sua concentração neste líquido é reduzida, e, para realçar as suas propriedades funcionais, tais como solubilidade, emulsificação e formação de espuma, são necessárias etapas de concentração como a

Ultrafiltração (UF) onde o teor de lactose é reduzido, gerando um produto com alto teor de proteína, como o isolado proteico de soro de leite.

Além das propriedades nutricionais, as proteínas do soro do leite são conhecidas pela versatilidade de suas propriedades funcionais tecnológicas como ingredientes em produtos alimentícios, principalmente pela elevada solubilidade e propriedades emulsificantes. A solubilidade é a mais importante característica de uma proteína, pois esta tem a capacidade de afetar de maneira favorável ou desfavorável sua funcionalidade. Com a chegada de novas tecnologias e com as novas descobertas da importância das proteínas do leite em Ciência e Tecnologia de Alimentos e na Nutrição, ocorreu grande aumento das pesquisas procurando intensificar o uso dessas proteínas. O IPS tem em sua composição de proteínas de 90% a 80%, em média 1% de lactose, 1% de gordura e 3% de cinzas (BRANS et al., 2004).

Nota-se na literatura trabalhos voltados para desenvolvimento de filmes, nas mais diversas abordagens, com o uso do isolado proteico de leite devido às suas características, sendo estes filmes utilizados principalmente para produção de embalagens alimentícias (RAMOS et al., 2012; FERNANDÉZ-PAN et al., 2013; PHUPOKSAKUL et al., 2014; SILVA et al., 2016).

A maior parte das pesquisas sobre as proteínas existentes no soro buscavam identificar o valor nutricional para fins alimentícios e como suplemento para atividade muscular, mas vem crescendo o número de pesquisas com interesse nas propriedades funcionais importantes que ela tem na formação de biofilme. As proteínas do soro são utilizadas como subprodutos na fabricação de queijo por conter duas proteínas, a R-lactalbumina e a lactoglobulina. A produção mundial em larga escala em torno de 10-20 (t) produzida por ano é sub utilizada (KINSELLA e WHITEHEAD, 1989). Grande parte era descartado em rios, gerando problemas para o meio Ambiente, conforme analisado por Le Tien et al. (2000).

Wang et al. (2010) produziram filmes para fins de embalagens utilizando concentrado proteico de soro de leite (WPC) como matéria-prima principal usando o glicerol e carboximetilcelulose obtendo bons resultados em valores baixos de concentração e que valores elevados de WPC provoca diminuição das propriedades de barreira do filme. Mas por outro lado, melhora as propriedades mecânicas.

Oliveira et al. (2017) prepararam filmes à base de proteína de soro de leite incorporados com óleo essencial de orégano em diferentes concentrações e tinha o

propósito de avaliar as propriedades e atividade antimicrobiana. Obtiveram filmes mais flexíveis com o aumento da concentração do óleo e diminuição da solubilidade do mesmo. Os resultados mostraram que os filmes à base de proteínas do soro incorporados ao óleo essencial de orégano têm potencial aplicação como embalagem ativa.

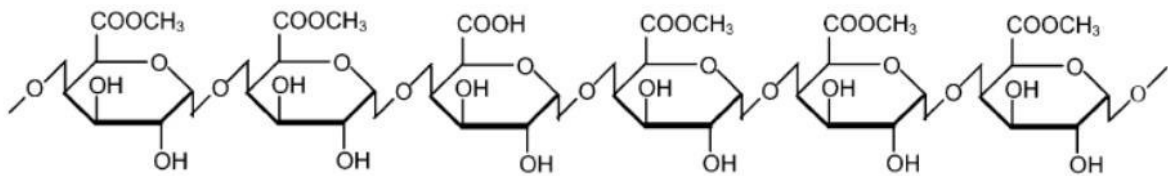
### **1.2.1.2 Pectina**

As pectinas podem ser descritas como hidrocolóides naturais, presentes nas paredes celulares de certas frutas como maçã e polpa de cítricos. As pectinas também podem ser definidas como polissacarídeos que possuem entre 150 e 500 unidades de ácido galacturônico, ligadas por ligações (1→4), parcialmente esterificadas com grupos metoxi, separadas por regiões ramificadas contendo vários açúcares (PAIVA et al., 2009).

Segundo Canteri et al. (2012), a descoberta da pectina, como composto químico, data do ano de 1790, sendo que apenas em 1824 foi feita a sua caracterização, como sendo um composto presente nas frutas e responsável pela formação de gel. Considerava-se que a pectina fosse uma pequena estrutura cíclica, porém, em 1923, foi observado a partir de análises de raio-X que a pectina era um polímero bastante complexo. Dependendo da origem botânica do produto vegetal, o teor de substâncias pécticas pode variar. No entanto, há quatro subprodutos da agroindústria e da indústria alimentícia que são ricos em substâncias pécticas (teor superior a 15% em base seca): bagaço de maçã, albedo cítrico, polpa de beterraba e pétalas de girassol (CANTERI, 2012).

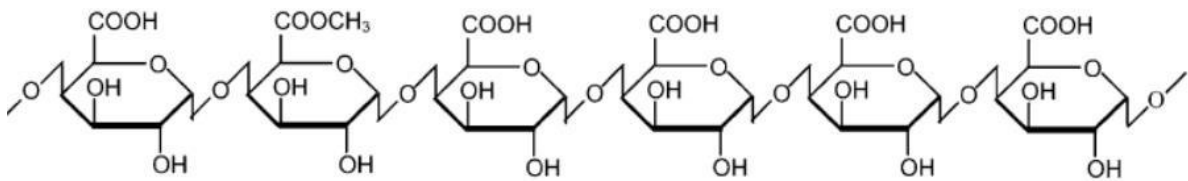
Pectinas comerciais têm como característica expressiva, seu grau de metoxilação, o que se relaciona a quantidade de ácidos galacturônicos esterificados com grupamentos metílicos (CH<sub>3</sub>). De acordo com o grau de metoxilação as pectinas são divididas em dois grupos: as pectinas de alta metoxilação (ATM), que contêm 50% ou mais das unidades de ácido galacturônico esterificadas; e as de baixa metoxilação (BTM), que apresentam unidades de ácido galacturônico esterificadas inferiores a 50%. O grau de metoxilação influencia diretamente as propriedades funcionais das pectinas, como a solubilidade, temperatura e condição de gelificação (LICODIEDOFF, 2010) (Figuras 1 e 2).

**Figura 1**-Pectina com alto teor de metoxilação.



Fonte: Tharanathan (2003).

**Figura 2** - Pectina com baixo teor de metoxilação.



Fonte: Tharanathan (2003).

Paiva et al. (2009), afirmam que o uso e importância das pectinas na indústria de alimentos, se dá devido à sua função de conferir firmeza, retenção de sabor e de aroma, assim como, ao seu desempenho na dispersão e estabilização de diversas emulsões. Para que a pectina possa formar gel, característica esperada para o seu uso, deve-se considerar o pH do meio submetido para formação do gel, teor de sólidos solúveis e o grau de metoxilação.

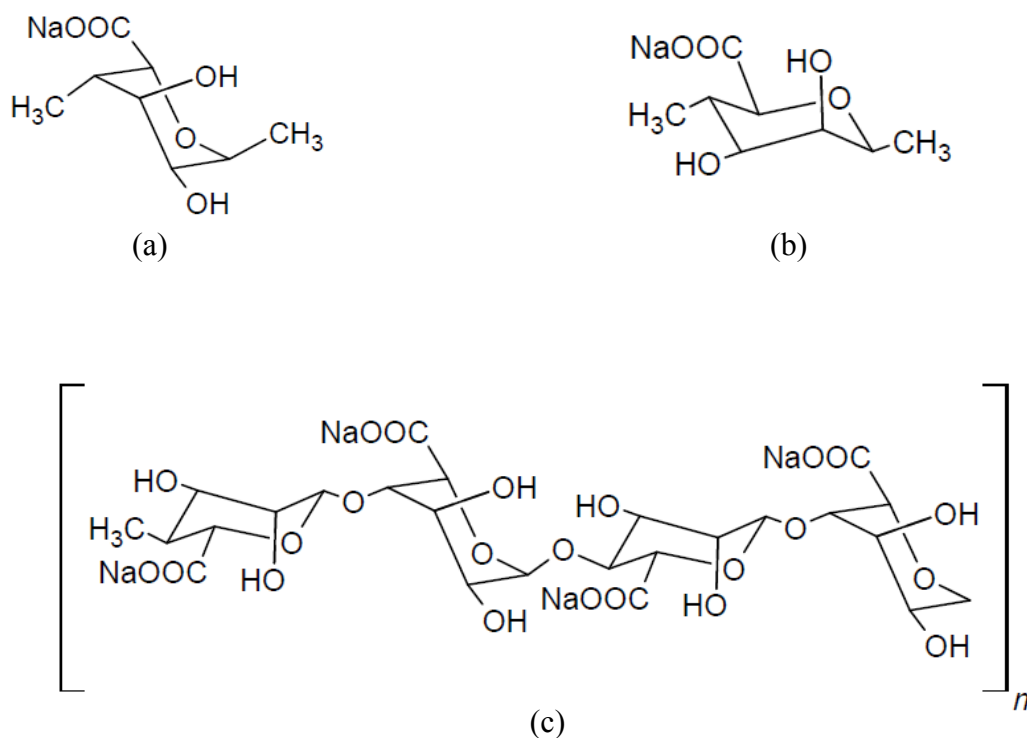
### 1.2.1.3 Alginato

O alginato de sódio é um polissacarídeo linear obtido a partir de algas marrons ou bactérias, sendo composto por resíduos dos ácidos  $\beta$ -D-Manurônico e  $\alpha$ -L-Gulurônico na forma de sal de sódio, unidos por ligações glicosídicas e distribuídos em diferentes proporções ao longo da cadeia. O alginato pode ser utilizado em inúmeras aplicações nas indústrias alimentícias, farmacêuticas, têxteis e papel, e em processos para tratamento de água pelo fato de apresentar características tais como; ação gelificante e espessante, biodegradabilidade, biocompatibilidade e ausência de toxidez (SANTANA e

KIECKBUSCH, 2013). Os filmes de alginato são estudados, visando sua utilização em embalagens, cobertura e proteção de alimentos, matriz ou cobertura reticulada para sistemas de liberação de fármacos e no encapsulamento de células vivas (LIMA et al., 2007; SANTANA e KIECKBUSCH, 2013).

Silva et al. (2012) afirmam que a composição da molécula básica de alginato se dá por monômeros de Gulurônico (G) e Manurônico (M), formando regiões de M-blocos, G-blocos e blocos de sequência alternativa (MG-blocos), conforme Figura 3, onde a proporção relativa de cada organização sequencial depende da fonte natural do alginato. De acordo com Santana e Kieckbusch (2013), a viscosidade de soluções de alginato depende da organização dos blocos M e G. Na Tabela 1 são apresentadas algumas características de alginatos obtidos dos dois principais tipos de algas, uma rica em grupos M e outra em grupos G. Comercialmente eles são divididos em três classes de acordo com a viscosidade: baixa viscosidade (LV), média viscosidade (MV) e alta viscosidade (HV).

**Figura 3** - Estrutura do: (a) ácido  $\beta$ -D-manurônico, (b)  $\alpha$ -L-gulurônico e (c) alginato.



Fonte: O autor.

**Tabela 1** - Propriedades químicas (X<sub>G</sub> e X<sub>M</sub>) e físicas ( $\mu$ , M<sub>n</sub> e d<sub>p</sub>) do alginato.

Alga	Composição	Reologia	X <sub>G</sub>	X <sub>M</sub>	$\mu$ (dL/g)	M <sub>n</sub> (kDa)	d <sub>p</sub>
<i>Macrocystis pyrifera</i>	Alto - M	LV	0,38	0,62	5,9	72,7	367
		MV	0,35	0,65	9,6	119,9	606
		HV	0,37	0,63	10,7	134,5	679
<i>Laminaria hyperborea</i>	Alto - G	LV	0,63	0,37	5,9	73,1	369
		MV	0,57	0,43	6,8	84,6	427
		HV	0,63	0,37	17,0	217,7	1099

Fonte: Clementi et al., (1999)

Em que: X<sub>G</sub> é a fração de ácidos Gulurônico (G); X<sub>M</sub> é a fração de ácidos Manurônico (M);  $\mu$  (dL/g) é a viscosidade intrínseca em NaCl 0,1 M; M<sub>n</sub> (kDa) é a massa molecular média; d<sub>p</sub> é o grau de polimerização.

O alginato de sódio é um polissacarídeo abundante, apresentando propriedades úteis e favoráveis ao meio ambiente, visto que, é renovável, biodegradável e seguro. É amplamente utilizado em alimentos, tecidos, e no campo médico, devido às suas notáveis propriedades de gelificação à aplicação de materiais hemostáticos. O uso de alginatos se dá basicamente por três principais propriedades. A primeira é a sua capacidade de aumentar a viscosidade de soluções aquosas. A segunda é a capacidade de formar géis. E a terceira, é a capacidade de formar películas de sódio ou de alginato de cálcio e fibras de alginato de cálcio (MOLLAN e KHAN, 2012; PEREIRA et al., 2013; HARPER et al., 2016).

A preparação de filmes de alginato, como a maioria dos biopolímeros, ocorre pela evaporação de solvente, sendo variável a temperatura de secagem. As películas usando alginato podem ser secas em temperatura ambiente; e a 36 °C, 40 °C, 50 °C, 60 °C e 80 °C. Dependendo da temperatura utilizada, do volume, da concentração da solução, e da umidade relativa do ar, o tempo de secagem pode variar (SILVA et al., 2012). Os filmes de alginato têm sido desenvolvidos amplamente na literatura (PEREIRA et al., 2013; BIEHARLZ et al., 2012; NGO et al., 2018) incorporando agentes para compor embalagens, materiais funcionais e confeccionando blendas.

#### 1.2.1.4 Amido

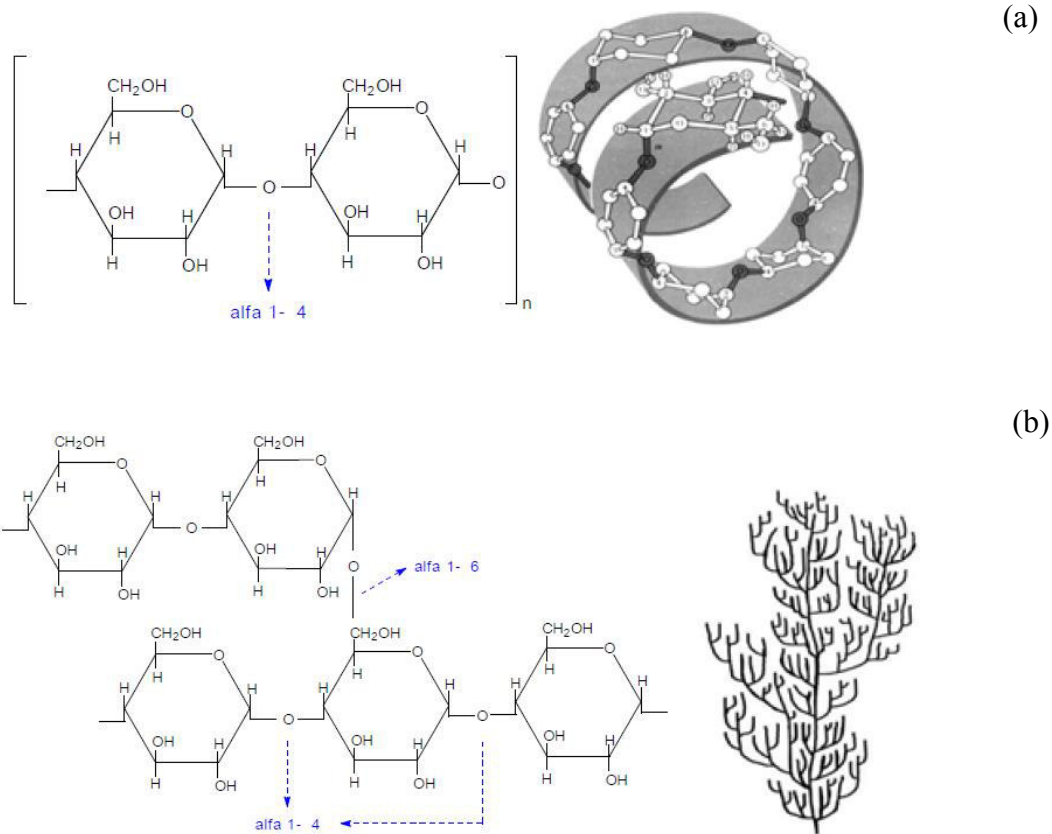
O amido é um polímero natural formado por monômeros de glicose unidos por ligações glicosídicas e, portanto, classificado como um homopolissacarídeo (FOOD INGREDIENTS BRASIL, 2015; KHAN et al., 2016). Apresenta-se como um pó branco, insolúvel em água fria e destituído de sabor (VILLELA et al., 1978). Ele é sintetizado no estágio final da fotossíntese, constituindo a principal fonte de reserva energética das plantas (SILVA et al., 2008). O amido pode ser extraído das células de frutos, sementes, raízes e tubérculos na forma de grânulos de 1 a 100 $\mu$ m de diâmetro (SILVA et al., 2008; KHAN et al., 2016). A forma, tamanho e estrutura desses grânulos dependem da origem botânica e do estágio de desenvolvimento da planta (SPIER, 2013). O amido também é encontrado, em menores proporções, em microrganismos (VILLELA et al., 1978).

Além de pequenas quantidades de proteínas, lipídeos e cinzas, os grãos de amido contêm, majoritariamente, duas macromoléculas: a amilose e a amilopectina. A amilose é um polímero, essencialmente linear, composto principalmente de ligações  $\alpha$ -1,4 nas unidades de D-glicose (SPIER, 2013). Já a amilopectina, possui peso molecular superior, é formada por ligações glicosídicas  $\alpha$ -1,4 e  $\alpha$ -1,6, dando origem a uma molécula altamente ramificada. As proporções dessas estruturas nos grânulos variam de acordo com a variedade e maturação da planta, o que resulta em amidos com propriedades físico-químicas e funcionais diferenciadas. Em média, a amilose corresponde cerca de 15 a 30% do amido, enquanto a amilopectina corresponde de 70 a 85% (SANTANA et al., 2013).

A Figura 4 ilustra as estruturas químicas tanto da amilose quanto da amilopectina, mostrando como elas se distribuem espacialmente. Observa-se que a amilose, apesar de linear, apresenta uma conformação helicoidal, o que dificulta sua associação regular com outras cadeias (CORRADINI et al., 2005). No entanto, essa conformação permite que a amilose forme complexos corados ou insolúveis com substâncias como o iodo, timol e butanol (VILLELA et al., 1978). Quanto maior a afinidade por iodo, maior será o teor de amilose do amido (TÔRRES, 2014). A linearidade da amilose torna seu comportamento mais próximo dos polímeros sintéticos, característica interessante para determinadas aplicações dos amidos (HORN, 2012).



**Figura 4** - Estrutura da amilose e respectiva conformação helicoidal (a) e da amilopectina e sua forma ramificada (b).



Fonte: Adaptado de CEREDA e VILPOUX, 2003.

Ainda na Figura 4 é possível perceber o aspecto ramificado da amilopectina, responsável pela cristalinidade dos grãos de amido. Ela se distingue da amilose por formar pseudo-soluções menos viscosas, mais estáveis e avermelhadas na presença de iodo (VILLELA et al., 1978). Os segmentos lineares da amilopectina formam estruturas helicoidais duplas, estabilizadas por pontes de hidrogênio, entre os grupos hidroxilas da molécula, que se agregam em regiões semicristalinas. As cadeias de amilose e as ramificações da amilopectina compõem a região amorfa dos grãos (SANTOS, 2012).

Embora sua maior aplicação seja no setor alimentício, o amido também é utilizado em outras indústrias como a química, farmacêutica, papelreira, de construção civil, têxtil e petrolífera (FOOD INGREDIENTS BRASIL, 2015). Possui destaque na área de biocombustíveis, como uma das fontes para a obtenção do etanol (PAVLAK et al., 2007). Na indústria de papel o amido é largamente utilizado como coadjuvante, na forma de agente de revestimento ou como adesivo. Melhora as propriedades mecânicas do papel,

formando um filme protetor, que aumenta sua resistência, assim como, permite uma melhor ligação entre os componentes do papel e papelão (ROYAL INGREDIENTS, 2019; TOLVANEN et al., 2009). O amido vem sendo usado na indústria de plásticos e embalagens (KHAN et al., 2016; PEELMAN et al., 2015). O alto teor de amilose leva a formação de filmes mais homogêneos, enquanto, maior proporção de amilopectina provoca aumento na tendência de separação de fases do gel (sinérese). Os biopolímeros produzidos com amido com maior concentração de amilose apresentam melhores propriedades mecânica e barreira e os de amilopectina são mais frágeis e quebradiços.

## **1.3 O BABAÇU**

### **1.3.1 A Palmeira**

As palmeiras constituem formas vegetais de ampla distribuição, ocorrendo principalmente na região intertropical com raras ou nenhuma presença em regiões desértica e polar. Apresentam hábitos variados em relação ao tipo de caule, podendo apresentar estipes de médio e grande porte, isolado ou cespitoso e lianas com ou sem espinhos no caule e folhas. Sobrevivem a longos períodos de estiagem e incêndios ocasionais, mas raramente toleram baixas temperaturas (HENDERSAN, 1995; MARTINS, 2001). A família *Arecaceae* registra aproximadamente 240 gêneros e 2700 espécies no mundo (LORENZI et al., 2010). Há registro de ocorrência no Brasil de 39 gêneros e 264 espécies, sendo 109 endêmicas (LEITMAN et al., 2013). Destacam-se como interesse para a sobrevivência e a subsistência do homem pelo uso de frutos e palmito, sendo as regiões da Amazônia e Cerrado com registro de maior número de espécies, 146 e 82 respectivamente.

Outra maneira de aproveitamento é o processamento na forma de doces, bebidas, óleos e no artesanato com grande variedade nas espécies dos gêneros *Attalea*, *Orbygnia*, *Syagrus*, *Acrocomia* e *Mauritia* (PEREIRA, 1996; LIMA et al., 2003). Nos gêneros *Attalea* e *Orbygnia* destaca-se o Babaçu (Figura 5), de estipe único variando de 10 a 30 metros de altura, com 20 a 60 centímetros de diâmetro, podendo conter de 7 a 22 folhas pinadas, geralmente medindo de 4 a 8 metros de comprimento (RAMÍREZ, 2004; LORENZI et al., 2010; CARRAZA et al., 2012). A produção do fruto (coco babaçu), apreciado tanto pelo homem como por animais silvestres (roedores), varia conforme a região e condições

naturais (CARRAZA et al., 2012). Por esta razão é de relevância na subsistência de muitas comunidades tradicionais (LIMA et al., 2003).

**Figura 5** – Palmeira de babaçu.



Fonte: Próprio autor.

As folhas são usadas na cobertura de casas (GALDINO e DA SILVA, 2009; REZENDE et al., 2010), no artesanato (CORREIA et al., 2010), o estipe na estrutura e parede das moradias (NASCIMENTO et al., 2009). Do endocarpo dos frutos é produzido o carvão como fonte de energia, do mesocarpo como complemento alimentar e as amêndoas como alimento animal, condimento culinário, na composição de cosmético e na produção de biodiesel (ALVIN, 2014).

O nome do babaçu tem origem Tupi-Guarani: ba = fruto; açu = grande. É uma palmeira nativa das regiões Norte, Nordeste e Centro do Brasil. O babaçu é o nome dado ao fruto e a palmeira oleaginosa da família botânica *Arecaceae*. Ele está presente em vários países da América Latina como Brasil, Bolívia e Suriname (CRUZ e ALMEIDA, 2014).

No gênero *Attalea* engloba espécies nativas da região norte do Brasil, e que ocorrem, principalmente, na Mata dos Cocais (transição entre Caatinga, Cerrado e Amazônia) nos estados do Maranhão, Tocantins e Piauí, sendo o Maranhão o maior produtor do babaçu, possuindo 2/3 de toda a produção no Brasil. Já as espécies do gênero

*Orbignya* são mais comuns nos estados de Goiás, Minas Gerais e Bahia (CRUZ e ALMEIDA, 2014; CARRAZA et al., 2012).

A importância da planta relaciona-se à grande quantidade de produtos e subprodutos que derivam dela, mas apesar do imenso valor dessa palmeira, o potencial atrativo dela continua atualmente pouco explorado, devido à baixa eficiência dos modos de produção, especialmente no que se refere a tecnologias de aproveitamento integral do babaçu em agroindústrias de base familiar (CARRAZA et al., 2012). De acordo com SANTANA et al. (2017) apenas o óleo e a torta (massa residual da prensagem) extraídos das amêndoas do coco, são produzidos industrialmente.

### **1.3.2 O Fruto e o Mesocarpo de Coco Babaçu**

O coco babaçu (fruto da palmeira de babaçu) é oval alongado, de coloração castanha e surge de agosto a janeiro e, é composto por quatro partes principais (Figura 6):

- a) Epicarpo (camada externa fibrosa);
- b) Mesocarpo (camada intermediária que fica entre o epicarpo e o endocarpo, fibrosa e amilácea, com 0,5 a 1,0 cm de espessura);
- c) Endocarpo (camada interna lenhosa, onde ficam alojadas as amêndoas de 2 a 3 cm de espessura), e
- d) Amêndoas (de cor branca, coberta por uma película de cor castanha, de 3 a 6 por fruto, com 2,5 a 6 cm de comprimento e 1 a 2cm de largura) (SANTOS, 2014; SOLER et al., 2007).

A avaliação proporcional das diferentes partes que correspondem ao fruto do babaçu mostra que cerca de 13% do peso total do fruto corresponde ao epicarpo; 20% ao mesocarpo, 60% ao endocarpo e 7% as amêndoas (TÔRRES, 2014).

**Figura 6** - Composição do coco babaçu.



Fonte: Da Sousa et al. (2019).

Do mesocarpo, é obtida uma farinha amplamente comercializada no Maranhão. A farinha é obtida a partir da secagem e trituração do mesocarpo (ALMEIDA et al., 2011). O mesocarpo de coco babaçu é geralmente obtido por meio do descascamento manual por comunidades tradicionais (Figura 7).

**Figura 7** – Descascamento manual para a obtenção do mesocarpo de coco babaçu:  
descascamento com uso de facão



Fonte: Próprio autor.

Após retirada do epicarpo por este método, o mesocarpo fica exposto para ser extraído no formato de flocos que são posteriormente secos e triturados para a obtenção da farinha do mesocarpo seco (farinha de babaçu) (CARRAZA et al., 2012). Esta apresenta uma cor castanha devido aos taninos, substâncias naturais de natureza fenólica (MANIGLIA & TÁPIA-BLÁCIDO, 2016).

A farinha serve de alimento para pessoas e animais, como na forma de farinha substitutiva da mandioca. A farinha do mesocarpo de coco babaçu não é um produto muito valorizado, sobretudo pela falta de uniformidade. As diferenças nas farinhas oferecidas ao mercado são decorrentes de vários fatores como cultivar, clima, solo, ponto de colheita, variabilidade genética, matéria-prima e outros, mas o principal fator responsável é o método de processamento (ALMEIDA et al., 2011; CARRAZA et al., 2012).

A heterogeneidade da farinha é devida, principalmente, à fabricação por pequenos produtores para seu uso diário, utilizando-se de técnicas e processos diversos. O mesocarpo, quando fresco, apresenta cor creme clara e pode ser facilmente reduzido a pó. À medida que envelhece, vai adquirindo rigidez lenhosa e cor castanho-avermelhada e, quando seco, ao ser embebido em água, apresenta textura semelhante ao látex, sendo dificilmente moído ou triturado (CARRAZA et al., 2012).

No conhecimento tradicional o mesocarpo é utilizado no tratamento de diversas doenças como dismenorreia, constipação, obesidade, reumatismo, úlceras, doenças venosas e inflamatórias e no tratamento de leucemias e tumores, visto que é rico em carboidratos e sais minerais. No mesocarpo pode-se encontrar além dos taninos, substâncias como açúcares, saponinas, compostos esteroides e triterpenos (FORTES et al., 2009; AZEVEDO et al., 2007).

O mesocarpo de babaçu apresenta uma composição rica em amido, entre 50% e 68,3% (m/m) (CRUZ, 2011; TÔRRES, 2014). Recentemente, foram desenvolvidas técnicas de extração e purificação deste amido (ARARUNA, 2015; MANIGLIA e TÁPIA-BLÁCIDO, 2016), o que favorece seu potencial de aplicação nas áreas alimentícias quanto no uso como biomaterial.

## 1.4 REFERÊNCIAS

- ASTM – American Society for Testing Materials. Standard Terminology Relating to Plastics (ASTM D883–99), 1999.
- ALMEIDA, R. R. et al. Thermal analysis as a screening technique for the characterization of babassu flour and its solid fractions after acid and enzymatic hydrolysis. *Thermochimica Acta*. v. 519, n. 1-2, p. 50-54, 2011.
- ARARUNA, F.O.S. Obtenção e caracterização do amido do mesocarpo do coco babaçu (*Orbignya phalerata* Mart.) como agente espessante para o auxílio na alimentação de pacientes com disfagia. Dissertação de mestrado. UFPI. 2015.
- AZEVEDO, A.P.S.; FARIAS, J.C.; FERREIRA, S.C.; ARAGÃO FILHO, W.C.; SOUSA, P.R.; PINHEIRO, M.T.; MACIEL, M.C.; SILVA, L.A.; LOPES, A.S.; BARROQUEIRO, E.S.; GUERRA, R.N.; NASCIMENTO, F.R. Anti-thrombotic effect of chronic oral treatment with *Orbignya phalerata* Mart. *Journal Ethnopharmacologic*, v. 11, p. 155-159, 2007.
- BIERHALZ, A. C.; DA SILVA, M. A.; KIECKBUSCH, T. G. Natamycin release from alginate/pectin films for food packaging applications. *Journal of Food Engineering*, v.110, p.18-25, 2012.
- BIJI, K. B.; RAVISHANKAR, C. N.; MOHAN, C. O.; GOPAL, T. K. S. Smart Packaging systems for food application: a review. *Journal of Food Science and Technology*, v.52, p.6125-6135, 2015.
- BRANS, G. C. G. P. H.; SCHROEN, R. G.M.; van der Sman, R. M. BOOM. Membrane fractionation of milk: state of the art and challenges. *Journal of Membrane Science*, v.243, p.263-272, 2004.
- CALLISTER JR., William D.; RETHWISCH, David G. *Ciência e engenharia de materiais: uma introdução*. 9 ed. Rio de Janeiro: LCT, 2016.
- CANTERI, M. H. G.; MORENO, L.; WOSIACKI, G.; SCHEER, A. P. Pectina: da matéria-prima ao produto final. *Polímeros*, v. 22, nº. 2, p. 149-157, 2012.
- CEREDA, M. P.; VILPOUX, O. F. (Coord.) *Tecnologia, usos e potencialidades de tuberosas amiláceas latino americanas*. São Paulo: Fundação Cargill, 2003, 771 p.
- CLEMENTI, F.; CRUDELE, M. A.; PARENTE, E.; MANCINI, M.; MORESI, M. Production and characterization of alginate by *Azotobacter vinelan*, *J. Science Food Agr.*, v. 79, n. 4, p. 602-610, 1999.

CORRADINI, E. et al. Estudo comparativo de amidos termoplásticos derivados do milho com diferentes teores de amilose. *Polímeros: Ciência e Tecnologia*, vol. 15, n. 4, p. 268-273, 2005.

CRUZ, E. R. S.; ALMEIDA, J. J. S. Qualidade do óleo de babaçu (*Orbignya spp*) expressado pelas análises físico-químicas extraído das amêndoas coletadas na zona rural (Vila Conceição) de Imperatriz – Maranhão. *Educação Ambiental em Ação*, n. 46, 2014. ISSN 1678-0701. Disponível em < <http://revistaea.org/artigo.php?idartigo=1729>>. Acesso em: 26/04/19.

DEMARQUETE, R. *Estrutura e Propriedade de Polímeros*. Rio de Janeiro: UFRJ PMT 2010 - Introdução à Ciência dos Materiais para Engenharia. Disponível em: [www.pmt.usp.br/pmt5783/Polimeros.pdf](http://www.pmt.usp.br/pmt5783/Polimeros.pdf). Acesso em: 24/04/19.

DOMÍNGUEZ, R.; BARBA, F. J.; GÓMEZ, B.; PUTNIK, P.; KOVACEVIC, D. B.; PATEIRO, M.; SANTOS, E. M.; LORENZSO, J. M. Active packaging films with natural oxidants to be used in meat industry: a review. *Food Research International*, v. 113, p. 93-101, 2018.

ENCALADA, A. M. I.; BASANTA, M. F.; FISSORE, E. N. DE'NOBILI, M. D.; ROJAS, A. M. Carrot fiber (CF) composite films for antioxidant preservation: Particle size effect. *Carbohydrate Polymers*, v. 136, p. 1041-1051, 2016.

FERNÁNDEZ-PAN, I.; MENDOZA, M.; MATÉ, J. I. Whey protein isolate edible films with essential oils incorporated to improve the microbial quality of poultry, *Journal of Science Food and Agriculture*, v. 93, p. 2986-2994, 2013.

FOOD INGREDIENTS BRASIL. Amidos. *Food Ingredients Brasil*, n. 35, p. 31-56, 2015.

FONTOURA, Denize Rocha Santos; CALIL, Ricardo Moreira; CALIL, Ercilia Maria Borgheresi. A importância das embalagens para alimentos-aspectos socioeconômicos e ambientais. *Atas de Saúde Ambiental ASA (ISSN 2357-7614)*, v. 4, n. 1, p. 138-160, 2016.

FORTES, T.S.; FIALHO, E.M.S.; REIS, A.S.; ASSUNÇÃO, A.K.M.; PINHEIRO, M.T.; AZEVEDO, A.P.S.; BARROQUEIRO, E.S.B.; GUERRA, R.N.M.; NASCIMENTO, F.R.F. Desenvolvimento do tumor de Ehrlich em camundongos após a incubação in vitro com mesocarpo de babaçu. *Revista de Ciências e Saúde*, v. 11, n. 1, p. 11-18, 2009.

GALDINO, Yara da Silva Nogueira; DA SILVA, Carolina Joana. *Casa e Paisagem pantaneira: conhecimento e práticas tradicionais*. Cuiabá, MT: Carlini & Cniato, 2009.

GARCIA-CRUZ, C. H.; FOGGETTI, U.; SILVA, A. N. da. Alginato bacteriano: aspectos tecnológicos, características e produção. *Química Nova*, São Paulo, v. 31, n. 7, 2008.



HARPER B. S.; BARBUT, S.; SMITH, A.; MARCONE, M. F. Mechanical and microstructural properties of “wet” alginate and composite films containing various carbohydrates. *E. Food Engineering & Materials Science*, v. 80, p. E85-E92, 2016.

HORN, M. M.; MARTINS, V. C. A.; PLEPIS, A. M. G. Effects of starch gelatinization and oxidation on the rheological behavior of chitosan/starch blends. *Polymer International*, 2011.

KINSELLA, J. E.; WHITEHEAD, D. M. Proteins in Whey: Chemical, Physical, and Functional Properties. *Advanced Food Nutritional Research*, v.33, p.343-438, 1989.

KECHICHIAN, V.; DITCHFIELD, C.; VEIGA-SANTOS, P.; TADINI, C. C. Natural antimicrobial ingredients incorporated in biodegradable films based on cassava starch. *LWT – Food Science and Technology*, p. 1-7, 2010.

KHAN, B.; NIAZI, M. B. K.; SAMIN, G.; JAHAN, Z. Thermoplastic starch: a possible biodegradable food packaging material – a review. *Journal of Food Process Engineering*, n. 0, 2016.

LAFTAH, W. A. Starch Based Biodegradable Blends: A Review. *International Journal of Engineering Research & Technology*, v. 6, n. 6, p. 1151-1168, 2017.

LE TIEN, C.; LETENDRE, M.; ISPAS-SZABO, P.; MATEESCU, M. A.; DELMAS-PATTERSON, G.; YU, H.-L.; LACROIX, M. Development of Biodegradable Films from Whey Proteins by Cross-Linking and Entrapment in Cellulose. *J. Agric. Food Chem.* 2000, 48, 5566–5575.

LICODIEDOFF, S.; AQUINO, D. A.; GODOY, C. B. R. ; LEDO, C. A. S. . Avaliação da sinérese em geléia de abacaxi por meio de análise uni e multivariada. *Semina. Ciências Exatas e Tecnológicas*, v. 31, p. 51-56, 2010.

LIMA, Edson S. FELFILI, Jeanine M.; MARIMON, Beatriz S.; SCARIOT, A. Diversidade, estrutura e distribuição espacial de palmeiras em um cerrado sensu stricto no Brasil Central - DF. *Revista Brasil. Bot.*, V.26, n.3, p.361-370, jul./set. 2003.

LIMA, A. M. F.; ANDREANI, L.; SOLDI, V. Influência da adição de plastificante e do processo de reticulação na morfologia, absorção de água e propriedades mecânicas de filmes de alginato de sódio. *Química Nova*, v. 30, nº. 4, p. 832-837, 2007.

MANIGLIA, B. C.; TAPIA-BLÁCIDO. Isolation and characterization of starch from babassu mesocarp. *Food Hydrocolloids*, n. 55, p. 47-55, 2016.

MORAES, J. O.; MULLER, C. M. O. ; LAURINDO, J. B. Influence of the simultaneous addition of bentonite and cellulose fibers on the mechanical and barrier properties of starch composite-films. *Food Science and Technology International*, v. 1, p. 23-28, 2012.

NGO, T. M.; DANG, T. M.; TRAN, T. X.; RACHTANAPUN, P. Effects of Zinc Oxide Nanoparticles on the Properties of Pectin/Alginate Edible Films. *International Journal of Polymer Science*, p. 1-9, 2018.

OLIVEIRA, S. P. L. F.; BERTAN, L. C.; DE RENSIS, C. M. V. B.; BILCK, A. P.; VIANNA, P. C. B.. Whey protein-based films incorporated with oregano essential oil. *Polímeros*, v.27(2), p.158-164, 2017.

PAIVA, E. P.; LIMA, M. S.; PAIXÃO, J. A. Pectina: Propriedades químicas e importância sobre a estrutura da parede celular de frutos durante o processo de maturação. *Revista Iberoamericana de Polímero*, v. 10, nº. 4, p. 196-211, 2009.

PAVLAK, M. C. M.; ZUNIGA, A. D.; LIMA, T. L. A.; ARÉVALO-PINEDO, A.; CARREIRO, S. C.; FLEURY, C. S.; SILVA, D. L. Aproveitamento da farinha do mesocarpo do babaçu (*Orbignya martiana*) para obtenção de etanol. *Evidência*, v.7, n.1, p. 7-24, 2007.

PEELMAN, N.; RAGAERT, P.; RAGAERT, K.; MEULENAER, B. D.; DEVLIEGHERE, F.; CARDON, L. Heat resistance of new biobased polymeric materials, focusing on starch, cellulose, PLA, and PHA. *Journal of Applied Polymer Science*, v. 132, 2015.

PHUPOKSAKUL, T.; LEAUNGSUKERK, M.; NUMPIBOONMARN, P.; SOMWANGTHARANOJ, A.; JANJARASSKUL, T. Properties of poly(lactide) – whey protein isolate laminated films. *Journal of Science Food and Agriculture*, v. 95. p. 715-721, 2015.

PEREIRA, R.; CARVALHO, A.; VAZ, D. C.; GIL, M. H.; MENDES, A.; BÁRTOLO, P. Development of novel alginate based hydrogel films for wound healing applications. *International Journal of Biological Macromolecules*, Vol. 52, p. 221-230, 2013.

PEREIRA, B. A. S. Flora nativa. In: Dias, B. F. S (Coord.). *Alternativas de desenvolvimento dos cerrados: conservação dos recursos naturais renováveis*. Fundação Pró-Natureza, Brasília, 1996. p.53-57.

RAMIREZ, M. M. Flora de palmeras de Bolivia. La Paz, ed. Universidad Mayor de San Andrés, 2004.

RAMOS, O. L.; FERNANDES, J.; DA SILVA, S. B.; PINTADO, M. E. Edible Films and Coatings from Whey Proteins: A Review on Formulation, and on Mechanical and Bioactive Properties. *Critical reviews in food science and nutrition*, v. 52, p. 533-552, 2012.

REZENDE, J. B. A.; LIMA, J.; MEIRA, F. M.; LIMA, P.; TENÓRIO, G.; et al.. Manejo de Caraná no Alto Tiquié. In: CABALZAR, Aloisio (Org.). *Manejo do mundo:*

conhecimento e práticas dos povos indígenas do Rio Negro, noroeste Amazônico. São Paulo: FOIRN & ISA, 2010.

RHIM, J. W.; NG, P. K. W. Natural biopolymer-based nanocomposite films for packaging applications. *Critical Reviews in Food Science and Nutrition*, Boca Raton, v. 47, n. 4, p. 411-433, 2007.

ROYAL INGREDIENTS, Papel e papelão. Disponível em <<http://www.royal-ingredients.com/pt/applications/paper-and-board>>. Acesso em: 24/04/19.

SANTANA, A. A.; KIECKBUSCH, T. G. Physical evaluation of biodegradable films of calcium alginate plasticized with polyols. *Brazilian Journal of Chemical Engineering*, v. 30, nº. 4, p. 835-845, 2013.

SANTANA, A. A.; DE OLIVEIRA, R. A.; PINEDO, A. A.; KUROZAWA, L. E., PARK, K. J. Microencapsulation of babassu coconut milk. *Food Science and Tehcnology*, Campinas, v. 33, n. 4, p. 737-744, 2013.

SANTANA, A.A.; MARTIN, L.G.P.; OLIVEIRA, R.A.; KUROZAWA, L.E.; PARK, K.J. Spray drying of babassu coconut milk using different carrier agents. *Drying Technology*, v. 35, p. 76-87, 2017.

SANTOS, A. E. F.; BASTOS, D. C.; DA SILVA, M. L. V. J.; THIRÉ, R. M. S. M.; SIMÃO, R. A. Chemical analysis of a cornstarch film surface modified by SF<sub>6</sub> plasma treatment. *Carbohydrate Polymers*, v. 87, p. 2217-2222, 2012.

SILVA, M. A.; BIERHALZ, A. C. K.; KIECKBUSCH, T. G. Influence of drying conditions on physical properties of alginate films. *Drying Technology: An International Journal*, v. 30, p. 72-79, 2012.

SILVA, R. M. et al. Características físico-químicas de amidos modificados com permanganato de potássio/ácido láctico e hipoclorito de sódio/ácido láctico. *Ciência e Tecnologia de Alimentos*, 28, p. 66-77, 2008.

SILVA, K. S.; MAURO, M. A.; GONÇALVES, M. P.; ROCHA, C. M. R. Synergistic interactions of locust bean gum with whey proteins: Effect on physicochemical and microstructural properties of whey protein-based films. *Food Hydrocolloids*, v. 54, p. 179-188, 2016.

SPIER, F.; ZAVAREZE, E. R. ; SILVA, R. M. E.; ELIAS, M. C.; DIAS, A. R. G. Effect of alkali and oxidative treatments on the physicochemical, pasting, thermal and morphological properties of corn starch. *Journal of the Science of Food and Agriculture*, v. 3, 2013.

STEINHOFF, B.; WANG, S.; ALIG, I. Uma análise da degradação do poli(ácido láctico) (PLA) induzida pelo processo de transformação, Revista Plástico Industrial, São Paulo, v. 11, n. 126, p. 78-83, 2009.

TAN, Z.; YI, Y.; WANG, H.; ZHOU, W.; YANG, Y.; WANG, C. Physical and Degradable Properties of Mulching Films Prepared from Natural Fibers and Biodegradable Polymers. Applied sciences, v. 6, p. 1-11, 2016.

THARANATHAN, R. N. Biodegradable films and composite coatings: past, present and future. Trends in Food Science & Technology, v. 14, n. 3, p. 71-78, 2003.

TOLVANEN, P.; MAKI-ARVELA, P.; SOROKIN, A. B.; SALMI, T.; MURZIN, D. Yu. Kinetics of starch oxidation using hydrogen peroxide as an environmentally friendly oxidant and an iron complex as a catalyst. Chemical Engineering Journal, 154, p.52-59, 2009.

TÔRRES, Y. J. S. S. Estudo da hidrólise enzimática do amido do mesocarpo de babaçu. 2014. 63 f. (Mestrado em Química) – Programa de Pesquisa e Pós-graduação em Química, Universidade Federal do Maranhão, São Luís, 2014.

VARTIAINEN, J.; VAHA-NISSI, HARLIN, A. Biopolymer Films and Coatings in Packaging Applications - A Review of Recent Developments. Materials Sciences and Applications, v. 5, p. 708-718, 2014.

VICENTINI, N. M.; CEREDA M. P. Uso de filmes de fécula de mandioca em conservação pós-colheita de pepino (*Cucumissativus* L.). Brazilian Journal of Food Technnology. v. 2, n. 1-2, p. 87-90, 1999.

VILLADIEGO, A. M. D.; SOARES, N. F. F.; ANDRADE, N. J.; PUSCHMANN, R.; MINIM, V. P. R.; CRUZ, R. Filmes e revestimentos comestíveis na conservação de produtos alimentícios. Revista Ceres, v. 52, nº. 300, p. 221-244, 2005.

VILLELA, G. G.; BACILA, M.; TASTALDI, H. Bioquímica. 4ª Ed. Rio de Janeiro: Guanabara Koogan, 1978.

WANG HONG-JIANG, SUN CHENG; HUANG LI-QIANG. Preparation and Properties of Whey Protein Packaging Film (Tianjin University of Science & Technology) Tianjin, China. 17th IAPRI- World Conference on Packaging- 2010.

**CAPÍTULO 2: CHARACTERIZATION OF PECTIN  
BIOFILMS WITH THE ADDITION OF BABASSU  
MESOCARP AND WHEY PROTEIN CONCENTRATE**

**Trabalho publicado na Revista *American Journal of Materials Science* em  
2017**

# Characterization of Pectin Biofilms with the Addition of Babassu Mesocarp and Whey Protein Concentrate

Lopes I. A.<sup>1</sup>, Santos Jr J.<sup>1</sup>, Da Silva D. C.<sup>1</sup>, Da Silva L. J. S.<sup>1</sup>, Barros A. K.<sup>2</sup>, Villa-Vélez H. A.<sup>1\*</sup>, Santana A. A.<sup>1</sup>

<sup>1</sup>Chemical Engineering Coordination, Federal University of Maranhão, São Luís, Brazil.

<sup>2</sup>Department of Electrical Engineering, Federal University of Maranhão, São Luís, Brazil.

**Abstract:** Biofilms are defined as flexible films prepared from biological materials with the potential for application in the pharmaceutical and food areas, their use depending on various parameters such as the mechanical properties, barrier properties and water solubility, amongst others. The present work aims to characterize pectin (P) biofilms composed of babassu mesocarp (BM) and whey protein concentrate (WPC), prepared by the casting method. Thus physical attributes such as moisture content, water soluble mass, thickness, water vapor permeability and degradation were determined. Fourier-transform infrared spectroscopy and scanning electron microscopy were used in order to determine the chemical composition and surface structure, respectively, of the biofilms. Calcium crosslinked and non-reticulated films were considered. The biofilms composed of 100%P and 50%P+50%WPC were more hygroscopic than those composed of 50%P+50%BM and 50%P+25%BM+25%WPC. The lowest water vapor permeability and solubility values were found for the films plasticized with 50%P+50%BM. The films plasticized with 50%P+50%BM and 50%P+25%BM+25%WPC showed very similar functional attributes regarding their application as food wrappings and/or production bags.

**Keywords** Babassu mesocarp, Casting method, Physical characterization, Whey protein concentrate, Glycerol

## 1. Introduction

Biofilms are natural polymers formed from biological, animal or vegetable materials such as microorganisms, lipids, proteins and polysaccharides. These materials, obtained from the growth of microorganisms or from animal protein and plants, are currently replacing the plastic materials synthesized from petroleum due to their environmental friendliness [1, 2]. Recently, the production of biofilms combining different polysaccharides, proteins and lipids has been the focus of research to improve their functionality (e.g., mechanical and barrier properties), showing synergistic advantages when compared with the pure components [3].

Pectin is an anionic polysaccharide widely used in the food industry due its high availability in citrus peels, with low extraction costs, high solubility, good gelling properties, high biocompatibility and simple modification by chemical and biochemical processes. In addition, pectin has great potential for use in the preparation of biofilms, as

food coverings and drug coating, amongst others [4, 5]. The characteristics of biofilms composed of pectin have been reported by Giancone et al., [6], where films made from high methoxyl pectin showed barrier properties comparable to commercial biodegradable film packaging and, according to Fishman et al., [7], where films made from mixtures of pectin/starch/plasticizer resulted in a very definite loss of brittleness of the film, making them much more flexible. Thus the physical, thermal and mechanical properties of pectin-based films, depends on the aggregated substances, such as plasticizers and emulsifiers, as well as the coverings used on the matrix.

Amongst the diversity of raw material that have been researched to produce biofilms, the babassu mesocarp and whey protein concentrate are two possible compounds that can be mixed with the filmogenic matrix containing pectin. The babassu (*Orbignyaphalerata* Mart.) mesocarp is produced during the separation of the babassu kernel, being widely marketed in the states of Maranhao, Piaui and Tocantins (Brazil) [8]. The dried babassu mesocarp flour is used as a substitute for cassava flour, and serves as food for both humans and animals [9], as well as in natural medicines for the treatment of multiple diseases [10-12]. Chemically, the babassu mesocarp flour contains 60% of starch (gelatinization temperature of the granules in the range from 63 to 73°C) [13] and a significant amylose content and its polymeric structure is highly crystalline, showing promising applications in the form of elastic matrices [14, 15]. On the other hand, the whey protein concentrate contains globular proteins such as  $\beta$ -lactoglobulin,  $\alpha$ -lactoalbumin and bovine serum albumin, presenting both thermo-reversible and thermo-irreversible gels when heated above 65-70°C, with wide applications for use in the food industry as an emulsifier [16]. Moreover, the emulsifying capacity depends on the composition of the matrix considered (e.g., ionic strength and pH), the processing to which it is submitted and the storage conditions that it experiences during its lifetime, e.g., heating, cooling, mechanical agitation [17, 18].

Both compounds show promising applications in the production of biofilms, since films prepared with pure pectin are completely soluble in water, besides having poor mechanical properties. Thus the combinations could provide new characteristics which should be researched. In addition, studies concerning the use of babassu and whey protein concentrate in the confection of biofilms have not been reported in the literature. Thus the present work aims to study the influence of the mixture of pectin/babassu mesocarp/whey protein concentrate, with added calcium chloride (crosslinking agent) and glycerol (plasticizing agent), on the chemical, barrier and mechanical properties of biofilms.

## **2. Material and Methods**

### **2.1. Raw Materials and Sample Preparation**

Citric pectin (P) (Isofar, Rio de Janeiro, Brazil), whey protein concentrate (WPC) (Alibra, Campinas, Brazil), anhydrous calcium chloride (Merck, Darmstadt, Germany), glycerol (Synth, São Paulo, Brazil) and babassu mesocarp (BM) were used in this research.

Babassu mesocarp (BM) was obtained from *in nature* coconut. The coconut was first peeled and the fiber and mesocarp extracted with a steel knife. The mesocarp was then milled in a ball mill (Model 460\*600, Yongsheng, China) and sieved through a No. 400 mesh screen (Tyler series, W.S. Tyler, USA) in order to obtain a powder with a diameter of 37  $\mu\text{m}$ . The chemical characteristics of the BM were determined according to the Standard Analytical Methods [19], obtaining values for moisture content of  $1.66\pm 0.03$  g/100g (w.b.), protein content of  $4.03\pm 0.58$  g/100g (w.b.), fat content of  $0.43\pm 0.10$  g/100g (w.b.), and ash content of  $2.34\pm 0.08$  g/100g (w.b.). The carbohydrate content was obtained by difference, obtaining a value of  $91.54\pm 0.08$  g/100g (w.b.).

### **2.2. Film Preparation**

Biofilms were prepared according to the methodology of Santana and Kieckbusch [20] with modifications. Citric pectin (P) together with babassu mesocarp (BM) and/or whey protein concentrate (WPC) and glycerol (3 ml) were dissolved in distilled water to a total volume of 200 ml, with constant magnetic stirring. After dissolution, 30 ml of the cross-linking solution was added and the temperature increased to 70°C. The cross-linking solution ( $\text{Ca}^{2+}$ ) was added slowly to the solution containing the citric pectin with babassu mesocarp and/or whey protein concentrate, using a peristaltic pump (model 77120-70, Masterflex, USA) with a maximum flow rate of 0.6 ml/min, to avoid local gelling. The films were obtained by the casting technique, i.e., aliquots of 50 g of the hot solution were poured into round Plexiglas pans (area = 172.03  $\text{cm}^2$ ) and slowly dried at 40°C in an oven with air recirculation (model 099EV, Fanem, Brazil) for 18 to 20 hours. The dried films were removed from the support and stored at 52% RH and 25°C for 48 hours. In all, four formulations were studied, 100%P, 50%P+50WPC, 50%P+50%BM and 50%P+25%BM+25%WPC.

### **2.3. Characterization of the Biofilms Film thickness**

The thickness of the biofilms ( $\delta$ ) was controlled by pouring a constant mass (50 g) into the film forming solution over the support. The thickness of the conditioned films was measured using a digital micrometer (model MDC-25S, Mitutoyo, Japan). Measurements were taken at five different positions on the film surface and the mean value reported.



### Moisture content

The moisture contents ( $w$ ) of the four formulations were determined in a vacuum oven (model MA030, Marconi, Brazil) at 60°C for 24 h using the gravimetric method AOAC 934.06 [19]. The analyses were carried out in triplicate and reported on a dry weight basis (d.b.).

### Matter dissolved in the water

The mass dissolved in the water ( $S$ ) was determined in triplicate according to the methodology proposed by Irissin-Mangata et al. [21]. The mass of a piece of film was determined and then immersed in 50 ml of distilled water under mild shaking action (175 rpm) at  $25 \pm 5^\circ\text{C}$  for 24 h, in an orbital controlled temperature shaker (model 3545-40-EA, Termo Fisher Sci Inc, USA). The sample was then transferred to a vacuum oven (60°C for 24 h) to determine the final dry matter. The soluble matter was expressed as a function of the initial dry matter according to Eq. (1):

$$S = \left[ \frac{m_i(1-w) - m_f}{m_i(1-w)} \right] \quad (1)$$

where  $w$  is the moisture content (d.b.),  $m_i$  is the initial mass and  $m_f$  is the final mass (g).

### Water vapor permeability

Water vapor permeability ( $WVP$ ) was determined using the ASTM E95-96 method [22] at 25°C in a small Plexiglas cell (25 ml) completely filled with calcium chloride granules in order to maintain the relative humidity (RH) of the system at 0%. The film was fitted tightly to the removable cell lid, covering a central rectangular opening (38.5 cm<sup>2</sup>). The cell was placed inside another hermetic Plexiglas jar ( $\approx 500$  ml) containing a saturated NaCl solution (Synth, São Paulo, Brazil) at the bottom, and submitted to intermittent agitation to keep the RH of the system at 75% and hence maintain a constant difference in water vapor pressure. After the system attained steady-state conditions ( $\approx 2$  h), the cell weight was measured every 12 h for 3 days using an analytical balance (model AP210, Ohaus, Switzerland) and the water vapor permeability [(g.mm)/(m<sup>2</sup>.day.kPa)] calculated from Eq. (2):

$$WVP = \left( \frac{G\delta}{A_e\Delta P_w} \right) F \quad (2)$$

where,  $\delta$  is the thickness of the film (mm),  $A_e$  is the area of the exposed surface of the film ( $m^2$ ),  $\Delta P_w$  is the partial water pressure difference across the film (kPa),  $G$  is the permeation rate (g/day) calculated by linear regression of the mass gain vs. time, and  $F$  is a correction factor that takes the additional diffusion resistance in the stagnant air gap between the surface of the calcium chloride layer and the film into account. In the geometry used, this correction was close to 1.0 and was therefore not considered [23].

### **Biodegradation test**

The biodegradation was determined according to the ASTM G160-98 method [24] under specified experimental conditions, breeding ground, soil pH between 6.5-7.5, relative humidity between 85-95%, temperature  $30 \pm 2^\circ C$  and analysis time of two weeks. Figure 1a shows a small packaging scheme of the test piece bodies. To determine the resistance to biodegradation, samples of each biofilm were weighed and placed in a container with mineral (ground), vegetable (grass) and animal (insect) matters, and exposed to the action of nature (living organisms, rain, wind and sun) (Figure 1b). After two weeks, samples were taken from the environment and weighed to determine the percent degradation ( $D$  %) according to Eq. (3):

$$D(\%) = \frac{m - m_i}{m_i} \times 100 \quad (3)$$

where  $m$  is the mass after the exposure time (g) and  $m_i$  is the initial mass of the sample (g).

### **2.4. Morphology**

Scanning electron microscopy (SEM) was employed to study the surface and cross-sectional morphologies of the biofilms produced. All the biofilms were dried in a vacuum oven at  $70^\circ C$  for 24 h and the samples mounted onto stubs, sputter coated with gold in a vacuum chamber and photographed (magnifications of x145, 265, 360, 620, 1,450, 3,100, 4,100 and 5,000) using the scanning electron microscope (model Phenom Pro, Phenom-World, Netherland) operated at 5 kV.

### **2.5. Fourier-transform Infrared Spectroscopy (FTIR)**

FTIR-ATR spectroscopy of the biofilms was carried out using a spectrometer (model IR-Prestige, Shimadzu, Japan) with 128 scans between  $400$  and  $5000 \text{ cm}^{-1}$  and  $4 \text{ cm}^{-1}$  resolution.

## 2.6. Statistical Analysis

All regressions were carried out using the Statistic V9 (Statsoft, Tulsa, USA) software. In addition, an analysis of variance and Tukey test were employed to determine any statistically significant differences ( $p < 0.05$ ) between the averages.

## 3. Results and Discussion

### 3.1. Biofilm Characterizations

Biofilms composed of pectin with the addition of babassu mesocarp and/or whey protein concentrate were formulated and prepared by the casting technique, obtaining the following four matrices 100%P, 50%P+50WPC, 50%P+50%BM and 50%P+25%BM+25%WPC. Visually, the 100%P and 50%P+50%WPC biofilms showed a slightly yellowish, translucent and homogeneous surface, flexible texture and were easily removed from the Plexiglas mold. On the other hand, the 50%P+50%BM and 50%P+25%BM+25%WPC biofilms showed a brown homogeneous surface and low flexibility as compared to the biofilms without BM (Fig. 2). Table 1 shows the filmogenic characteristics of thickness, moisture content, the matter dissolved in water, water vapor permeability and biodegradation data for the four formulations.

Table 1 shows that the biofilms composed of 100%P and 50%P+50%WPC showed thickness values ( $\delta$ ) that were 57% less than the biofilms composed of 50%P+50%BM and 50%P+25%BM+25%WPC. These results can be explained by the particle size of the babassu mesocarp of 37  $\mu\text{m}$ , this therefore being the minimum limit to forming a homogeneous biofilm. Moreover, the thickness of the films composed of the ternary mixture of 50%P+25%BM+25%WPC increased even more than the binary mixtures of P with BM and/or WPC. According to Silva et al. [5], this tendency at the macroscopic level can be attributed to an increase in molecular volume due to a more intense plasticizing effect at higher glycerol and citric pectin concentrations.

The moisture contents ( $w$ ) of the biofilms ranged from 6.30 to 7.41% (d.b.), the formulations with 100% pectin showing slightly higher moisture contents than the other formulations. This behavior was also observed by Bierhalz et al. [25] who attributed it to the high hydrophobicity of the pectin. For the other three formulations, the low moisture contents can be attributed to the intumescence power of the whey protein concentrate [26] and babassu mesocarp [13].

The water solubility (*S*) of the four formulations presented values between 51.12 and 73.98%. These values were higher than those reported by Silva et al. [5] of between 8.8 and 37.2%, by Seixas et al. [4] of between 32.88 and 51.98% and by Bierhalz et al. [25] of between 16.72 and 25.66, all for biofilms composed of pectin and alginate. In the present study, one can observe that the solubility decreased as the concentration of BM increased. This was because the BM promoted crosslinking of the polymer chains, and hence as the BM concentration increased, so the intermolecular bonds became more cohesive and organized in the matrix, making the biofilms more resistant to dissolution. Although high film solubility may be desirable in some applications, the low solubility of edible films is one of the most important requirements for food and pharmaceutical applications [3].

The water vapor permeability (*WVP*) ranged from 6.17 to 13.29 g.mm/m<sup>2</sup>.day.kPa for the four formulations, these values being similar to those found for biofilms composed of zein-oleic acids [27], high methoxyl pectin [6] and of PLA/nanoclay composite [28]. In general terms, the biofilms composed of citric pectin with BM presented moderate barriers to water vapor permeability. Also, the values found for *WVP* for the four formulations also exhibited an inverse relationship with the values for solubility (Table 1). This behavior can be attributed to the low level of reticulation with Ca<sup>2+</sup> in the formulations. Furthermore, for each type of formulation, the *WVP* increased with film thickness. In ideal homogeneous polymeric films, the permeability constants are independent of thickness. Water transport through hydrophilic films, however, is extremely complex due to non-linear moisture sorption isotherms and water content-dependent diffusivity [20, 29]. In the present study, the interfacial equilibrium with humid air promoted an incipient structure relaxation in the outer portion of the cross section of the film, increasing the permeation rate in this surface layer. The thicker film reduced the relative contribution of this layer to the total resistance and hence the *WVP* increased [20, 25].

**Figura 1** -Visual aspects of the four pectin biofilms with added babassu mesocarp and whey protein concentrate. (a) 100%P, (b), 50%P+50%WPC, (c) 50%P+50%BM (F3) and (d) 50%P+25%BM+25%WPC.

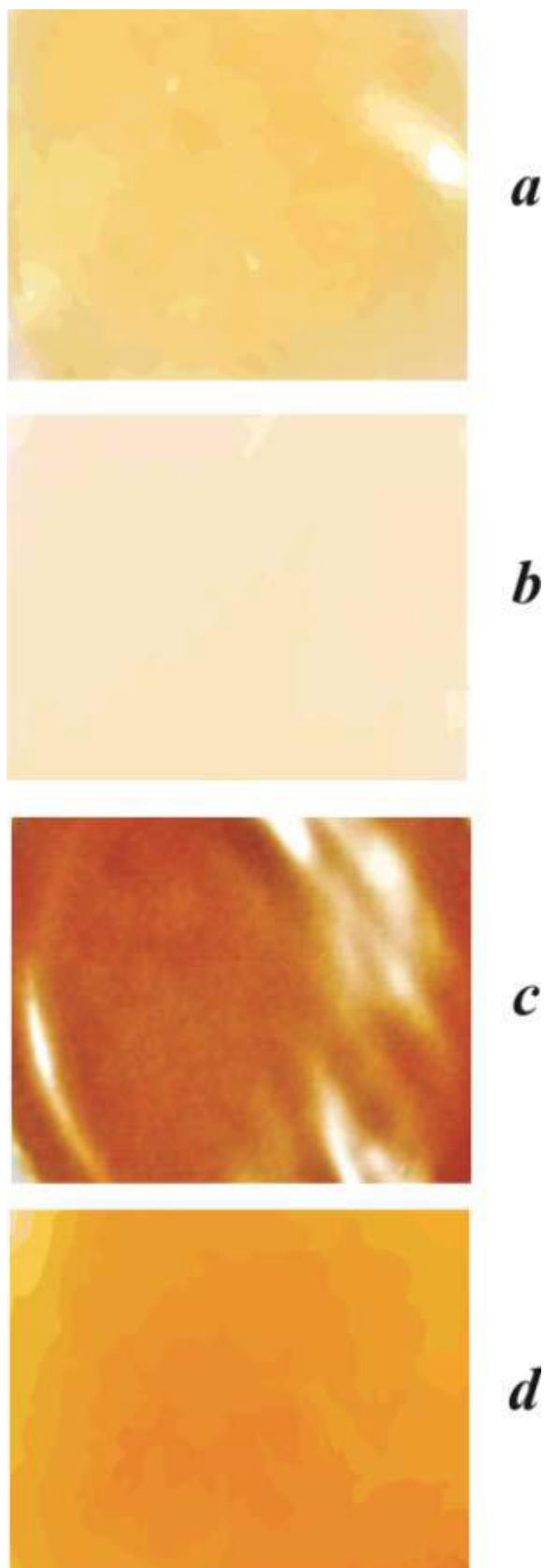


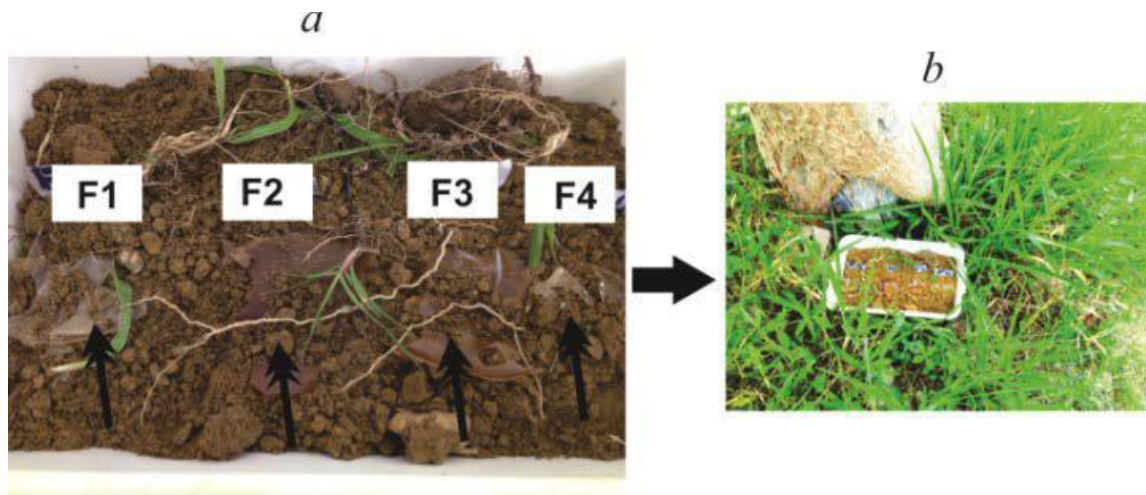
**Tabela 1** - Characterization of the biofilms made from the four formulations composed of citric pectin (P), babassu mesocarp (BM) and whey protein concentrate (WPC).

Biofilm formulation	$\delta$ (mm)	w (%, d.b.)	S (%)	WVP (gm/m <sup>2</sup> daykPa)	D (%)
100%P	0.22±0.01 <sup>b</sup>	7.41±0.33 <sup>b</sup>	73.98±0.04 <sup>c</sup>	11.52±0.11 <sup>c</sup>	100±0.02 <sup>a</sup>
50%P+50%WPC	0.16±0.01 <sup>a</sup>	7.06±0.68 <sup>ab</sup>	69.84±0.02 <sup>bc</sup>	13.29±1.66 <sup>d</sup>	100±0.02 <sup>a</sup>
50%P+50%BM	0.28±0.11 <sup>c</sup>	6.77±0.44 <sup>ab</sup>	51.12±0.30 <sup>a</sup>	6.17±0.49 <sup>a</sup>	100±0.03 <sup>a</sup>
50%P+25%BM+25%WPC	0.37±0.06 <sup>d</sup>	6.30±0.23 <sup>a</sup>	61.28±0.07 <sup>b</sup>	7.10±0.52 <sup>b</sup>	100±0.04 <sup>a</sup>

Means with the same letter in the same column indicate there is no significant difference ( $p < 0.05$ ) according to Tukey's Test.  $\delta$  is the thickness, w is the moisture content, S is the solubility of the matter in water, WVP is the water vapor permeability and D is the biodegradability.

The biodegradability test (D) showed complete biodegradation in the four biofilms. The degradation analysis was carried out for 7 days. During the first five days of monitoring, the weather was stable and the films suffered little degradation. However, on the last 2 days there was torrential rain and the films were completely biodegraded. This can be explained by the fact the natural macromolecules of the biofilms produced were formed of proteins and carbohydrates that are degradable in biological systems due to hydrolysis followed by oxidation. On the other hand, not all the biofilms were completely solubilized, since the action of the rain accelerated the biodegradation process. Furthermore, the films were also attacked by insects and microorganisms, which removed some of the biodegradable components. According to Tripathi et al. [30] and Chandra and Rustgi [1], during the biodegradation process in the soil, the amorphous fraction of the material is exposed to attack by microorganisms and the microbial degradation results in an increase in the degree of crystallinity of the biofilms.

**Figura 2** - Biodegradation analysis: (a) Biofilm packaging composed of 100%P (F1), 50%P+50%WPC (F2), 50%P+50%BM (F3) and 50%P+25%BM+25%WPC (F4) and, (b) biofilms in the natural environment.

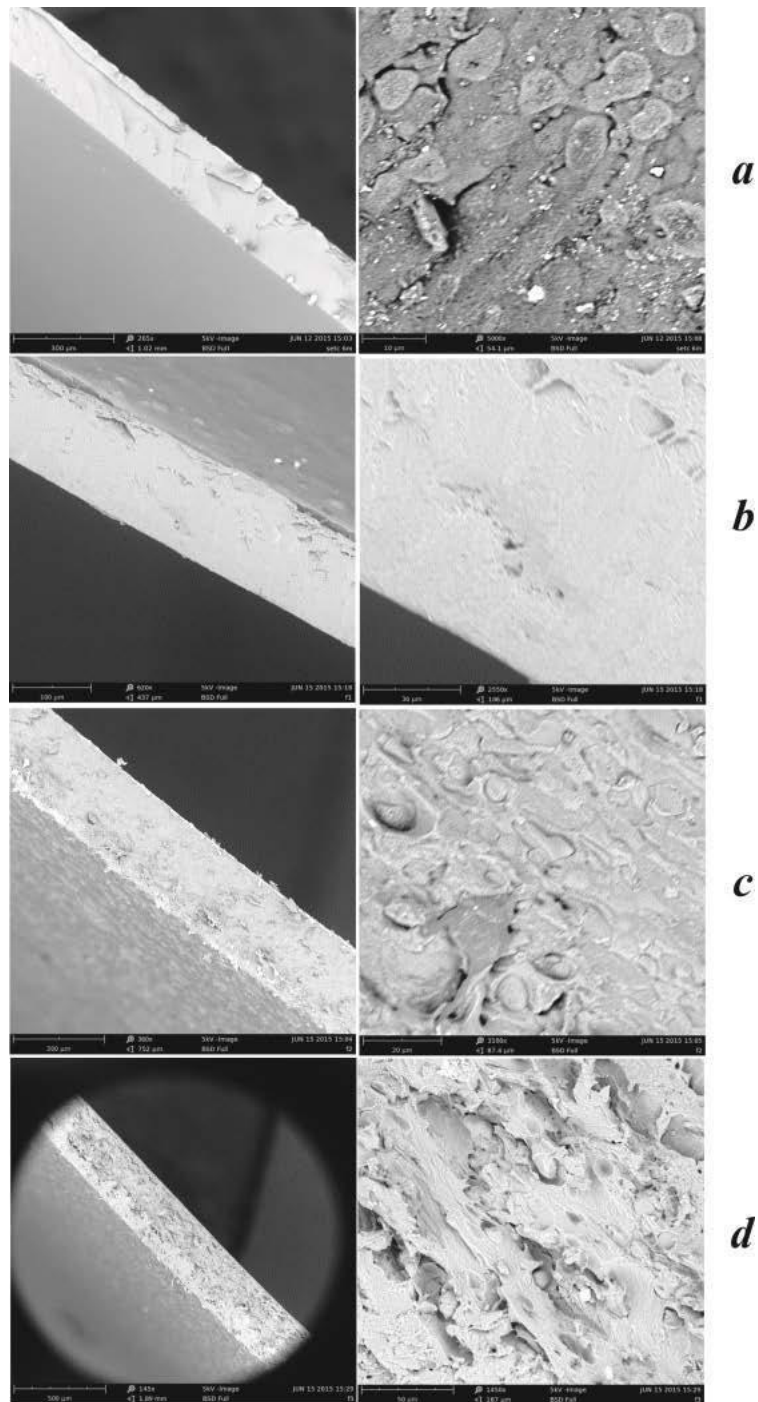


### 3.2. Morphology Results

Cross sectional images of the biofilms composed of 100%P and 50%P+50%WPC show a continuous and compact filmogenic matrix. Fig. 3 shows the formation of lumps on the surface of the biofilms composed of 100%P, a characteristic attributed to the gelling process of the pectin and the roughness of the surface. Moreover, as can be seen from the physical characterization, this formulation showed greater dissolution in water. A study by Cavallaro et al., [31] showed the peculiar effect on the wettability of the biomaterial generated by biofilms based on pectin/polyethylene glycol, which was ascribed to the increase in surface roughness, as confirmed by the SEM analyses, showing the surface to be very rough with many craters (size of ca. 2  $\mu\text{m}$ ).

Biofilms composed of 50%P+50%WPC showed micrographs with a homogeneous surface. In some areas, the surfaces presented small fragmentations and a sponge-like structure. The cross-sectional morphology was also smooth and jellylike in these films, although an incipient stratification could be identified. Similar results were reported by Fang et al. [32] for biofilms prepared with WPC+20% glycerol. These authors showed that the addition of  $\text{Ca}^{2+}$  caused greater protein aggregation in the biofilm, marked by the irregular but continuous surface. The cross-section revealed a sponge-like structure, in which the whey protein aggregates appeared to be bound by fine wires to form a continuous web. The existence of the net was reflected in the increase in tensile strength of this film.

**Figura 3** -shows the SEM images for the formulations 100%P, 50%P+50%WPC, 50%P+50%BM and 50%P+25%BM+25%WPC, respectively.



The biofilms composed of 50%P+50%BM and 50%P+25%BM+25%WPC were shown to be brown and have a voluminous appearance, due to the presence of the babassu mesocarp, which has a brown color. However, both formulations showed a homogeneous,



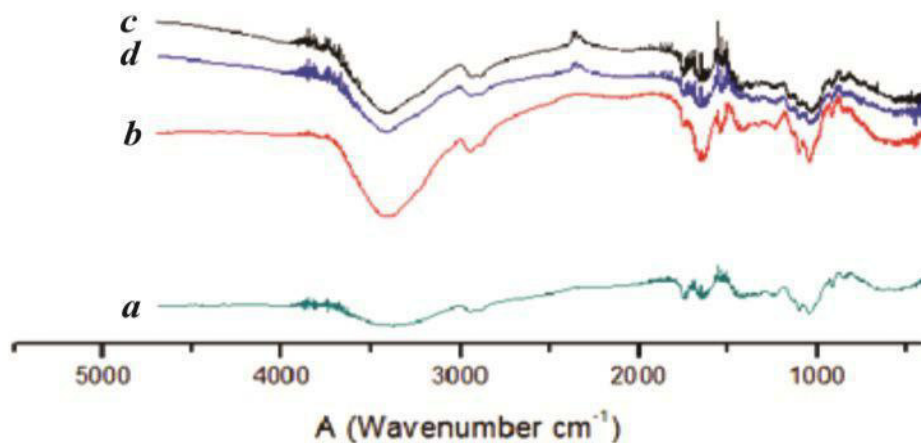
continuous and uniform aspect. The micrographs of the films with BM showed an intense formation of blocks on the surface, as well as in the cross section, due to the low solubility of the BM. This confirms the observation made from the visual aspect of the film. The blocks distributed over the surface impart the feeling of roughness and the bulky cross section, with an undulated fractured conformation which differs considerably from the well-aligned arrangement of the 50%P+50%WPC films. In general terms, the biofilms with BM in their composition showed an increase in roughness of the surface. They also became more flexible and consequently less resistant to tension, with lower permeability to water vapor since the area displayed became relatively greater. According to Arzate-Vásquez et al. [33], a strong film must have a more compact cross section.

### **3.3. Fourier-transform Infrared Spectroscopy (FTIR)**

The FTIR-ATR spectra obtained for the different biofilms can be seen in Figure 4. The characteristic pectin peaks can be observed at around 3400, 2900, 1700, and 1050  $\text{cm}^{-1}$ , attributed to the O-H,  $\text{COO}^-$  (asymmetric),  $\text{COO}^-$  (symmetric) and C-O-C stretching of the biopolymers, respectively. The peaks in the 1700 – 500  $\text{cm}^{-1}$  region corresponded to several vibrations of the carbohydrate ring [34].

A decrease in the overall absorbance in the 3290  $\text{cm}^{-1}$  region can be visualized for the formulation 50%P+50%BM. This peak appeared to be due to O-H stretching vibrations, associated with polar interactions between film components and unbound water present in the biofilms. The babassu mesocarp with pectin, together with calcium, promotes an increase in intermolecular hydrogen bonding on the polymer, and consequently, the decrease in intensity of this O-H peak can be related to a reduction in polymer-water interactions and moisture absorption [35]. This behavior is consistent with the moisture content, matter dissolved in water and water vapor permeability observed for the formulation 50%P+50%BM. Furthermore, the presence of WPC with BM and P also promoted shifts in the wave numbers of asymmetric and symmetric  $\text{COO}^-$  vibrations. For a possibly asymmetric  $\text{COO}^-$  peak, the wave numbers were 3002, 2998, 3000 and 3000  $\text{cm}^{-1}$  for the biofilms 100%P, 50%P+50%WPC, 50%P+25%BM+25%WPC and 50%P+50%BM, respectively. Thus the possibly symmetric vibration occurred at 2400  $\text{cm}^{-1}$  for all the formulations.

**Figura 4** - FTIR-ATR spectra of the four biofilm formulations. (a) 100%P, (b), 50%P+50%WPC, (c) 50%P+50%BM (F3) and (d) 50%P+25%BM+25%WPC.



Maniglia and Tapia-Blácido [14] studied the FIRT spectra of starch and fibers from babassu mesocarp, showing a high crystallinity index of the starches and the corresponding fiber residues. Since starch was the main component in these materials, the crystallinity index was mainly related to this structure, suggesting that the functional properties of the starch from babassu mesocarp could make it suitable for application as a food ingredient and in biodegradable film production.

#### 4. Conclusions

Biofilms prepared by blending pectin with babassu mesocarp and whey protein concentrate presented improved properties when compared to the films prepared from the pure polymers. The composite biofilms composed of 100%P and 50%P+50%WPC showed translucent and homogeneous appearances. Moreover, the biofilms prepared with 50%P+50%BM and 50%P+25%BM+25%WPC presented similar structures, confirming the strong presence of BM in the formulation, making a stronger and more compact biofilm. In the present study a filmogenic solution composed of 50%P+50%BM with the addition of glycerol (3%, v/v) and CaCl<sub>2</sub> (1% m/v) showed the best characteristics amongst the four biofilm formulations.

## ACKNOWLEDGEMENTS

The authors are grateful to the central analytical laboratory of CCET/UFMA and to Professors Arão Pereira da Costa Filho and Maria da Gloria Almeida Bandeira for offering their laboratories for the experimental procedures.

## REFERENCES

- [1] Chandra, R. and Rustgi, R., 1998, Biodegradable polymers. *Progress in Polymer Science*, 23(7), 1273-1335.
- [2] Lee, S. Y., 1996, Bacterial polyhydroxyalkanoates. *Biotechnology and Bioengineering*, 49(1), 1-14.
- [3] García, M. A., Pinotti, A., Martino, M. N., and Zaritzky, N. E., 2004, Characterization of composite hydrocolloid films. *Carbohydrate Polymers*, 56(3), 339-345.
- [4] Seixas, F. L., Turbiani, F. R. B., Salomão, P. G., Souza, R. P., and Gimenes, M. L., 2013, Biofilms composed of alginate and pectin: effect of concentration of crosslinker and plasticizer agents. *Chemical Engineering Transactions*, 23, 1693-1698.
- [5] Silva, M. A., Bierhalz, A. C. K., and Kieckbusch, T. G., 2009, Alginate and pectin composite films crosslinked with  $Ca^{2+}$  ions: Effect of the plasticizer concentration. *Carbohydrate Polymers*, 77(4), 736-742.
- [6] Giancone, T., Torrieri, E., Di Pierro, P., Cavella, S., Giosafatto, C. V. L., and Masi, P., 2011, Effect of Surface Density on the Engineering Properties of High Methoxyl Pectin-Based Edible Films. *Food and Bioprocess Technology*, 4(7), 1228-1236.
- [7] Fishman, M. L., Coffin, D. R., Onwulata, C. I., and Konstance, P., 2004, Extrusion of pectin and glycerol with various combinations of orange albedo and starch. *Carbohydrate Polymers*, 57(4), 401-413.
- [8] Silva, M. V. V., Sales, J. F., Silva, F. G., Rubio-Neto, A., Alberto, P. S., and Pereira, F. D., 2012, The influence of moisture on the vitro embryogeneration and morphogenesis of babassu (*Orbignya Phalerata* Mart.). *Acta Scientiarum Agronomy*, 34, 453-458.
- [9] Carneiro, A. P. M., Pascoal, L. A. F., Watanabe, P. H., Santos, B., Lopes, J. M., and Arruda, J. C. B., 2009, Farelo de babaçu em rações para frangos de corte na fase final:

desempenho, rendimento de carcaça e avaliação econômica. *Ciência Animal Brasileira*, 10(1), 40-47.

- [10] Pinheiro, M. M. G., Boylan, F., and Fernandes, P. D., 2012, Antinociceptive effect of the *Orbignyaspiciosa* Mart. (Babassu) leaves: Evidence for the involvement of apigenin. *Life Sciences*, 91(9–10), 293-300.
- [11] de Souza, P. A. V. R., Palumbo Jr, A., Alves, L. M., de Souza, P., Cabral, L. M., Fernandes, P. D., Takiya, C. M., Menezes, F. S., and Nasciutti, L. E., 2011, Effects of a nanocomposite containing *Orbignyaspiciosa* lipophilic extract on Benign Prostatic Hyperplasia. *Journal of Ethnopharmacology*, 135(1), 135-146.
- [12] Rego, T. J. A., *Fitogeografia das plantas medicinais no Maranhão*. 1. Ed. São Luís (MA): EDUFMA, vol. 1, 1995.
- [13] Cinelli, B. A., López, J. A., Castilho, L. R., Freire, D. M. G., and Castro, A. M., 2014, Granular starch hydrolysis of babassu agroindustrial residue: A bioprocess within the context of biorefinery. *Fuel*, 124, 41-48.
- [14] Maniglia, B. C. and Tapia-Blácido, D. R., 2016, Isolation and characterization of starch from babassu mesocarp. *Food Hydrocolloids*, 55, 47-55.
- [15] Baruque Filho, E. A., Baruque, M. d. G. A., and Sant'Anna Jr, G. L., 2000, Babassu coconut starch liquefaction: an industrial scale approach to improve conversion yield. *Bioresource Technology*, 75(1), 49-55.
- [16] Kinsella, J. E. and Whitehead, D. M., "Proteins in Whey: Chemical, Physical, and Functional Properties", in *Book* "Proteins in Whey: Chemical, Physical, and Functional Properties", E.K. John, Editor. 1989, Academic Press. p. 343-438.
- [17] Demetriades, K., Coupland, J. N., and McClements, D. J., 1997, Physical Properties of Whey Protein Stabilized Emulsions as Related to pH and NaCl. *Journal of Food Science*, 62(2), 342-347.
- [18] McClements, D. J. and Keogh, M. K., 1995, Physical properties of cold-setting gels formed from heat-denatured whey protein isolate. *Journal of the Science of Food and Agriculture*, 69(1), 7-14.
- [19] AOAC, "Official methods of analysis". 2007, AOAC International: Gaithersburg.

- [20] Santana, A. A. and Kieckbusch, T. G., 2013, Physical evaluation of biodegradable films of calcium alginate plasticized with polyols. *Brazilian Journal of Chemical Engineering*, 30, 835-845.
- [21] Irissin-Mangata, J., Bauduin, G., Boutevin, B., and Gontard, N., 2001, New plasticizers for wheat gluten films. *European Polymer Journal*, 37(8), 1533-1541.
- [22] ASTM, "Standard test method for water vapor transmission of materials". 1995, ASTM International: West Conshohocken.
- [23] McHugh, T. H., Avena-Bustillos, R., and Krochta, J. M., 1993, Hydrophilic Edible Films: Modified Procedure for Water Vapor Permeability and Explanation of Thickness Effects. *Journal of Food Science*, 58(4), 899-903.
- [24] ASTM, "Standard practice for evaluating microbial susceptibility of nonmetallic materials by laboratory soil burial". 1998, ASTM International: West Conshohocken.
- [25] Bierhalz, A. C. K., da Silva, M. A., and Kieckbusch, T. G., 2012, Natamycin release from alginate/pectin films for food packaging applications. *Journal of Food Engineering*, 110(1), 18-25.
- [26] Bernard, C., Regnault, S., Gendreau, S., Charbonneau, S., and Relkin, P., 2011, Enhancement of emulsifying properties of whey proteins by controlling spray-drying parameters. *Food Hydrocolloids*, 25(4), 758-763.
- [27] Pena-Serna, C. and Lopes-Filho, J. F., 2013, Influence of ethanol and glycerol concentration over functional and structural properties of zein-oleic acid films. *Materials Chemistry and Physics*, 142(2-3), 580-585.
- [28] Rhim, J.-W., Hong, S.-I., and Ha, C.-S., 2009, Tensile, water vapor barrier and antimicrobial properties of PLA/nanoclay composite films. *LWT - Food Science and Technology*, 42(2), 612-617.
- [29] Schwartzberg, H. G., "Modelling of gas and vapour transport through hydrophilic films", in *Book "Modelling of gas and vapour transport through hydrophilic films"*, M. Mathlouthi, Editor. 1986, Elsevier Science Publishing Co.: New York. p. 115-135.
- [30] Tripathi, S., Mehrotra, G. K., and Dutta, P. K., 2010, Preparation and physicochemical evaluation of chitosan/poly (vinyl alcohol)/pectin ternary film for food-packaging applications. *Carbohydrate Polymers*, 79(3), 711-716.

- [31]Cavallaro, G., Lazzara, G., and Milioto, S., 2013, Sustainable nanocomposites based on halloysite nanotubes and pectin/polyethylene glycol blend. *Polymer Degradation and Stability*, 98(12), 2529-2536.
- [32]Fang, Y., Tung, M. A., Britt, I. J., Yada, S., and Dalgleish, D. G., 2002, Tensile and Barrier Properties of Edible Films Made from Whey Proteins. *Journal of Food Science*, 67(1), 188-193.
- [33]Arzate-Vázquez, I., Chanona-Pérez, J. J., Calderón-Domínguez, G., Terres-Rojas, E., Garibay-Febles, V., Martínez-Rivas, A., and Gutiérrez-López, G. F., 2012, Microstructural characterization of chitosan and alginate films by microscopy techniques and texture image analysis. *Carbohydrate Polymers*, 87(1), 289-299.
- [34]Papageorgiou, S. K., Kouvelos, E. P., Favvas, E. P., Sapalidis, A. A., Romanos, G. E., and Katsaros, F. K., 2010, Metal–carboxylate interactions in metal–alginate complexes studied with FTIR spectroscopy. *Carbohydrate Research*, 345(4), 469-473.
- [35]Tapia-Blácido, D. R., Sobral, P. J. A., and Menegalli, F. C., 2010, Potential of *Amaranthus cruentus* BRS Alegria in the production of flour, starch and protein concentrate: chemical, thermal and rheological characterization. *Journal of the Science of Food and Agriculture*, 90(7), 1185-1193.

## **CAPÍTULO 3: PHYSICAL PROPERTIES OF FILMS BASED ON PECTIN AND BABASSU COCONUT MESOCARP**

**Trabalho publicado na Revista *International Journal of Biological  
Macromolecules* em 2019**

# Physical properties of films based on pectin and babassu coconut mesocarp

Da Silva, D. C.<sup>1</sup>; Lopes, I. A.<sup>1</sup>; Da Silva, L. J. S.<sup>1</sup>; Lima, M. F.<sup>1</sup>; Barros Filho, A. K. D.<sup>2</sup>; Villa-Vélez, H. A.<sup>1</sup>; Santana, A. A.<sup>1\*</sup>

<sup>1</sup> Faculty of Chemical Engineering, Federal University of Maranhão (UFMA), Avenida dos Portugueses, 1966, Bacanga, São Luís – MA, 65080-805, Brazil

<sup>2</sup> Faculty of Electrical Engineering, Federal University of Maranhão (UFMA), Avenida dos Portugueses, 1966, Bacanga, São Luís – MA, 65080-805, Brazil

## Abstract

The objective of this research was to study the physical properties, water sorption, thermal and structure of films made from citrus pectin (*CP*), babassu coconut mesocarp (*BCM*) and glycerol (*G*). Seventeen formulations were prepared according to a central compound rotational design combining different proportions of the materials and evaluating the films produced according to their moisture contents, solubility, thicknesses and water vapor permeability. The results showed a direct relationship between the composition of the film and each physical property, providing films with unique mechanical characteristics and barrier properties. In the second phase, the films were reformulated, maintaining the proportions of *CP* and *BCM* constant and altering the *G* content. The results showed films with permeable structures, thus favoring the use of high drying temperatures (up to 70 °C) for the confection of films, without altering their physical and structural properties.

**Keywords:** biodegradable films; babassu coconut mesocarp; mathematical modelling; drying.

## 1. Introduction

Research concerning biodegradable films of biofilms is an important area of study for the food, chemical and pharmaceutical industries [1, 2]. The casting method, commonly used to prepare biofilms, is a simple process whereby a filmogenic solution is first prepared and subsequently dried on an appropriate surface [3], allowing for the use of a wide range of materials of vegetable origin such as starches [2], amongst others. Between these materials, the babassu coconut mesocarp is a promise material studied as a raw material for ethanol production [4], thin film for application in electrochemical sensors [5] and bioactive film



[6, 7], showing great versatility for its technification and encourage the creation of local industries.

In order to elaborate these films, the interactions between the structural and plasticizer components must be studied in order to evaluate the cohesive and functional properties [8, 9]. This is important since the nature of biofilms, which is rigid and friable, causes limitations to their industrial applications, since it is well known that the mechanical properties of packaging films of synthetic origin are significantly better than those of edible origin [10]. Thus glycerol is the most widely used of the plasticizers in the elaboration of biofilms, so as to satisfy the mechanical property demands for packaging. Glycerol is becoming an attractive plasticizer, since it is a residue of the biodiesel industry produced in large amounts, and currently there are no applications for its use in large amounts [11, 12].

Amongst the different processes used in the preparation of biofilms, drying is one of the most important, since it is considered to be the process which most limits the final characteristics of biofilms [10, 13]. The impact of this process on edible films has been little studied, whereas it has been widely studied for thin films [14], particularly the effect of plasticizers on the moisture migration behavior of biofilms, which is based on the study of the diffusion rates and their relationship with the composition of the filmogenic solution [13, 15, 16].

It is also important to understand the relative importance of the different mechanisms that control moisture transfer through hygroscopic films, in order to project new films with improved and more selective barrier and mechanical properties. Consequently, the equilibrium properties and the kinetics of water transfer through the packaging material are of great importance. The selection of an appropriate mathematical model of the sorption behavior is a difficult task, due to the complex chemical composition and structure of biomaterials [17-19].

Thus the objective of this research was to study the physical, thermal, tensile strength, water sorption and structural properties of biofilms made from pectin and babassu coconut mesocarp, offering an ample study of the processing conditions, complemented by other research carried out with a starch matrix and babassu mesocarp powder.

## **2. Material and methods**

### **2.1. Raw materials**

The following raw materials were used: low methylesterified citrus pectin (Cpkelco, Limeira, Brazil), dihydrated calcium chloride (Merck, Darmstadt, Germany), glycerol (Synth, Diadema, Brazil), and babassu coconut (*Orbignya phalerata* Mart.) mesocarp powder with a moisture content of  $1.9\pm 0.1$  (g/100g, w.w.b.), ash content of  $2.34\pm 0.77$  (g/100g, w.w.b.), as determined by AOAC methods 926.12 and 900.02 respectively [20], and mean diameter ( $D_p$ ) of  $5330,867\pm 1980,585$  nm (determined by photon correlation spectroscopy using a dynamic light scattering ZetaPlus equipment (model 90Plus/BI-MAS, Brookhaven Instruments Corporation, USA) at wavelength of 625 nm, 25 °C and incidence angle of 90°), extracted manually from the whole fruit for use as the main matrix in biofilm manufacture.

### **2.2. Film preparation and experimental design**

The films were elaborated using the casting technique with modifications [3] by way of a central compound rotational design (CCRD) (Box et al., 1978), the variables being the citrus pectin (*CP*) mass, the babassu coconut mesocarp powder (*BCM*) mass and the glycerol (*G*) volume (see Table 1). A total of 17 films were prepared (8 factorial points, 6 axial points and 3 central points), where the different proportions of *CP*, *BCM* and *G* were dissolved in distilled water to give a total volume of 200 mL with constant stirring. After homogenization, 30 mL of the reticulating agent (dihydrated calcium chloride) were slowly added (with constant stirring) and the temperature increased to 70 °C

until the filmogenic matrix jellified. Having obtained the filmogenic solution, 50 mL volumes were poured over the surfaces of glass Petri dishes (diameter = 15 cm) and dried in an incubator with air circulation (Nova Técnica, model 400-1ND, Brazil) at 40 °C for 24 hours. Finally the films were removed from the plates and stored in desiccators, with the relative humidity controlled at 52%.

### **2.3. Characterization of the biofilms**

The 17 film formulations were first characterized by the tests for moisture content, water solubility, thickness and water vapor permeability. Based on the best physical characteristics of the formulations, two films were reformulated and the same analyses repeated plus the analyses of the grammage, sorption isotherms, drying kinetics, scanning microscopy and water sorption of the films.

### 2.3.1 Determination of the moisture content

The moisture content was determined by way of the AOAC 926.12 gravimetric method [20] using a vacuum oven at 105 °C for 24 h, and expressed as a fraction of the mass according to Eq. (1).

$$\omega = \left( \frac{m_i - m_f}{m_i} \right) \times 100 \quad (1)$$

where  $\omega$  is the moisture content (g/100g, w.w.b.),  $m_i$  is the initial mass of the material (g), and  $m_f$  is the final mass of the dry material (g).

### 2.3.2. Water solubility

The water solubility of the films ( $S$ , g/100g, w.w.b.) was determined according to the methodology of Gontard et al. (1992), as represented by Eq. (2).

$$S = \left( \frac{m_i - m_f}{m_i} \right) \times 100 \quad (2)$$

For this purpose, the initial mass ( $m_i$ , g) of the film sample was quantified after immersion in 50 mL of distilled water, with stirring (175 rpm) at 25 °C for 24 h, using an orbital shaker (Tecnal, model TE-145, Brazil). The diluted solutions were then dried in an incubator with air circulation to determine the final mass of the dry material ( $m_f$ , g).

### 2.3.3. Thickness

The thickness ( $\delta$ , mm) of the films was determined as the arithmetic mean of ten points measured at random on the surface of the biofilm using a digital micrometer with a resolution of 0.001 mm (Mitutoyo, model MDC-25S, Japan). These measurements were obtained after a conditioning period at 25 °C with a relative humidity of 52%.

### 2.3.4. Water vapor permeability

The water vapor permeability [ $WVP$ , (g.mm)/(m<sup>2</sup>.day.kPa)], was determined according to the ASTM norm [21]. Thus the film was fixed in an acrylic cell at 25±1 °C. The bottom of the cell was filled with granulated calcium chloride (Ecibra, São Paulo, Brazil) to maintain the relative humidity at 0 %. This cell was placed inside another acrylic recipient, which was hermetically sealed and contained a saturated NaCl solution (Synth, Diadema, Brazil) at the bottom to maintain the environment with a relative humidity of 74 %, thus obtaining a constant difference in the water vapor pressure ( $\Delta P_{\omega}$ , kPa). The increase in total mass of the cell, which was monitored with time (for about 72 hours), corresponded to the rate the

water permeated through the film ( $\varphi$ , g/day) and was introduced into Eq. (3) to calculate the WVP.

$$WVP = \left( \frac{\varphi \delta}{A_e \Delta P_w} \right) F \quad (3)$$

where  $A_e$  is the area of the film surface exposed ( $m^2$ ),  $\varphi$  is the angular coefficient of the straight line drawn through the experimental points on a graph of mass versus time (g/day).  $F$  is a correction factor which takes into account the additional resistance to the transfer of a mass of water vapor through a film stagnated with air between the surface of the calcium chloride layer and the film (Santana and Kieckbusch, 2013). For the methodology used, this correction was very close to 1.0 and was not considered.

### 2.3.5. Grammage

The grammage was determined according to Sobral (2000) by weighing a defined area of the biofilm on an analytical balance and using Eq. (4).

$$\varepsilon = 100000 \left( \frac{m}{A} \right) \quad (4)$$

where  $\varepsilon$  is the grammage ( $g/m^2$ ),  $m$  is the weight of the film (g) and  $A$  is the area of the film ( $cm^2$ ).

### 2.3.6. Mechanical properties

The tensile strength ( $TS$ , MPa), the elongation at break ( $E$ , %) and the elasticity modulus ( $EM$ , MPa) were directly determined for both formulations (through six samples of  $10 \times 2.5$  cm) in a universal testing machine (model XLW(B), Labthink, USA) at temperature of  $25 \pm 1$  °C and relative humidity of  $55 \pm 3\%$ , following the standard method D-882 of the ASTM International [22]. Results of the stress-strain curves and tensile properties calculations were determined by the machine software.

### 2.3.7. Color measurements

Color analyzes were performed on a CR-5 (Konica Minolta, Ramsey, New Jersey, USA) colorimeter with a  $10^\circ$  observer and D65 illuminant, measuring the parameter  $L$  (brightness) and chromatic coordinates  $a$  ( $+a$  = red;  $-a$  = green), and  $b$  ( $+b$  = yellow,  $-b$  = blue). These parameters were used to calculate the color saturation ( $C$ ) and the chromatic hue angle ( $h^\circ$ ) according to the Eqs. (5) and (6).

$$C = \sqrt{a^2 + b^2} \quad (5)$$

$$h^o = \operatorname{tg}^{-1}\left(\frac{b}{a}\right) \quad (6)$$

### 2.3.8. Sorption isotherms

The sorption isotherms of the films were studied in order to evaluate the bonding capacity of the films at a specific water activity ( $a_w$ , non-dimensional) [23, 24]. The equilibrium moisture contents of the samples were determined by the static gravimetric method using saturated salt solutions (LiCl, CH<sub>3</sub>COOK, MgCl<sub>2</sub>, KI, K<sub>2</sub>CO<sub>3</sub> and NaCl) in the water activity ( $a_w$ ) range from 0.111 – 0.753 [25]. The triplicate samples were placed in 10 mL filter weights each containing approximately 0.5 g of material. The filter weights were placed in supports inside hermetically sealed plastic pots containing the saturated salt solutions at the bottom, and stored in B.O.D. incubators (SPLabor, model SP-500) maintained at 25 °C. The samples were weighed on an analytical balance at 5-day intervals, to constant weight. The equilibrium moisture content was determined in an incubator at 105 °C for 24 hours.

The following theoretical models were used to fit the desorption isotherms: GAB (Eq. (7)) and BET (Eq. (8)), and also the following empirical models: Oswin (Eq. (9)), Halsey (Eq. (10)), Henderson (Eq. (11)) and Chung-Pfost (Eq. (12)) [26, 27].

$$X_e = \frac{X_m C K a_w}{(1 - K a_w) [1 + (C - 1) + K a_w]} \quad (5)$$

$$X_e = \frac{X_m C a_w}{(1 - a_w) [1 + (C - 1) a_w]} \quad (8)$$

$$X_e = a \left( \frac{a_w}{1 - a_w} \right)^b \quad (9)$$

$$X_e = \left( \frac{-a}{\ln a_w} \right)^{\frac{1}{b}} \quad (10)$$

$$X_e = \left( \frac{-\ln(1 - a_w)}{a} \right)^{\frac{1}{b}} \quad (11)$$

$$X_e = a + b(\ln a_w) \quad (12)$$

Where  $X_e$  is the equilibrium moisture content (kg/kg, d.w.b.),  $X_m$  is the equilibrium moisture content of the monolayer (kg/kg, d.w.b.),  $C$  and  $K$  are parameters of the GAB and BET models (non-dimensional), and  $a$  and  $b$  are the parameters of the empirical models (non-dimensional) (Rizvi, 2005).

### 2.3.9. Drying kinetics

The drying kinetics were studied by taking fragments of the films elaborated, drying them in a convective air incubator (Pardal, model PE14, Brazil) at temperatures of 50, 60 and 70 °C, and weighing at pre-defined intervals to constant weight. The final moisture content of the films was determined at the end of the drying process, the kinetic results being represented as a function of the moisture content on a dry weight basis. The kinetic models of Weibull (Eq. (13)), Peleg (Eq. (14)), Logarithmic (Eq. (15)), Lewis (Eq. (16)), Page (Eq. (17)), Midilli (Eq. (18)), Two terms (Eq. (19)) and Diffusion approach (Eq. (20)) were used to model and simulate the behavior of the drying kinetics of the films at the different temperature levels [28-31].

$$X = X_e + (X_0 - X_e) \exp\left(-\frac{t}{k_1}\right) \quad (13)$$

$$X = X_0 - \left(\frac{t}{k_1 + k_2 t}\right) \quad (14)$$

$$X = X_e + (X_0 - X_e) k_1 \times \exp(-k_2 t) + k_3 \quad (15)$$

$$X = X_e + (X_0 - X_e) \exp(-k_1 t) \quad (16)$$

$$X = X_e + (X_0 - X_e) \exp(-k_1 t^{k_2}) \quad (17)$$

$$X = X_e + (X_0 - X_e) \exp(-k_1 t^{k_2}) + k_3 t \quad (18)$$

$$X = X_e + (X_0 - X_e) (k_1 \exp(-k_2 t) + k_3 \exp(-k_4 t)) \quad (19)$$

$$X = X_e + (X_0 - X_e) k_1 \exp(-k_2 t) + (1 - k_1) \exp(-k_2 (k_3 t)) \quad (20)$$

where  $X$  is the moisture content (kg/kg, d.w.b.),  $X_e$  is the equilibrium moisture content (kg/kg, d.w.b.),  $X_0$  is the initial moisture content (kg/kg, d.w.b.),  $t$  is the drying time (s), and  $k_1, k_2, k_3$  and  $k_4$  are the parameters of the drying models.

### **2.3.10. Scanning electronic microscopy**

The structure of the films was evaluated using a model XL30-FEG scanning electronic microscope (SEM) (Philips, Amsterdam, Netherlands) operating at 5 kV [32]. The samples were mounted on a carbon tape and impregnated with a layer of gold. The structure of each sample was evaluated using dispersive energy and density displacement spectrometry to resolve the microscope data.

### **2.3.11. Fourier Transform Infrared Spectroscopy**

Fourier transform infrared spectroscopy (FTIR-ATR) was used to examine the selected films using a Shimadzu model IR-Prestige spectrometer (Japan) with 128 scans and 4 cm<sup>-1</sup> of resolution, between 400 and 5000 cm<sup>-1</sup>[33].

### **2.3.12. TGA and DTA analysis**

Thermal measurements TGA/DTA was carried out using a DTG equipment (model DTG-60, Shimadzu, Japan) under a nitrogen atmosphere at a flow rate of 50 mL/min, heating rate of 10C°/min, and a temperature range of 30 to 1000 °C. The mass of the samples was of 2,827 mg and 4.650 mg for film A and B respectively. Both samples were covered in aluminum plates.

## **2.4. Mathematical modelling and statistical analysis**

In the present research, all the mathematical and statistical approaches employed in the development of the best models were carried out using the functions of the Matlab® R2013a program (The Mathworks Inc., Natick, MA, USA).

Tukey's test was used to study and compare the physical properties of the films for each response, using the "multicompare" function. The "multicompare" function allows one to determine the difference between the means of a determined data group with  $\alpha = 95\%$ .

Having evaluated the interaction and significance between the variables for each response, a mathematical model was prepared for each response using stepwise regression by way of the stepwisefit function, using the best combination of the factors as a base for the addition or exclusion of terms to establish the model, subsequently being evaluated using the significance test ( $p < 0.05$ ) [34, 35]. On the other hand, in order to model the sorption isotherms and drying kinetics, the parameters of the simulation models were estimated from the fit of the equations of the experimental data using the "nlinfit" function [36].

The determination coefficient ( $R^2$ ) (Eq. (21)) and the relative mean error ( $RME$ ) (Eq. (22)) were used to statistically validate the modelling and simulation. The value for  $R^2$  determines the efficiency of the proposed models according to the data variation, and the statistical parameter  $RME$  is the criterion that evaluates the precision of the estimate. A model with a  $RME$  value below 10% is considered to be a highly precise model, whereas a model with a  $RME$  value between 10 and 15 % can be considered acceptable [37].

$$R^2 = \frac{\sum_{k=1}^{\beta} (y_k^* - \bar{y})^2}{\sum_{k=1}^{\beta} (y_k - \bar{y})^2} \quad (21)$$

$$RME = \frac{100}{\beta} \sum_{k=1}^{\beta} \frac{|y_k - y_k^*|}{y_k^*} \quad (22)$$

In equations (21) – (22),  $y$  represents the experimental values,  $y^*$  represents the calculated values,  $k$  is the mean of the experimental values and  $\beta$  is the number of experimental values.

### 3. Results and discussion

#### 3.1. Physical properties of the films formulated using an experimental design

Table 1 shows the results obtained for the physical properties of the films elaborated with citrus pectin, babassu coconut mesocarp and glycerol.

The table shows a variation in the physical properties of each formulation, providing evidence that the results obtained were directly related to the proportion of each component ( $CP$ ,  $BCM$  and  $G$ ) in the film. Thus films with  $BCM > 2.5$  g and  $G < 2.0$  mL showed low moisture contents ( $\omega < 19.122$  g/100g, w.w.b.), and those with  $BCM < 1.5$  g and  $G > 3.0$  mL showed high moisture contents ( $\omega > 24.381$  g/100g, w.w.b.). Only the formulation with  $CP = 8.4$  g,  $BCM = 1.5$  g and  $G = 4.2$  mL showed intermediary results, which could be explained due to the high citrus pectin content and its hydrophobic nature [38]. On the other hand, the babassu coconut mesocarp has high swelling capacity (Cinelli et al., 2014), and, when mixed with glycerol, creates a plasticizing system which maintains the moisture of the biofilm matrix controlled [7, 39]. This synergic effect is associated with the process of dispersing the babassu mesocarp in the glycerol [6, 40], which reduces the availability of hydroxyl groups to interact with the water, a determining factor for the characteristic moisture content of each film.



**Table 1:** Experimental results obtained for the physical characterizations of the different filmformulations.

<b>Biofilm</b>	<b>CP (g)</b>	<b>BCM (g)</b>	<b>G (mL)</b>	<b><math>\omega</math> (g/100g, w.w.b)</b>	<b>S (g/100g, w.w.b)</b>	<b><math>\delta</math> (mm)</b>	<b>WVP (g.mm)/(m<sup>2</sup>.dya.kPa)</b>
1	4.4	1.5	2.2	28.109±1.588 <sup>cd</sup>	34.494±2.839 <sup>abcd</sup>	0.109±0.017 <sup>bc</sup>	5.513±1.130 <sup>bcd</sup>
2	8.4	1.5	2.2	21.284±0.933 <sup>def</sup>	27.829±4.958 <sup>bcde</sup>	0.168±0.028 <sup>ab</sup>	6.713±0.789 <sup>abcd</sup>
3	4.4	4.0	2.2	23.565±6.031 <sup>cf</sup>	43.211±14.090 <sup>ab</sup>	0.162±0.019 <sup>ab</sup>	5.270±0.435 <sup>bc</sup>
4	8.4	4.0	2.0	14.979±2.390 <sup>f</sup>	23.949±4.112 <sup>de</sup>	0.164±0.017 <sup>ab</sup>	7.973±0.873 <sup>ac</sup>
5	4.4	1.5	4.2	39.384±2.211 <sup>ab</sup>	48.202±0.819 <sup>a</sup>	0.116±0.004 <sup>bc</sup>	6.247±0.845 <sup>abcd</sup>
6	8.4	1.5	4.2	21.453±4.771 <sup>def</sup>	37.069±2.679 <sup>abcd</sup>	0.144±0.011 <sup>ab</sup>	6.360±1.259 <sup>abcd</sup>
7	4.4	4.0	4.2	31.001±0.905 <sup>bc</sup>	42.397±2.658 <sup>abc</sup>	0.170±0.022 <sup>ab</sup>	6.313±0.834 <sup>abcd</sup>
8	8.4	4.0	4.2	25.602±1.499 <sup>ce</sup>	39.194±9.695 <sup>abcd</sup>	0.203±0.004 <sup>a</sup>	9.583±0.196 <sup>a</sup>
9	2.0	2.5	3.0	43.404±5.037 <sup>a</sup>	50.642±5.471 <sup>a</sup>	0.130±0.002 <sup>ac</sup>	6.873±0.593 <sup>abcd</sup>
10	10.0	2.5	3.0	22.100±1.231 <sup>cf</sup>	22.776±1.392 <sup>de</sup>	0.166±0.011 <sup>ab</sup>	4.507±0.106 <sup>bc</sup>
11	6.0	0.0	3.0	41.534±3.024 <sup>a</sup>	38.996±10.570 <sup>abcd</sup>	0.113±0.012 <sup>bc</sup>	3.933±1.716 <sup>bd</sup>
12	4.4	1.5	4.2	24.381±1.533 <sup>ce</sup>	25.678±2.798 <sup>cde</sup>	0.170±0.026 <sup>ab</sup>	5.357±0.605 <sup>bc</sup>
13	6.0	2.5	1.0	19.122±0.132 <sup>ef</sup>	13.894±3.752 <sup>e</sup>	0.128±0.013 <sup>ab</sup>	6.173±0.659 <sup>abcd</sup>
14	6.0	2.5	5.0	41.811±0.418 <sup>a</sup>	14.654±4.281 <sup>e</sup>	0.164±0.040 <sup>ab</sup>	6.387±3.574 <sup>abcd</sup>
15	6.0	2.5	3.0	28.636±1.682 <sup>cd</sup>	37.662±1.268 <sup>abcd</sup>	0.159±0.055 <sup>ab</sup>	7.647±0.120 <sup>abc</sup>
16	6.0	2.5	3.0	25.568±5.345 <sup>ce</sup>	35.650±2.586 <sup>abcd</sup>	0.156±0.045 <sup>ab</sup>	8.123±0.120 <sup>ad</sup>
17	6.0	2.5	3.0	30.997±0.307 <sup>bc</sup>	34.361±1.864 <sup>abcd</sup>	0.156±0.045 <sup>ab</sup>	8.613±0.130 <sup>ad</sup>

\*Mean of triplicates ± standard deviation. The same letters in the same column indicate no significant difference between the values for the means ( $p < 0.05$ ). *CP*:citrus pectin, *BCM*: babassu coconut mesocarp, *G*: glycerol,  $\omega$ : moisture content, *S*: solubility,  $\delta$ : thickness, and *WVP*: water vapor permeability.

The results obtained for solubility ( $S$ ) showed that for proportions of  $CP > 8.4$  g,  $BCM < 2.5$  g and  $G > 2.2$  mL values of up to 27.829 g/100g (w.w.b.), were obtained. These values could be considered as intermediary-low, such that when the  $CP$  concentration of the film was reduced, high solubility values of around 50.642 g/100g (w.w.b.) were obtained for film 9 ( $CP = 2.0$  g,  $BCM = 2.5$  g and  $G = 3.0$  mL). According to Dias et al., [17], the solubility of biofilms depends on the interaction between cellulosic fibers and the plasticizer, where a high lignin content on the surface promotes a high resistance of the biofilm surface, making chemical, absorption and thermal reactions difficult. In this case, the  $BCM$  concentration promotes reticulation of the biofilms, due to lining up of the fibers of the polymeric matrix [6, 7], making them more resistant to dissolution.

The film thickness did not vary significantly, where film 1 ( $CP = 4.4$  g,  $BCM = 1.5$  g and  $G = 2.2$  mL) and film 11 ( $CP = 6.0$  g,  $BCM = 0$  g and  $G = 3.0$  mL) were those showing the lowest values of around  $\delta = 0.109$  mm and  $\delta = 0.113$  mm, respectively. In general terms the thickness of these films is thin when compared to those made with zein [11] and mixtures of nanoclay/starch [40], and similar to biofilms elaborated with citrus pectin/babassu mesocarp/milk protein isolate (Lopes et al., 2017).

Similar to the results obtained for thickness, the water vapor permeability showed the highest value of ( $WVP = 9.583$  (g.mm)/(m<sup>2</sup>.day.kPa)) for the formulation  $CP = 8.4$  g,  $BCM = 4.0$  g and  $G = 4.2$  mL, and low values ( $WVP < 5.513$  (g.mm)/(m<sup>2</sup>.day.kPa)) for films 1, 3 and 12, with no variability in the results obtained for the other filmogenic formulations. In addition, no correlation was observed between the water vapor permeability and the other properties analyzed. The conjugation of the three components ( $CP$ ,  $BCM$  and  $G$ ) was determinant for the results obtained for  $WVP$ . According to Lopes et al. (2017) the interfacial equilibrium with the moist air promotes an incipient relaxation of the structure in the external portion of the cross-section of the film, increasing the permeation rate through this surface layer. However, a thicker film reduces the relative contribution of this layer to the total resistance, increasing the  $WVP$  of the biofilm [3]. This level of agreement is highly reasonable when one considers the more significant variations in the determinations of vapor pressure for components with similar vapor pressures, such as carboxylic acids, sugars and celluloses [41]. Finally, the volatility of the glycerol drops could interfere with the vapor pressures measured inside the cell when these are found in excess and not completely mixed in the solution [42].

### 3.1.1. Mathematical simulation of the physical properties of the biofilms

The modelling of the experimental results obtained for the physical properties of the different film formulations was carried out by stepwise regression, obtaining second and third degree linear correlations with respect to the concentrations of citrus pectin, babassu mesocarp and glycerol. Table 2 shows the values obtained for the coefficients of the terms and their statistical validation.

**Table 2:** Simulation of the physical properties using the stepwise-fit method.

Property	Parameter	Valueoftheparameter	$R^2$	RME (%)
W (g/100g, w.w.b.)	Intercept	-226.240	0.903	9.836
	CP	98.931		
	BCM	99.662		
	G	-15.791		
	CP <sup>2</sup>	-7.543		
	BCM <sup>2</sup>	3.610		
	CP×BCM	-43.368		
	CP×G	13.380		
	CP <sup>2</sup> ×BCM	3.405		
	BCM <sup>2</sup> ×G	-2.195		
	CP <sup>3</sup>	0.039		
G <sup>3</sup>	0.056			
S (g/100g, w.w.b.)	Intercept	20.903	0.890	14.737
	CP	-6.177		
	G	31.527		
	BCM <sup>2</sup>	-13.610		
	G <sup>2</sup>	6.149		
	CP <sup>2</sup> ×BCM	-0.905		
	BCM <sup>2</sup> ×CP	1.995		
	CP <sup>2</sup> ×G	0.096		
	CP <sup>3</sup>	0.112		
	BCM <sup>3</sup>	0.630		
G <sup>3</sup>	-1.288			
δ (mm)	Intercept	8.712×10 <sup>-2</sup>	0.915	12.880
	CP	5.081×10 <sup>-3</sup>		
	BCM	4.043×10 <sup>-3</sup>		

	$BCM \times G$	$3.147 \times 10^{-3}$		
	Intercept	-6.757		
	$BCM$	12.361		
	$BCM^2$	-3.727		
	$G^2$	0.703		
	$CP \times G$	-0.122		
$WVP$ (g.mm)/(m <sup>2</sup> .day.kPa)	$CP \times BCM \times G$	0.038	0.890	11.758
	$CP^2 \times BCM$	-0.395		
	$BCM^2 \times CP$	0.938		
	$CP^3$	0.046		
	$BCM^3$	-0.305		
	$G^3$	-0.129		

$CP$ : citrus pectin,  $BCM$ : babassu coconut mesocarp,  $G$  glycerol,  $\omega$ : moisture content,  $S$ : solubility,  $\delta$ : thickness, and  $WVP$ : water vapor permeability.  $RME$ : relative mean error.  $R^2$ : correlation coefficient.

For  $\omega$ ,  $S$ ,  $\delta$  and  $WVP$ , all the coefficients selected were statistically significant at the confidence level of 95 %, obtaining values of  $R^2 > 0.890$  and  $RME < 14.737$  %, indicating good agreement between the experimental and calculated values. Thus values for  $CP$ ,  $BCM$  and  $G$  within the range of the study could be incorporated in order to predict the values of the physical properties cited above [43].

### 3.2. Reformulated films

Based on the results previously obtained, two film formulations were improved, A and B, corresponding to the concentrations of  $CP = 10.0$  g,  $BCM = 5.0$  g and  $G = 5.0$  mL, and  $CP = 10.0$  g,  $BCM = 5.0$  g and  $G = 1.0$  mL respectively.

#### 3.2.1. Physical properties

Table 3 shows the results obtained for the physical properties of the reformulated films. The statistical results showed a significant difference between the films for all the physical properties. The  $CP$  and  $BCM$  concentrations were maintained constant, only varying the concentration of  $G$ . This reaffirms the discussions made in sections above concerning the effect of each component on the physical properties.

**Table 3:** Results obtained for the physical properties of the reformulated films\*.

Physical properties		Film A	Film B
<i>RH</i> (g/100g, w.w.b.)( $\omega$ at 52%)		74.178±0.02 <sup>a</sup>	85.674±0.03 <sup>b</sup>
<i>S</i> (g/100g, w.w.b.)		49.462±2.390 <sup>a</sup>	60.737±3.810 <sup>b</sup>
$\delta$ (mm)		0.201±0.029 <sup>a</sup>	0.165±0.023 <sup>b</sup>
<i>WVP</i> (g.mm)/(m <sup>2</sup> .day.kPa)		6.226±0.745 <sup>a</sup>	8.973±1.383 <sup>b</sup>
$\epsilon$ (g/cm <sup>2</sup> )		247.857±7.937 <sup>a</sup>	196.786±0.975 <sup>b</sup>
<i>TS</i> (MPa)		49.410±15.484 <sup>a</sup>	226.673±71.312 <sup>b</sup>
<i>E</i> (%)		10.412±1.259 <sup>b</sup>	3.768±0.940 <sup>a</sup>
<i>EM</i> (MPa)		4.669±1.036 <sup>a</sup>	60.797±12.476 <sup>b</sup>
Color (CIELab)	<i>L</i> <sup>*</sup>	29.813±0.025 <sup>a</sup>	33.343±0.111 <sup>b</sup>
	<i>a</i> <sup>*</sup>	7.590±0.000 <sup>b</sup>	4.463±0.095 <sup>a</sup>
	<i>b</i> <sup>*</sup>	11.280±0.036 <sup>a</sup>	16.490±0.026 <sup>b</sup>
	<i>C</i> <sup>*</sup>	13.597±0.025 <sup>a</sup>	17.083±0.042 <sup>b</sup>
	<i>h</i> <sup>o</sup>	56.067±0.078 <sup>a</sup>	74.850±0.305 <sup>b</sup>

\*Mean of triplicate  $\pm$  standard deviation. The same letters in the same line indicate no significant difference between the values for the means ( $p < 0.05$ ).  $\omega$ : moisture content, *S*: solubility,  $\delta$ : thickness, *WVP*: water vapor permeability,  $\epsilon$ : grammage, *TS*: tensile strength, *E*: elongation at break, *EM*: elastic modulus, *L*<sup>\*</sup>:indicates lightness, *a*<sup>\*</sup>:red-green axis, *b*<sup>\*</sup>:yellow-blue axis, *C*<sup>\*</sup>: chroma, and *h*<sup>o</sup>: hue angle.

From a technical aspect, film B showed a greater moisture content and solubility than biofilm A due to the smaller amount of plasticizer (glycerol) in the filmogenic matrix, since this facilitates breaking of the polymer molecules on the surface [11, 39]. On the other hand, film A showed a greater grammage than film B, which can be attributed to the larger amount of mass in the filmogenic solution, principally due to the larger amount of glycerol added. Thus the formulation with a higher glycerol concentration could present better mechanical resistance characteristics [1, 44].

The above argument is evidenced in the results of the mechanical properties, where the film A presented lower tensile strength (*TS*) and higher elasticity (*E*) compared to film B, which obtained high values of *TS* and low values of *E*. The modulus of elasticity (*EM*), which correlates the *TS* and *E* properties, shows values of 4,669 MPa for film A and 60,797 MPa for film B, showing the effect of the concentration of glycerol as plasticizing agent, higher in film A. Similar results were related by Maniglia et al. [6] where an increase in elongation can be obtained with a higher concentration of hydrophilic plasticizers (in this case glycerol). This plasticization of the film implies, however, a decrease in tensile strength and an increase in the hydrophilicity and water vapor

permeability [45]. According to Khalil et al. [46] films with a higher elongation at rupture presents a material that will have a better resistance to impact, as well easily to processing.

Already the color parameters ( $L^*$ ,  $a$  and  $b$ ) showed results where the yellow color predominate than the red color. The hue angle ( $h^\circ$ ) showed values of  $74.850^\circ$  for film A and  $56.067^\circ$  for film B, showing a yellow hue (reference value of  $90^\circ$ ). According to Brandelero et al. [47] the tonality of biodegradable films is influenced in large part by the increase of the concentration of the plasticizer, crosslinker and coating material (in this case the babassu mesocarp). Thus, the yellow color is more predominant in film A than in film B.

### 3.2.2. Sorption isotherms

Figure 1 shows the absorption isotherms of films A and B at a temperature of  $25^\circ\text{C}$ .

The results in the above figure show equilibrium moisture contents ( $X_e$ ) varying in the range from  $0.360 - 0.939$  kg/kg (d.w.b.) for film A, and from  $0.113 - 0.604$  kg/kg (d.w.b.) for film B, in the water activity range from  $0.122 - 0.843$ . These values were similar to those found for films made from sodium alginate and pectin [9], nut starch and carrageenan [10] and amaranth [13]. The difference in the equilibrium moisture content ranges, which was greater for film A than for film B, can be attributed to hydrophobic sites created by the citrus pectin in the film and the greater amount of glycerol, where the plasticizing effect of this component impedes the exchange of water from the inside of the film to the atmosphere [9, 48].

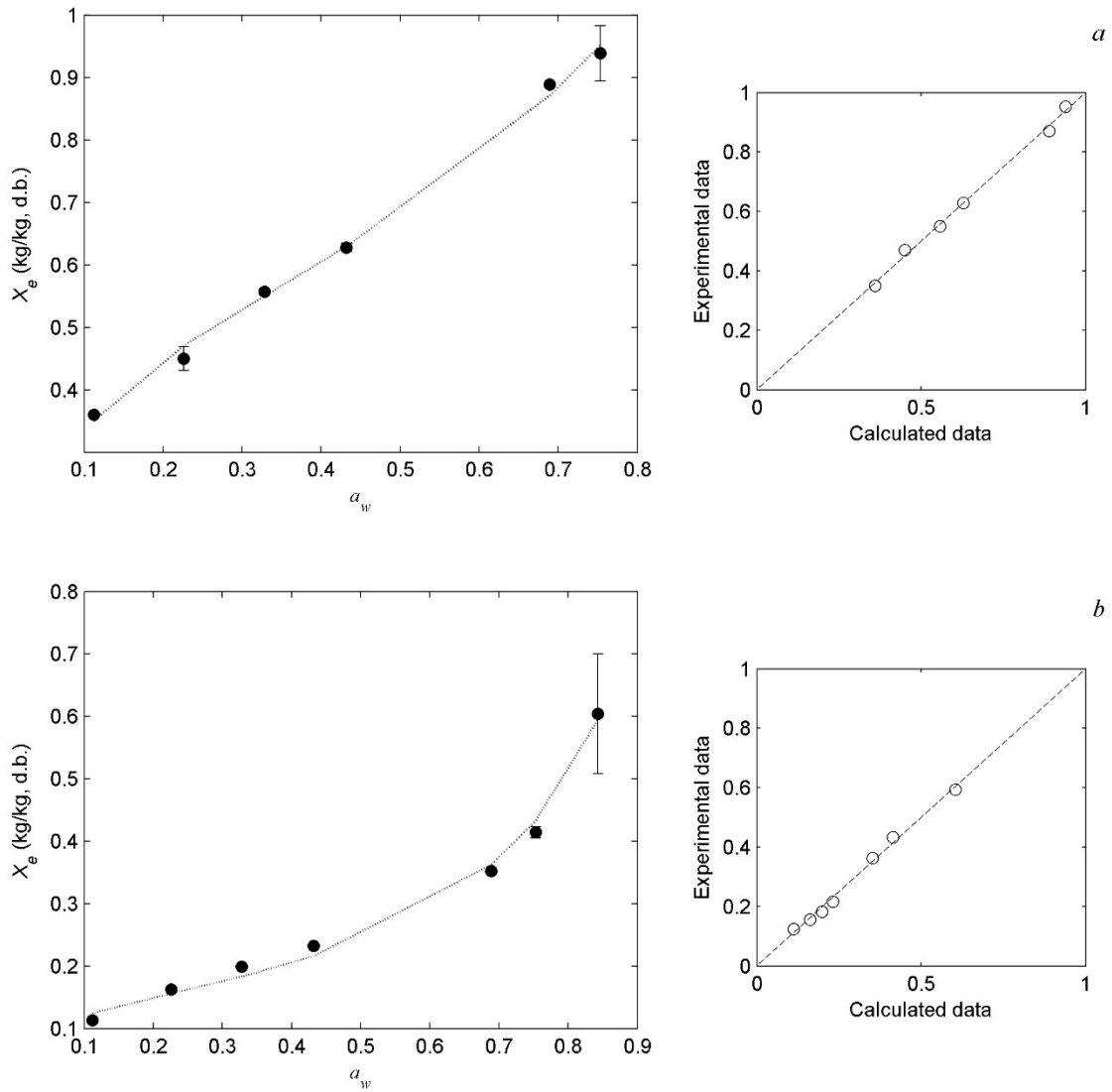


**Figure 1:** Experimental values for the sorption isotherms (●) of the films A (a) and B (b) and simulated using the GAB model (—). The figure on the right indicates the residuals between the experimental values and those predicted by the model.

The results for the mathematic modelling of the isotherms, presented in Table 4, show that the GAB model best represented the experimental values for both films, with values for  $R^2 > 0.989$  and for  $RME < 5.447\%$ .

**Table 4:** Results of the modelling and simulation of the sorption isotherms of films A and B at 25 °C.

Model	Parameter	Biofilm A	Biofilm B
GAB	$X_m$	0.731	0.147
	$C$	15.895	38.910
	$K$	0.664	0.918
	$R^2$	0.993	0.989
	$RME$ (%)	2.014	5.447
BET	$X_m$	0.274	0.102
	$C$	$1.051 \times 10^8$	$1.475 \times 10^7$
	$R^2$	0.910	0.981
	$RME$ (%)	17.458	11.650
Oswin	$a$	0.680	0.262
	$b$	0.306	0.466
	$R^2$	0.994	0.981
	$RME$ (%)	1.750	6.508
Halsey	$a$	0.265	0.073
	$b$	2.271	1.621
	$R^2$	0.978	0.992
	$RME$ (%)	4.817	4.858
Henderson	$a$	1.613	4.408
	$b$	2.397	1.445
	$R^2$	0.994	0.946
	$RME$ (%)	2.417	11.706
Chung & Pfof	$a$	0.962	0.483
	$b$	0.311	0.203
	$R^2$	0.892	0.707
	$RME$ (%)	11.133	26.652

$X_m$ : equilibrium moisture content of the monolayer,  $C$ : parameter of the GAB & BET models,  $K$ : parameter of the GAB model,  $a$  &  $b$ : parameters of the empirical models.  $RME$ : relative mean error.  $R^2$ : correlation coefficient. Biofilm A ( $CP = 10.0$  g,  $BCM = 5.0$  g and  $G = 5.0$  mL), Biofilm B ( $CP = 10.0$  g,  $BCM = 5.0$  g and  $G = 1.0$  mL).

### 3.2.3. Drying kinetics

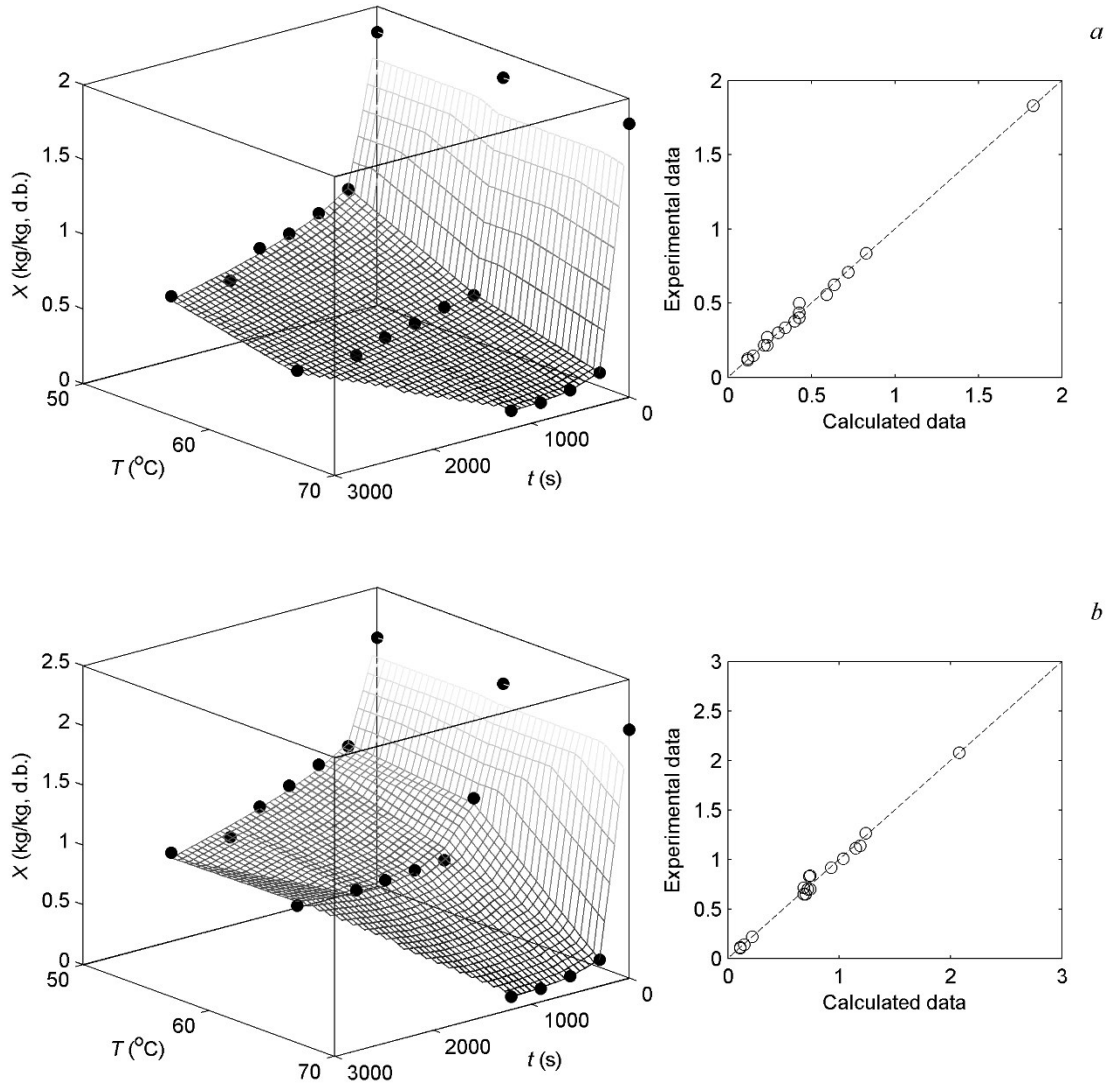
The drying kinetics of the reformulated films were determined at different temperatures, and the experimental results are shown in Figure 2.

Figure 1 shows equilibrium moisture contents ( $X_e$ ) of 0.740, 0.680 and 0.108 kg/kg (d.w.b.), for film A, and of 0.428, 0.236 and 0.118 kg/kg (d.w.b.), for film B, corresponding to the drying times of 2100, 2100 and 1200 s at temperatures of 50, 60 and



70 °C respectively. In addition, the initial moisture contents ( $X_0$ ) were 2.078 and 1.829 kg/kg (d.w.b.), for films A and B, respectively. These results show that the formulation with the larger amount of plasticizer presented the highest water evaporation rate from the filmogenic matrix, this rate being more expressive in decreasing temperature order, that is, 70 °C > 60 °C > 50 °C. It can be said that the two films presented a microstructure with open channels that permitted the exchange of water to the desiccating system [49]. These channels are formed by the regrouping of the mesocarp and of the citrus pectin with the plasticizer, forming a homogenous surface, as can be seen in the microscope analyses. These results were similar to those reported for amaranth/glycerol/sorbitol biofilms [13], nut starch/glycerol/carrageenin hybrid [10] and sodium alginate/pectin [9].

Table 5 shows the results obtained in the modelling of the drying kinetics, where the Midilli empirical model best represented the behavior of the data for both films, with  $R^2 > 0.983$  and  $RME < 5.929$  %, as can be seen from the graph of the residues in Figure 2.



**Figure 2:** Experimental values for the drying kinetics (●) of the films A (a) and B (b) and simulated using the Midilli model (mesh, ○). The figure on the right indicates the residuals between the experimental values and those predicted by the model.

**Table 5:** Results of the modelling and simulation of the drying kinetics of films A and B.

Model	Parameter	Biofilm A			Biofilm B		
		50 °C	60 °C	70 °C	50 °C	60 °C	70 °C
Weibull	$k_1$	668.75	225.01	106.47	1223.8	819.03	105.45
	$R^2$	0.883	0.968	0.999	0.870	0.831	0.999
	$RME$ (%)	26.817	41.062	3.923	14.638	27.709	4.582
Peleg	$k_1$	113.16	32.329	15.015	199.92	114.93	12.679
	$k_2$	0.677	0.622	0.570	0.668	0.629	0.495
	$R^2$	0.985	0.995	0.999	0.970	0.976	0.999
	$RME$ (%)	7.919	8.694	2.342	6.036	6.175	2.852
Logarithmic	$k_1$	0.761	0.895	0.994	0.631	0.721	0.995
	$k_2$	$3.971 \times 10^{-3}$	$7.757 \times 10^{-3}$	$9.710 \times 10^{-3}$	$2.476 \times 10^{-3}$	$3.708 \times 10^{-3}$	$9.803 \times 10^{-3}$
	$k_3$	0.395	0.178	$8.574 \times 10^{-3}$	0.685	0.557	0.010
	$R^2$	0.956	0.986	0.999	0.933	0.989	0.999
	$RME$ (%)	12.560	13.182	5.712	8.253	3.264	6.861
Lewis	$k_1$	$1.495 \times 10^{-3}$	$4.444 \times 10^{-3}$	$9.392 \times 10^{-3}$	$8.171 \times 10^{-4}$	$1.221 \times 10^{-3}$	$9.483 \times 10^{-3}$
	$R^2$	0.882	0.968	0.999	0.870	0.831	0.999
	$RME$ (%)	26.817	41.062	3.923	14.638	27.709	4.582
Page	$k_1$	0.106	0.414	0.113	1.335	0.107	0.117
	$k_2$	0.362	0.240	0.564	$4.759 \times 10^{-10}$	0.337	0.560

	$R^2$	0.992	0.997	0.999	0.795	0.958	0.999
	$RME$ (%)	5.049	5.934	3.131	28.217	8.704	3.776
Midilli	$k_1$	0.213	0.850	0.196	0.117	$8.764 \times 10^{-3}$	0.203
	$k_2$	0.238	0.113	0.466	0.255	0.773	0.462
	$k_3$	$-8.122 \times 10^{-5}$	$-6.032 \times 10^{-5}$	$-9.490 \times 10^{-6}$	$-1.314 \times 10^{-5}$	$2.534 \times 10^{-5}$	$-1.068 \times 10^{-5}$
	$R^2$	0.992	0.998	0.999	0.983	0.984	0.999
	$RME$ (%)	4.679	4.712	2.322	4.024	5.292	2.813
		$k_1$	0.515	0.773	0.792	0.351	0.495
Twoterm	$k_2$	0.993	0.993	0.993	0.993	0.993	0.993
	$k_3$	0.484	0.226	0.207	0.648	0.504	0.201
	$k_4$	$5.255 \times 10^{-4}$	$6.360 \times 10^{-4}$	$4.229 \times 10^{-3}$	$3.786 \times 10^{-4}$	$3.783 \times 10^{-4}$	$4.229 \times 10^{-3}$
	$R^2$	0.990	0.998	0.999	0.980	0.888	0.999
	$RME$ (%)	4.314	4.219	2.435	3.629	11.121	2.938
		$k_1$	0.620	0.834	0.999	0.741	0.666
Diffusion approach	$k_2$	$7.789 \times 10^{-4}$	$3.428 \times 10^{-3}$	$9.391 \times 10^{-3}$	$4.981 \times 10^{-4}$	$6.531 \times 10^{-4}$	$6.408 \times 10^{-3}$
	$k_3$	223.23	$7.552 \times 10^8$	$2.480 \times 10^4$	223.23	129.01	$3.463 \times 10^8$
	$R^2$	0.911	0.929	0.999	0.899	0.788	0.984
	$RME$ (%)	11.326	39.141	3.926	7.461	16.631	17.649

$k_1, k_2, k_3, k_4$ : parameters of the empirical models.  $RME$ : relative mean error.  $R^2$ : correlation coefficient. Biofilm A ( $CP = 10.0$  g,  $BCM = 5.0$  g and  $G = 5.0$  mL), Biofilm B ( $CP = 10.0$  g,  $BCM = 5.0$  g and  $G = 1.0$  mL).

### 3.2.4. Scanning electronic microscopy

Figure 3 shows the surface micrographs of the formulations  $CP = 10.0$  g,  $BCM = 5.0$  g and  $G = 5.0$  mL, and  $CP = 10.0$  g,  $BCM = 5.0$  g and  $G = 1.0$  mL, corresponding to films A and B, respectively.

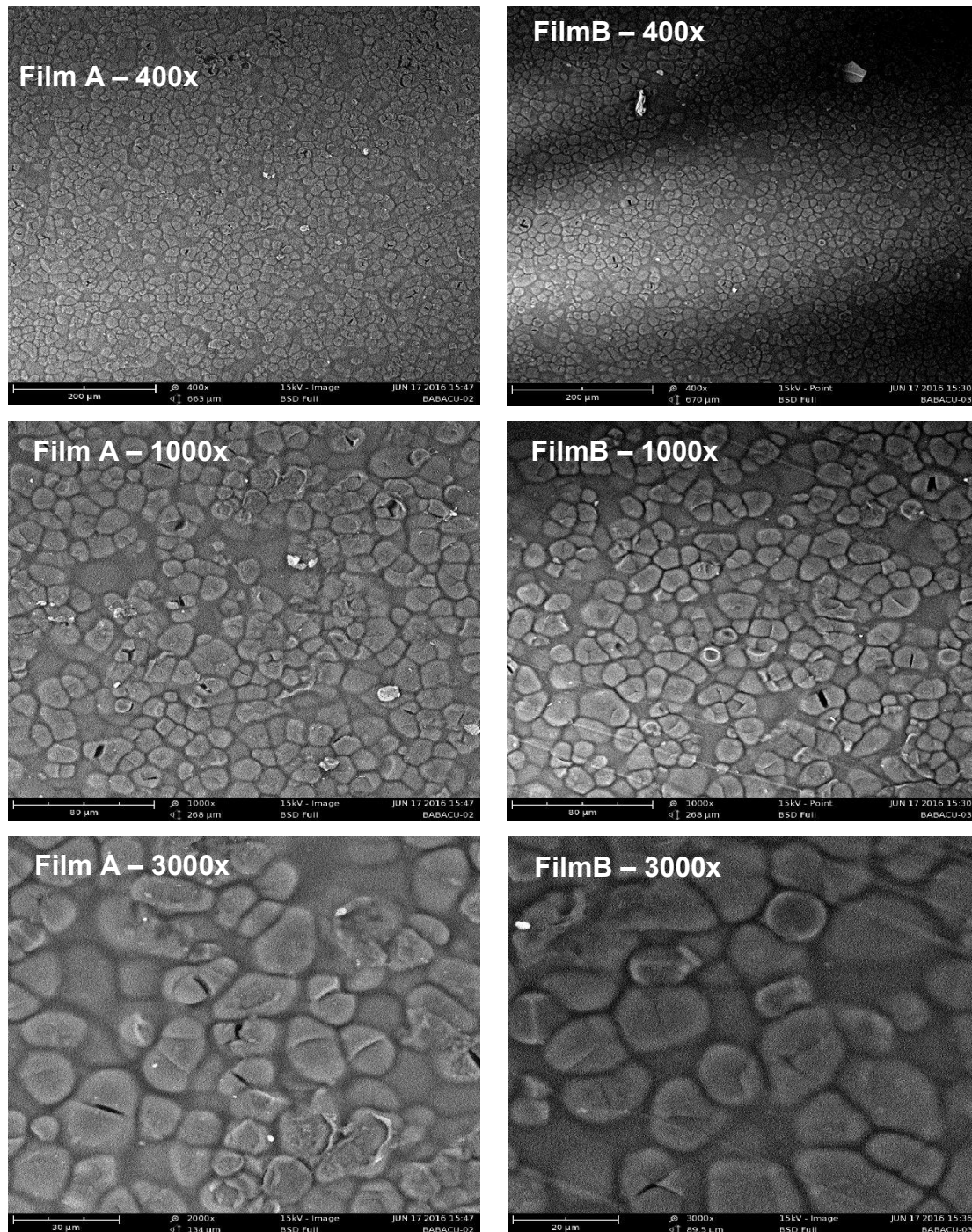


**Figure 3:** Surface micrographs of films A and B at different magnifications

Both films presented similar structures in the different magnifications, where one can observe a plasticized surface with small agglomerates of babassu mesocarp particles with sizes between 10 and 15  $\mu\text{m}$ . An interstitial space can be observed between each particle, filled with citrus pectin and plasticized by glycerol. According to Maniglia et al., [6, 50] the glycerol is responsible for potentiating the organization of the crystalline structure of the polymers (starch) in the filmogenic matrix, and, in the case of the biofilms based on babassu mesocarp, the crystalline cellulosic structure. Thus the images show the synergism of the components (*CP*, *BCM* and *G*) in the confection of the films, the addition of different concentrations of glycerol being reflected in the increase or decrease of the mechanical resistance of the film [7, 11].

### 3.2.5. Fourier Transform Infrared Spectroscopy

Figure 4 shows the infrared spectra obtained for formulations A and B. From the spectra it was possible to identify the dimers that produced intense and very wide axial deformation absorption of the O-H in the  $3443 - 2362 \text{ cm}^{-1}$  region. The characteristic peaks for pectin can be found around  $3443 - 3335$ ,  $2931$ ,  $1444 - 400$  and  $538 \text{ cm}^{-1}$ , attributed to O-H,  $\text{COO}^-$  (asymmetric),  $\text{COO}^-$  (symmetric), and C-O-C on stretching the biopolymers, respectively.

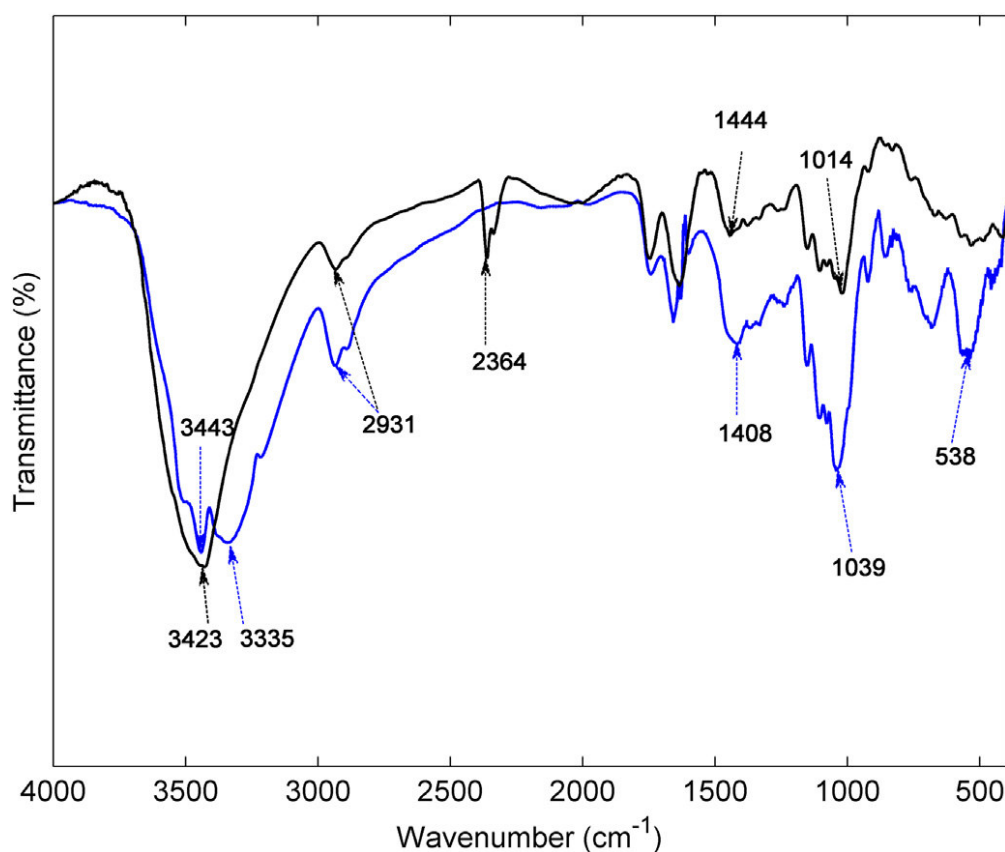


**Figure 4:** FTIR-ATR spectra of the films A (black –) and B (blue –).

Variation in the amount of glycerol caused changes in the spectrum, causing a shortening of two bands, 1000 and 3500. These shortenings could be explained due to the stretching of the O-H vibrations, associated with polar interactions between the components of the films and the water present. The mesocarp with pectin, together with the calcium, caused an increase in binding of the intermolecular hydrogen of the polymer, and consequently the reduction in intensity of the O-H peak can be related to the reduction in polymeric interactions in the water and the absorption of moisture [7, 50].

### 3.2.6. Thermal analyses

In the TGA/DTA curves presented in Figure 5 for both reformulated biofilms three stages of decomposition were observed.

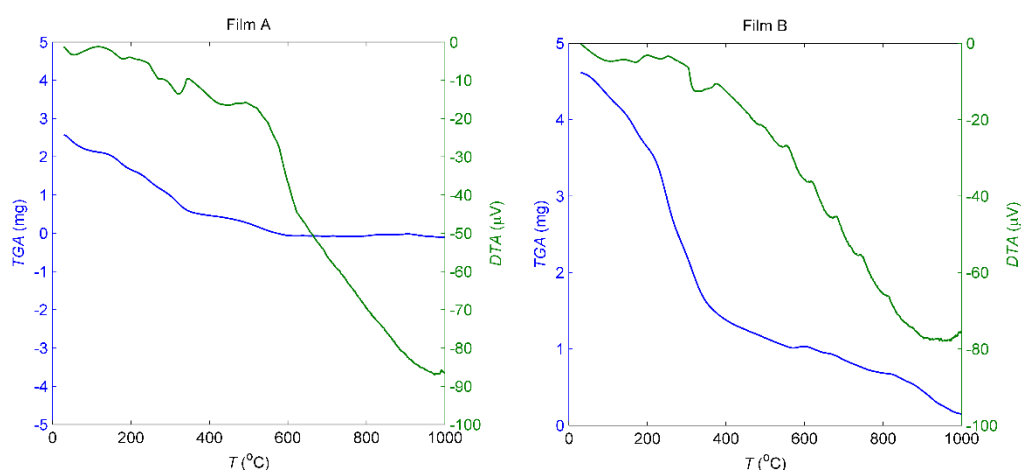


**Figure 5:** TGA (blue –) and DTA (green –) curves of the reformulated films.

In the first temperature region up to 200 °C, the endothermic peak situated at ~180 °C for film A and ~150 °C for film B results from the evaporation of excess water. The second stage shows one endothermic peak situated at ~320 and 330 °C for film A and B respectively, representing the decomposition of the organic compounds, babassu mesocarp and citrus pectin. A previous peak in the second stage at ~230 °C for both reformulated films can be attributed by the glass transition of glycerol [51]. The third weight loss at ~520 and ~490 °C for film A and B respectively, can be associated with an exothermic peak, points out the transformation of amorphous degradation of the films. According to Teixeira et al. [5], these alterations can be attributed to the rupture of inter and intramolecular hydrogen bonds between the hydroxyl groups of the precursor material, which occurs after the reaction with

the glycerol, becoming weaker bonds and less intense between the groups present on the surface in the final material.

#### **4. Conclusions**

By using an experimental design, the effects of the film composition (citrus pectin, babassu coconut mesocarp and glycerol) on the moisture content, solubility, thickness and water vapor permeability could be observed, and adequately represented using the stepwise regression method. The models obtained allow for the simulation of the properties within the range of concentration of the materials employed in the films. On the other hand, the reformulated films showed that the higher the babassu mesocarp and glycerol concentrations, the greater the mechanical resistance of the films. The water absorption properties and drying kinetics showed that the biofilms presented water permeability characteristics with similar structural characteristics for both films. Finally, thermal analyses show three stages of decomposition for both films, since their results are important to controlling the process at industrial scaling.

#### **5. Acknowledgements**

The authors are grateful to the Research and Technological Development Foundation of Maranhão (FAPEMA), Brazil, for the financial support given to the projects UNIVERSAL-00752/17 e UNIVERSAL-01190/17.

#### **6. References**

- [1] M. Ramos, A. Valdés, A. Beltrán, M. Garrigós, Gelatin-Based Films and Coatings for Food Packaging Applications, *Coatings* 6(4) (2016) 41.
- [2] F.M. Fakhouri, S.M. Martelli, T. Caon, J.I. Velasco, L.H.I. Mei, Edible films and coatings based on starch/gelatin: Film properties and effect of coatings on quality of refrigerated Red Crimson grapes, *Postharvest Biology and Technology* 109(Supplement C) (2015) 57-64.
- [3] A.A. Santana, T.G. Kieckbusch, Physical evaluation of biodegradable films of calcium alginate plasticized with polyols, *Braz J Chem Eng* 30 (2013) 835-845.
- [4] B.A. Cinelli, J.A. López, L.R. Castilho, D.M.G. Freire, A.M. Castro, Granular starch hydrolysis of babassu agroindustrial residue: A bioprocess within the context of biorefinery, *Fuel* 124 (2014) 41-48.
- [5] P.R.S. Teixeira, A.S.d.N.M. Teixeira, E.A.d.O. Farias, D.A. da Silva, L.C.C. Nunes, C.M. da Silva Leite, E.C. da Silva Filho, C. Eiras, Chemically modified babassu coconut (Orbignya



sp.) biopolymer: characterization and development of a thin film for its application in electrochemical sensors, *Journal of Polymer Research* 25(5) (2018) 127.

[6] B.C. Maniglia, L. Tessaro, A.A. Lucas, D.R. Tapia-Blácido, Bioactive films based on babassu mesocarp flour and starch, *Food Hydrocoll* 70 (2017) 383-391.

[7] I.A. Lopes, J. Santos Jr, D.C. Da Silva, L.J.S. Da Silva, A.K. Barros, H.A. Villa-Vélez, A.A. Santana, Characterization of Pectin Biofilms with the Addition of Babassu Mesocarp and Whey Protein Concentrate, *American Journal of Materials Science* 7(3) (2017) 64-70.

[8] S. Santacruz, C. Rivadeneira, M. Castro, Edible films based on starch and chitosan. Effect of starch source and concentration, plasticizer, surfactant's hydrophobic tail and mechanical treatment, *Food Hydrocoll* 49(Supplement C) (2015) 89-94.

[9] S. Galus, A. Lenart, Development and characterization of composite edible films based on sodium alginate and pectin, *J Food Eng* 115(4) (2013) 459-465.

[10] R. Moreira, F. Chenlo, M.D. Torres, C. Silva, D.M. Prieto, A.M.M. Sousa, L. Hilliou, M.P. Gonçalves, Drying Kinetics of Biofilms Obtained from Chestnut Starch and Carrageenan with and without Glycerol, *Drying Technology* 29(9) (2011) 1058-1065.

[11] C. Pena-Serna, J.F. Lopes-Filho, Influence of ethanol and glycerol concentration over functional and structural properties of zein–oleic acid films, *Mater Chem Phys* 142(2–3) (2013) 580-585.

[12] N.L. García, L. Ribba, A. Dufresne, M. Aranguren, S. Goyanes, Effect of glycerol on the morphology of nanocomposites made from thermoplastic starch and starch nanocrystals, *Carbohydr Polym* 84(1) (2011) 203-210.

[13] D.R. Tapia-Blácido, P.J.d.A. Sobral, F.C. Menegalli, Effect of drying conditions and plasticizer type on some physical and mechanical properties of amaranth flour films, *LWT - Food Sci Technol* 50(2) (2013) 392-400.

[14] R. Sothornvit, J.M. Krochta, 23 - Plasticizers in edible films and coatings A2 - Han, Jung H, *Innovations in Food Packaging*, Academic Press, London, 2005, pp. 403-433.

[15] H.C.F. Carneiro, R.V. Tonon, C.R.F. Grosso, M.D. Hubinger, Encapsulation efficiency and oxidative stability of flaxseed oil microencapsulated by spray drying using different combinations of wall materials, *J Food Eng* 115(4) (2013) 443-451.

- [16] P. Moser, R.T.D. Souza, V.R. Nicoletti Telis, Spray Drying of Grape Juice From Hybrid CV. BRS Violeta: Microencapsulation of Anthocyanins Using Protein/Maltodextrin Blends as Drying Aids, *Journal of Food Processing and Preservation* 41(1) (2017) n/a-n/a.
- [17] A.B. Dias, C.M.O. Müller, F.D.S. Larotonda, J.B. Laurindo, Mechanical and barrier properties of composite films based on rice flour and cellulose fibers, *LWT - Food Sci Technol* 44(2) (2011) 535-542.
- [18] C.M.O. Müller, J.B. Laurindo, F. Yamashita, Effect of cellulose fibers addition on the mechanical properties and water vapor barrier of starch-based films, *Food Hydrocoll* 23(5) (2009) 1328-1333.
- [19] J.-W. Rhim, S.-I. Hong, C.-S. Ha, Tensile, water vapor barrier and antimicrobial properties of PLA/nanoclay composite films, *LWT - Food Sci Technol* 42(2) (2009) 612-617.
- [20] AOAC, Official methods of analysis AOAC International, Gaithersburg, 2007.
- [21] ASTM-E9596, Standard test method for water vapor transmission of materials, ASTM International, West Conshohocken, 1995.
- [22] ASTM D882-18, Standard test method for tensile properties of thin plastic sheeting, ASTM International, West Conshohocken, PA, 1995.
- [23] B. Saberi, Q.V. Vuong, S. Chockchaisawasdee, J.B. Golding, C.J. Scarlett, C.E. Stathopoulos, Water Sorption Isotherm of Pea Starch Edible Films and Prediction Models, *Foods* 5(1) (2016) 1.
- [24] T. Chowdhury, M. Das, Moisture sorption isotherm and isosteric heat of sorption of edible films made from blends of starch, amylose and methyl cellulose, *International Food Research Journal* 19(4) (2012) 1699-1678.
- [25] T.P. Labuza, A. Kaanane, J.Y. Chen, Effect of Temperature on the Moisture Sorption Isotherms and Water Activity Shift of Two Dehydrated Foods, *J Food Sci* 50(2) (1985) 385-392.
- [26] E.O. Timmermann, J. Chirife, H.A. Iglesias, Water sorption isotherms of foods and foodstuffs: BET or GAB parameters?, *J Food Eng* 48 (2001) 19-31.
- [27] S.S.H. Rizvi, Thermodynamic properties of foods in dehydration, in: M.A. Rao, S.S.H. Rizvi (Eds.), *Engineering Properties of Foods*, Taylor & Francis, Boca Raton, 2005, pp. 259-346.

- [28] A. Midilli, H. Kucuk, Z. Yapar, A new model for single-layer drying, *Drying Technology* 20(7) (2002) 1503-1513.
- [29] E. Akpınar, A. Midilli, Y. Bicer, Single layer drying behaviour of potato slices in a convective cyclone dryer and mathematical modeling, *Energy Conversion and Management* 44(10) (2003) 1689-1705.
- [30] B. Singh, A.K. Gupta, Mass transfer kinetics and determination of effective diffusivity during convective dehydration of pre-osmosed carrot cubes, *J Food Eng* 79(2) (2007) 459-470.
- [31] Z. Erbay, F. Icier, A Review of Thin Layer Drying of Foods: Theory, Modeling, and Experimental Results, *Critical Reviews in Food Science and Nutrition* 50(5) (2010) 441-464.
- [32] A.N. Parvulescu, P.J.C. Hausoul, P.C.A. Bruijninx, R.J.M. Klein Gebbink, B.M. Weckhuysen, Synthesis of octyl-ethers of biomass-based glycols through two competitive catalytic routes: Telomerization and etherification, *Catalysis Today* 158(1) (2010) 130-138.
- [33] K.K. Chittur, FTIR/ATR for protein adsorption to biomaterial surfaces, *Biomaterials* 19(4) (1998) 357-369.
- [34] A. Cevik, Unified formulation for web crippling strength of cold-formed steel sheeting using stepwise regression, *Journal of Constructional Steel Research* 63(10) (2007) 1305-1316.
- [35] Y. Chen, R. Shi, S. Shu, W. Gao, Ensemble and enhanced PM10 concentration forecast model based on stepwise regression and wavelet analysis, *Atmospheric Environment* 74(Supplement C) (2013) 346-359.
- [36] D.M. Cano-Higueta, H.A. Villa-Vélez, J. Telis-Romero, H.A. Váquiro, V.R.N. Telis, Influence of alternative drying aids on water sorption of spray dried mango mix powders: A thermodynamic approach, *Food and Bioprocess Processing* 93(Supplement C) (2015) 19-28.
- [37] S.S. Sablani, O.-D. Baik, M. Marcotte, Neural networks for predicting thermal conductivity of bakery products, *J Food Eng* 52(3) (2002) 299-304.
- [38] A.C.K. Bierhalz, M.A. da Silva, T.G. Kieckbusch, Natamycin release from alginate/pectin films for food packaging applications, *J Food Eng* 110(1) (2012) 18-25.
- [39] C.M.O. Müller, F. Yamashita, J.B. Laurindo, Evaluation of the effects of glycerol and sorbitol concentration and water activity on the water barrier properties of cassava starch films through a solubility approach, *Carbohydr Polym* 72(1) (2008) 82-87.

- [40] C.M.O. Müller, J.B. Laurindo, F. Yamashita, Effect of nanoclay incorporation method on mechanical and water vapor barrier properties of starch-based films, *Industrial Crops and Products* 33(3) (2011) 605-610.
- [41] M. Bocqué, C. Voirin, V. Lapinte, S. Caillol, J.-J. Robin, Petro-based and bio-based plasticizers: Chemical structures to plasticizing properties, *Journal of Polymer Science Part A: Polymer Chemistry* 54(1) (2016) 11-33.
- [42] M.I. Cotterell, B.J. Mason, A.E. Carruthers, J.S. Walker, A.J. Orr-Ewing, J.P. Reid, Measurements of the evaporation and hygroscopic response of single fine-mode aerosol particles using a beam optical trap, *Physical Chemistry Chemical Physics* 16 (2014) 2118-2128.
- [43] H.A. Villa-Vélez, H.A. Váquiro, J. Telis-Romero, The effect of power-ultrasound on the pretreatment of acidified aqueous solutions of banana flower-stalk: Structural, chemical and statistical analysis, *Industrial Crops and Products* 66 (2015) 52-61.
- [44] F.L. Seixas, F.R.B. Turbiani, P.G. Salomão, R.P. Souza, M.L. Gimenes, Biofilms composed of alginate and pectin: effect of concentration of crosslinker and plasticizer agents, *Chem Eng Trans* 23 (2013) 1693-1698.
- [45] R.M. Daudt, R.J. Avena-Bustillos, T. Williams, D.F. Wood, I.C. Kulkamp-Guerreiro, L.D.F. Marczak, T.H. McHugh, Comparative study on properties of edible films based on pinhão (*Araucaria angustifolia*) starch and flour, *Food Hydrocoll* 60 (2016) 279-287.
- [46] H.P.S. Abdul Khalil, A. Banerjee, C.K. Saurabh, Y.Y. Tye, A.B. Suriani, A. Mohamed, A.A. Karim, S. Rizal, M.T. Paridah, Biodegradable Films for Fruits and Vegetables Packaging Application: Preparation and Properties, *Food Engineering Reviews* 10(3) (2018) 139-153.
- [47] R.P.H. Brandelero, E.M. Brandelero, F.M.d. Almeida, Biodegradable films of starch/PVOH/alginate in packaging systems for minimally processed lettuce (*Lactuca sativa* L.), *Ciência e Agrotecnologia* 40 (2016) 510-521.
- [48] T. Giancone, E. Torrieri, P. Di Pierro, S. Cavella, C.V.L. Giosafatto, P. Masi, Effect of Surface Density on the Engineering Properties of High Methoxyl Pectin-Based Edible Films, *Food Bioprocess Technol* 4(7) (2011) 1228-1236.
- [49] Z. Maache-Rezzoug, S.A. Rezzoug, K. Allaf, Kinetics of drying and hydration of the scleroglucan polymer. A comparative study of two conventional drying methods with a new

drying process: dehydration by successive pressure drops *Drying Technology* 19(8) (2001) 1961-1974.

[50] B.C. Maniglia, D.R. Tapia-Blácido, Isolation and characterization of starch from babassu mesocarp, *Food Hydrocoll* 55 (2016) 47-55.

[51] K.Z. Win, N. Menon, Glass transition of glycerol in the volume-temperature plane, *Physical review. E, Statistical, nonlinear, and soft matter physics* 73(4 Pt 1) (2006) 040501.

**CAPÍTULO 4: ELABORATION AND CHARACTERIZATION  
OF BIOPOLYMER FILMS WITH ALGINATE AND BABASSU  
COCONUT MESOCARP**

**Trabalho aceito na Revista *Carbohydrate Polymers* em 2019**

## **CAPÍTULO 4: Elaboration and characterization of biopolymer films with alginate and babassu coconut mesocarp**

Ilmar Alves Lopes<sup>a</sup>; Louryval Coelho Paixão<sup>b</sup>; Layrton José Souza da Silva<sup>a</sup>; Adones Almeida Rocha<sup>a</sup>; Allan Kardec D. Barros Filho<sup>c</sup>; Audirene Amorim Santana<sup>a</sup>

<sup>a</sup>*Faculty of Chemical Engineering, Federal University of Maranhão (UFMA), Avenida dos Portugueses, 1966, Bacanga, São Luís – MA, 65080-805, Brazil*

<sup>b</sup>*Interdisciplinary Bachelor of Science and Technology, Federal University of Maranhão (UFMA), Avenida dos Portugueses, 1966, Bacanga, São Luís - MA, 65080-805, Brazil*

<sup>c</sup>*Faculty of Electrical Engineering, Federal University of Maranhão (UFMA), Avenida dos Portugueses, 1966, Bacanga, São Luís – MA, 65080-805, Brazil*

\* *Corresponding authors. Tel. and Fax: +55 98 32729239. Prof. Dr. Audirene Amorim Santana ([audirene.amorim@gmail.com](mailto:audirene.amorim@gmail.com))*

**ABSTRACT:** Biopolymers as films are defined as materials prepared from biological molecules with filmogenic morphology that can be versatile uses. The present research aimed to study formulations of natural polymeric composites based on babassu coconut mesocarp (BCM), alginate and glycerol, to verify the effect of these components on moisture, solubility, thickness and water vapor permeability (WVP) parameters for different cross-linking stages. After a second cross-linking was applied, they presented lower thickness, solubility, and WVP values than first cross-linking. Consecutive analyses for selected film formulations showed that the formulation to solutions of 400 mL with 3g of BCM, 7.5g of alginate and 4.0g of glycerol had the most promising results when correlating physical parameters with thermal analyses, chemical and mechanical properties. Films with amount of babassu coconut mesocarp in the proportion established were sturdy to solubility, leaching and thermal degradation, improved by second cross-linking applied.

**Keywords:** Biopolymer, Babassu coconut mesocarp, Sodium alginate

## 1. Introduction

Natural composites formed from biopolymers such as proteins and polysaccharides have a low impact on the environment and are considered possible substitutes for non-biodegradable petroleum-based polymers in many specific applications such as plastic bag production, food packaging and medical use (Landim et al., 2016). Demand for sustainable materials has increased the interest in this area of research in recent years, due to their wide applicability in the diversity process and products according the characteristics of each composite. Usually in a laboratory scale, the casting technique is used, which consists in adding diluted biocomposites in water in a plate to subsequent drying. While that technique has shown exciting results on the laboratory scale, for industrial scale the extrusion process is usually recommended (Silva et al., 2016; Seixas et al., 2013; Mali, Grossmann, & Yamashit et al., 2010; Fishman et al., 2004).

*Babassu* trees cover about 196 thousand km<sup>2</sup> of Brazilian territory, occurring in the states of Maranhão, Tocantins and Piauí, in the region known as Mata dos Cocais (Carrazza, Ávila, & Da Silva et al., 2012). The palm bark consists of four usable parts, formed by the epicarp (11%), mesocarp (23%), endocarp (59%) and almonds (7%). However, this bark is usually wasted during manual breaking processes (EMBRAPA, 1984). Thus, the development of alternatives that expand their use and make use of these wastes, adding value, has grown.

The mesocarp, found below the epicarp, is usually turned into flour and applied to human food. To obtain this, several processing steps are necessary, starting with the palm collection and ending with the storage of the final product, going through the processes of selection, washing, peeling, drying, grinding the flakes and sieving. Its chemical composition consists mainly of 66.51% starch, 6.8% dietary fiber, 1.19% protein, 0.29% ether extract (Carrazza, Ávila, & Da Silva et al., 2012), among other elements. The starch is formed by amylopectin and amylose, and has the physical, chemical and functional properties to form gels and films (Mali, Grossmann, & Yamashit et al., 2010). Therefore, considering the high concentration of starch in the mesocarp, its application in the production of biopolymers becomes feasible. The application of babassu coconut mesocarp has been studied for the production of films and blends, among other applications (Cinelli et al., 2014; Maniglia et al., 2017; Teixeira et al., 2018; Nunes et al., 2018; Da Silva et al., 2019), mainly considering its anti-inflammatory potential, as studied by Barroqueiro et al. (2011, 2016), Maniglia & Tapia-Blácido (2016) and Maniglia et al. (2017). Da Silva et al. (2018) studied the effect of babassu coconut mesocarp with anti-inflammatory effect on leishmaniasis infection.



Alginate is a polysaccharide extracted from brown algae called *Phaeophyceae*, which, in molecular terms, consists of copolymers of 1-4 bonds of  $\beta$ -D-manuronic acid (M) and  $\alpha$ -L-guluronic acid (G), of varying composition and sequential structure. In addition to applications in the food and pharmaceutical industries, it is also considered a potential structural component of films and coatings due to its unique colloidal properties, including thickening, emulsion stabilization, suspension, gel production, etc. (Moe, 1995; Harper et al., 2015). According to Bierhalz et al. (2014), the different alginate sources and variations in their structure influence one of the main characteristics of this polysaccharide: the ability to form thermostable gels in the presence of divalent ions (such as calcium ions).

Cross-linking the polymeric structure with calcium considerably reduces the water solubility of alginate films as well as their flexibility, furthermore, a plasticizer is added to improve physical and mechanical properties. The choice of the plasticizer depends on its compatibility with the polymer and solvent used. In the case of sodium alginate biopolymers, glycerol is the plasticizer that has proven to be very practical and efficient (Santana & Kieckbusch, 2013). Extant literature points to the use of a second cross-linking to increase the effect of improving these properties (Bierhalz et al., 2014; Santana & Kieckbusch, 2013; Silva, Bierhalz, & Kieckbusch, 2009).

From a socio-economic point of view, it is important to notice the regional relevance of the use of babassu coconut in Northeast of Brazil, particularly in Maranhão State, as it usually increases the economic value of residues. Moreover, one has to consider the potential use of those products to improve the quality of life in the communities involved in the coconut extractivism (Campos et al., 2015; Souza et al., 2011). The choice of alginate is mainly linked to films as well as to blends and composites in industrial and medical applications (Parreidt et al., 2018; Bierhalz & Moraes, 2017). Glycerol is non-expensive, non-toxic while being excellent plasticizer agent to biopolymers and a residue in biodiesel production (Paixão et al., 2019).

Considering the above, bioplastics were elaborated using different concentrations of babassu coconut mesocarp, alginate and glycerol, and cross-linking with calcium chloride in order to evaluate the effect of these components on the final characteristics of these films before and after complementary cross-linking.

## **2. Material and methods**

### **2.1 Materials**

Alginic acid sodium salt (A-2033, average molar mass of 90 kDa, intrinsic viscosity of 690 mL/g at 25 °C, composed of 61% mannuronic acid and 39% guluronic acid) was obtained from Sigma-Aldrich (USA). Dihydrated calcium chloride (Merck, Darmstadt, Germany), glycerol (Synth, Diadema, Brazil), and babassu coconut (*Orbignya phalerata* Mart.) mesocarp powder with a moisture content of  $1.9 \pm 0.1$  (% w.w.b), ash content of  $2.34 \pm 0.77$  (g/100g, w.w.b), determined by AOAC method 926.12 (AOAC, 2006), and mean diameter ( $D_p$ ) of  $5330.867 \pm 1980.585$  nm (determined by photon correlation spectroscopy using a dynamic light scattering ZetaPlus equipment (model 90Plus/BI-MAS, Brookhaven Instruments Corporation, USA) at a 625 nm wavelength, 25 °C and incidence angle of 90°), extracted manually from the whole fruit, washed with distilled water, dried at 70 °C in an air recirculating oven (Fanem, model 099EV, Brazil) and sieved on a vibratory table by a Tyler sieve.

### **2.2 Elaboration of Composites**

The elaboration of bioplastics was based on the methodology by Santana and Kieckbusch (2013) with some modifications. The composites were made by casting with a two-stage cross-linking. In the first stage, the sodium alginate and the babassu coconut mesocarp (Table 1) were dissolved in distilled water (400 mL) under constant magnetic stirring. The choice of formulations is grounded on the fact that films without glycerin have insufficient elasticity for the desired application. Glycerol plasticizer was then added at the concentrations shown in Table 1 at room temperature ( $25 \pm 1$  °C). The solution was mechanically stirred at 5,000 rpm (Fisaton, model 67, Brazil) for about 1 hour to ensure homogeneity and then heated to 70 °C using a heating blanket. Subsequently, 30 mL of a pre-cross-linking solution (1.0g/100mL  $\text{CaCl}_2 \cdot 2\text{H}_2\text{O}$ ) was slowly added at a flow rate of 0.6 mL/min using a peristaltic pump (Masterflex, model 77120-70, USA). A low flow rate and strong agitation were necessary to avoid local gelation. Aliquots of the solution (70 g) were placed in glass petri dishes (15 cm in diameter) which were dried at 40 °C in an air recirculating oven (Fanem, model 099EV, Brazil) for 24 hours with a flow of 1.1 m/s. After drying, the films were removed from the holder and stored at 52% RH and 25 °C for 48 hours.

**Table 1:** Planning for the elaboration of polymeric composites formulations.

<b>Formulation</b>	<b>BCM (g)</b>	<b>Alginate (g)</b>	<b>Glycerol (g)</b>
F1	1.0	6.0	3.0
F2	2.0	6.0	3.0
F3	3.0	6.0	3.0
F4	1.0	7.5	4.0
F5	2.0	7.5	4.0
F6	3.0	7.5	4.0
F7	1.0	9.0	5.0
F8	2.0	9.0	5.0
F9	3.0	9.0	5.0

BCM: Babassu coconut mesocarp

The cross-linking process was then completed soon after in the following stage (second stage) by fully immersing the films in 50 mL of an aqueous  $\text{Ca}^{2+}$  solution (3.0g/100 mL) for 5 min at room temperature ( $25 \pm 1^\circ\text{C}$ ). The treated films were removed from the bath, allowed to drain and placed on an acrylic plate, with the edges of the films fixed by the weight of a frame made of a stainless-steel tube to prevent wrinkling. These plates were then inserted into a tunnel-type dryer with a parallel air flow of 1.1 m/s at  $30^\circ\text{C}$  and RH above 60% for 24 hours. After this drying process, they were conditioned in the same condition as the films from the first stage, until the characterization tests were performed.

## **2.3 Physical characterization of composites**

### **2.3.1 Visual aspect**

A subjective evaluation was carried out according to visual and tactile observations with a view to using only films that were homogenous (absence of insoluble particles and uniform color), continuous (no ruptures or brittle zones), with a smooth surface which makes handling easier (easier to remove from support) and with good flexibility. Films not presenting these characteristics were disposed of.

### **2.3.2 Thickness ( $\delta$ )**

The film thickness was determined using a digital micrometer (Mitutoyo, model MDC-25S, Japan) with a resolution of 0.001 mm. The final thickness was calculated by the arithmetic mean of ten measurements at different symmetrical points over an area of  $32\text{ cm}^2$ .

### **2.3.3 Moisture content ( $\omega$ )**

The greenhouse-assisted gravimetric method (model SL-100/A, Solab, Brazil) was used at  $105^\circ\text{C}$  for 24h, according to AOAC 926.12 methodology (AOAC, 2006). Moisture was determined in triplicate for each formulation and expressed as mass fraction.

### 2.3.4 Water soluble mass (S)

The water soluble mass was determined in triplicate by adapting the methodology used by Da Silva et al. (2019). Determined masses of each film ( $m_i$ ) were immersed in 50 mL of distilled water and then placed under constant stirring, 100 rpm, on a shaking table (model 3545-40-EA, Termo Fisher SciInc, USA) for 24h at room temperature ( $25 \pm 1$  °C). The material was then dried in an oven (model SL-100/A, Solab, Brazil) for 24h at 105 °C, obtaining the dry mass ( $m_f$ ). Water soluble mass values were found according to Eq. 1.

$$S = \left\{ \frac{m_i(1-\omega) - m_f}{m_i(1-\omega)} \right\} \times 100 \quad (1)$$

### 2.3.5 Water vapor permeability (WVP)

Water vapor permeability was determined in triplicate using gravimetric method at room temperature ( $25 \pm 1$  °C) using E96M-16 (ASTM, 2016) methodology and acrylic containers filled with anhydrous calcium chloride granules (Ecibra, Brazil), which maintains the relative humidity of approximately 0%. The films were layed on an open container, in order to form a “membrane”. Then, it was placed in another container with sodium chloride (Synth, Brazil) with a thin solution of this salt at the bottom, which provides an environment with relative humidity of approximately 75%, closing the system difference in vapor pressure it is form, leading the water vapor from the bigger container, with contains the solution of sodium chloride, to the thinner container, with the anhydrous calcium chloride granules. The rate of increase in the total mass of the film was obtained by monitored measurements over 120h, corresponding to the water permeability rate across the film. WVP values were obtained using Eq. 2.

$$PVA = \left[ \frac{G\delta}{A_e \Delta P_a} \right] \quad (2)$$

Where: WVP is the water vapor permeability of the film [(g.mm)/(m<sup>2</sup>.day.kPa)];  $\delta$  is the thickness of the film (mm);  $A_e$  is the exposed area of the film (m<sup>2</sup>);  $\Delta P_a$  is the water vapor pressure (kPa),  $G$  is the water permeability rate (g/day), calculated by linear regression of the mass to time ratio.

## 2.4 Analysis of selected films

### 2.4.1 Scanning Electron Microscopy (SEM)

The morphology of the produced films was carried out using a Scanning Electron Microscope (model TM3030, Hitachi, Japan), operating at 5 kV. The samples were mounted on a carbon tape and impregnated using a gold layer. Observations of the surface and interior of the films were made (after breaking).

#### **2.4.2 Thermal Analysis: Thermogravimetry and Differential Exploratory Calorimetry**

Non-isothermal data and the gases distribution were identified using a NETZSCH Perseus STA 449 F3 STA/FT-IR coupled system. TG-DSC curves were carried out in an S-type carrier and a rhodium furnace with open alumina crucibles, helium atmosphere (50 mL.min<sup>-1</sup>), heating rate 10.0°C.min<sup>-1</sup>, temperature range of 35–400°C and sample weight of approximately 500.0 mg. Equal experimental parameters were adopted to both TGA and DSC runs.

#### **2.4.3 Fourier Transform Infrared Spectroscopy (FTIR)**

An infrared spectrometer (IR-Prestige model, Shimadzu, Japan) was used, with a resolution of 4 cm<sup>-1</sup> and a scanning range of 400 to 5000 cm<sup>-1</sup>, using powder from the material on pellets with potassium bromide (Da Silva et al., 2019).

#### **2.4.4 Mechanical properties**

Tensile strength, elongation at break and modulus of elasticity were determined for the film samples (through ten 10 × 2.5 cm samples) using ASTM standard method D882-12 (ASTM, 2012) at a temperature of 25 °C±1 °C and a relative humidity of 55±3%. The tensile test speed used was 1 cm/s.

#### **2.4.5 Time and degree of swelling**

The swelling time is a very important parameter for determining the durability of films in an aqueous medium. The procedure was performed by measuring the initial mass of the film and immersing it in distilled water at room temperature (25±1 °C) with low agitation. At certain times the film was removed, gently compressed on filter paper to remove excess surface water and weighed and then returned to the aqueous medium. The total swelling time was determined when the mass of the film became constant. The degree of swelling was calculated as a function of the total initial mass.

#### **2.4.6 Degradation**

Material degradability was determined according to ASTM G160-1998 in the following experimental conditions: soil pH 6.5-7.5 and soil relative humidity between 85-95%, temperature 22 ± 8°C over a period of 60 days. The material was exposed to soil with mineral, animal and vegetable matter. Eq. 3 was used to determine the lost mass:

$$D(\%) = \frac{m_f - m_i}{m_i} \times 100 \quad (3)$$

Where:  $m_f$  is the mass after the established period and  $m_i$  the initial mass of the samples.

## 2.5 Statistical Analysis

Analysis of variance and Tukey test were employed to determine statistically significant differences ( $p < 0.05$ ) between means using the Statistica V9 software (Statsoft, Tulsa, USA).

## 3. RESULTS AND DISCUSSION

### 3.1 Analysis of the visual aspect

After the 9 assays of the first stage, the films were characterized according to their visual aspect. In general, they were visually attractive, homogeneous, transparent, without brittle zones, with good flexibility as well as ease of detachment from the support. (Fig. 1).

Some formulations were found to be slightly stained and slightly opaquer than shown in Fig. 1. This decrease in film transparency, however, does not preclude their use. According to Maniglia et al. (2017), the reduction in the transparency of films can be explained by the higher amount of lipids and/or proteins present in the babassu coconut mesocarp. After the application of the cross-linking solution (second stage), the films were more compact and resistant and less flexible, but without brittle zones.

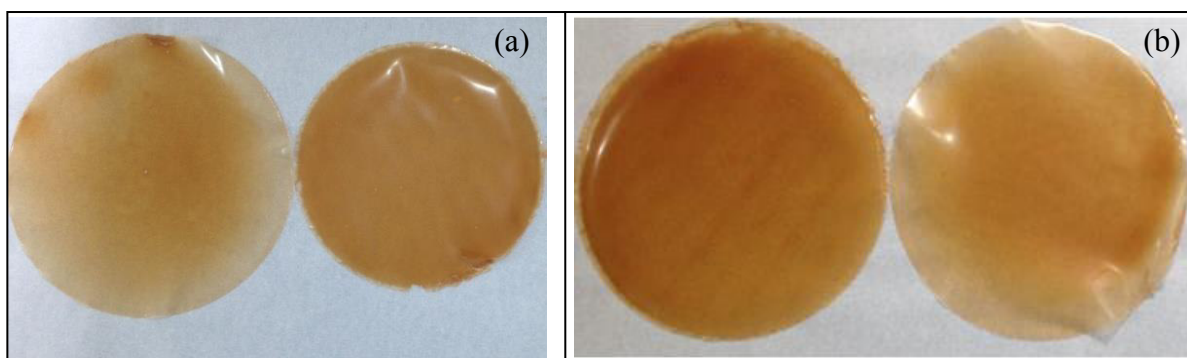


**Fig. 1:** Photographs of the film prepared with babassu coconut mesocarp, alginate, glycerol and cross-linked with  $\text{CaCl}_2 \cdot 2\text{H}_2\text{O}$ : (a) formulation F6, first stage on left, second stage on right; (b) formulation F7, first stage on left, second stage on right.

### 3.2 Physicochemical characterization

In Table 2, the mean values and standard deviation of the physical properties studied in the first and second stages (complementary cross-linking) were organized. Through multiple comparisons, the Tukey's test was exemplified by the insertion of alphabetic letters.

Considerable variations were observed in the moisture content and solubility for the different formulations, with mean values of moisture content ranging from 36.4 (F3 and F6) to 46.5% (F2) on first stage, 11.8 (F2) to 24.3% (F7) on second stage. Solubility ranged from 13.7 (F6) to 22.3% (F7) on first stage, 4.2 (F6) to 14.0% (F2 and F7) on the second stage, as it is showed in Table 2. In their studies of films prepared with babassu mesocarp flour or starch,

Maniglia et al. (2017) found lower moisture values (7.33 to 11.82%), compared with those obtained in the first stage and close to those found in the second stage herein. For solubility, the values obtained by these authors were close to those found in the first stage (24.32 to 39.02%). These results show the effect of the mesocarp on the biopolymer structure.

Statistically, the humidity values for all tests performed in the first stage did not differ. For solubility, there was variation at the 5% level of significance. Comparing the treatments with and without the application of complementary cross-linking, the moisture and solubility of the tests presented statistical difference, obtaining lower values in the second stage, confirming the expectations. This fact can be explained by the closure of the polymeric chain due to the addition of calcium chloride applied in the second treatment, making the composites less hygroscopic. Studying glycerol-plasticized alginate films in two treatments (first and second stage), Bierhalz et al. (2014) observed similar behavior.

The thickness of films composed of babassu coconut mesocarp and alginate as matrices did not present statistical significance between the assays in each treatment. However, comparing the treatments, only assays 3 and 6 were the same, while the other assays of the second stage were smaller than those of the first, indicating that the application of these films in a second solution of calcium chloride, makes them less thick. According to Santana and Kieckbusch (2013), an accurate determination of the biopolymer thickness is important, as it works as a basis for calculating various functional properties of films and is fundamental for repeatability analysis. However, film thickness is still a challenge for the commercialization of biopolymers, because while the polyethylene films have a low thickness and are resistant to water vapor permeation, the films made with babassu coconut mesocarp and alginate, for example, still leave a lot to be desired regarding this feature.

The lowest WVPs were obtained in F1 in both treatments, with values of 2.5 and 1.4 g.mm/m<sup>2</sup>.day.kPa for the first and second stages, respectively. Comparing the treatments, formulations F2 and F6 obtained statistically equal values. However, the other assays of the second stage were smaller than those of the first, showing that the immersion of these biopolymers in a second cross-linker solution makes them less permeable, and may be compared with commercial polyethylene films in the future.

Despite obtaining low WVP values compared to others in the literature (Bierhalz et al., 2014; Lopes et al., 2017), the films are within the average value range for the matrices used. These films may also have potential use in the biomedical area because they have bioactive constituents related to the antioxidant activity of the presence of phenolic compounds in the babassu coconut mesocarp (Maniglia & Tapia-Blácido, 2016).

### 3.3 Selected Films

Films were selected according to the physical parameters (moisture content, solubility, thickness and water vapor permeability) and repetition consistency established by Tukey's test. The selected conditions were: Formulation 1 (F1), with MCB = 1 g, A = 6.0 g and G = 5.0 g; Formulation 6 (F6), with MCB = 6.0 g, A = 7.5 g and G = 4.0 g; and Formulation 7 (F7), with MCB = 1.0 g, A = 9.0 g and G = 5 g.

#### 3.3.1 Fourier Transform Infrared Spectroscopy

Fig. 2 shows the spectrum of alginate and babassu coconut mesocarp powder. It shows alginate peaks on characteristics vibration zones of groups -OH, -CH, C-O-C, on bands around  $3400\text{ cm}^{-1}$ ,  $2930\text{ cm}^{-1}$  and  $1051\text{ cm}^{-1}$ , respectively.

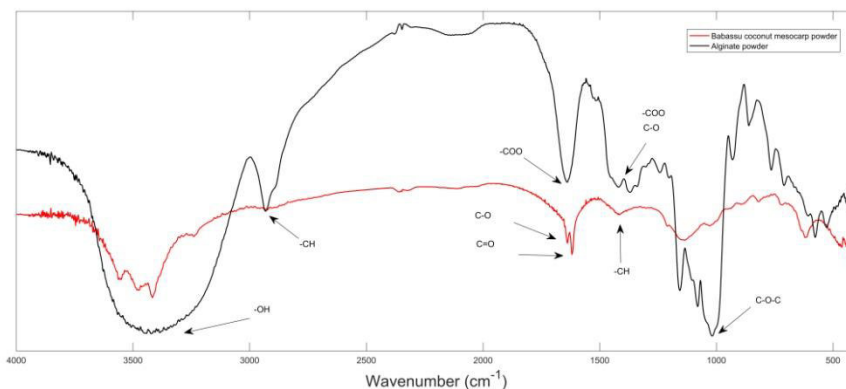


**Fig. 2:** Infrared spectra of alginate and babassu coconut mesocarp powder.

Fig. 3 shows the infrared spectra of the selected films. It is observed that the characteristic peaks of the alginate are in the region between  $1620\text{ cm}^{-1}$  related to the asymmetric  $-\text{COO}$  group elongations and at  $1400\text{ cm}^{-1}$  related to the symmetrical  $-\text{COO}$  groups. Peaks related to C-O-C groups are observed in the region of  $1050\text{ cm}^{-1}$ . A large area related to the presence of OH groups is present in the region between  $3600\text{--}3200\text{ cm}^{-1}$  (Pereira et al., 2012; Xiao, Gu, & Tan, 2014).

As observed in literature (Da Silva et al., 2019; Lopes et al., 2017; Maniglia et al., 2017), the presence of the mesocarp next to pectin, and especially the effect of the second cross-linking stage, caused a decrease in  $-\text{OH}$  peak intensity, related to the interaction properties of the polymer in relation to humidity, as expected, since it is evident as to the visual and tactile appearance that the films were more rigid and drier after complementary cross-linking.



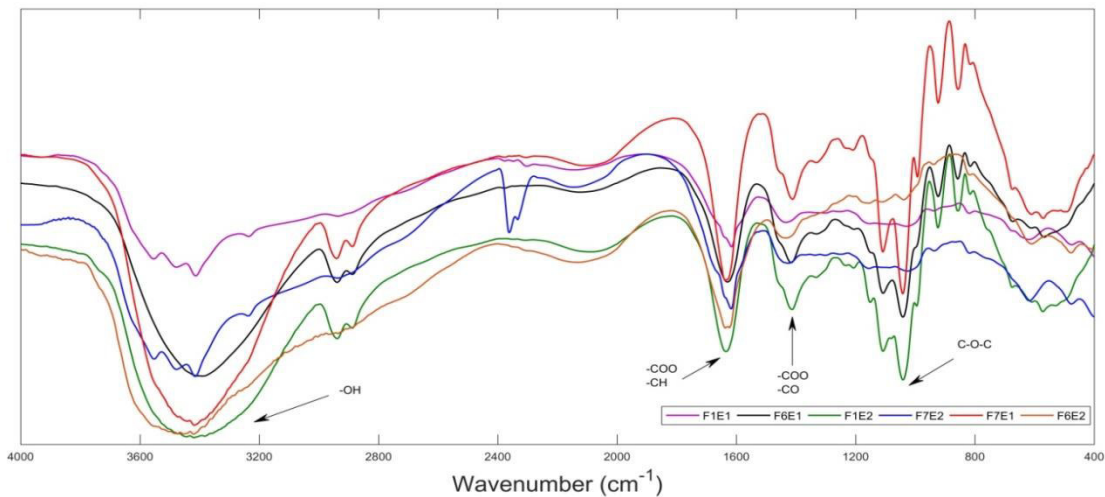


**Fig. 3:** Overlapping infrared spectra of selected polymer composites of alginate and babassu coconut mesocarp.

### 3.3.2 Thermal Analysis: Thermogravimetry and Differential Exploratory Calorimetry

The TGA graph is presented in Fig. 4(a). It is observed that the degradation process of the first stage films (F1E1, F6E1 and F7E1) started at a temperature of approximately 220 °C. After the complementary cross-linking (second stage), the same formulations began to degrade at higher temperatures, showing a slightly higher stability of these films (F1E2, F6E2 and F7E2). This degradation was similar to that observed by Pereira et al. (2012). Regarding the curved and slightly steep profile of mass loss, Tan et al. (2016) obtained results for starch films incorporated with higher fiber temperatures for onset of degradation, showing the possibility of incorporation of fibers into the matrices to obtain better thermal and, consequently, mechanical stability. The babassu coconut mesocarp may have played the role of fibers in the films.

In Fig. 4(b), the DSC graph obtained for the selected formulations can be observed. An endothermic peak at approximately 70 °C can be seen very clearly for all formulations, which may be associated with the sample dehydration process. Contrary to the observation of Pereira and collaborators (2012), peaks around 180 °C associated with the recrystallization phenomenon were not observed, except for a small exothermic peak at 204.4 °C of Formulation 1 film, of the first stage. The peaks at 220 °C in all films can be explained by the onset of total sample degradation, confirmed by the TGA graph (Fig. 3), which occurred quickly and unstably, demonstrating an abrupt thermal degradation of the material. No more evident peaks related to the presence of higher concentration of cross-linking agent were observed in the films, considering the films that underwent the second cross-linking. It was not possible to confirm the glass transition temperature of the material by DSC scanning,

since this is between -23 to 10 °C, as cited for alginate films (Harper et al., 2015; Bierhalz et al., 2014; Santana & Kieckbush, 2013; Chaudhary, Adhikari, & Kasapis, 2011), values not covered in the scan performed; This score denotes that the material may have elastic properties at low and environmental temperatures, such as natural rubber and low density polyethylene, the latter widely used in the manufacture of plastic bags. The presence of babassu coconut mesocarp may have contributed to the increase in glass transition temperature, as presented in the literature for starch films (Maniglia & Tapia-Blácido, 2016; Chuang et al., 2015; Souza & Andrade, 2000; Hermasson & Svegmarm, 1996).

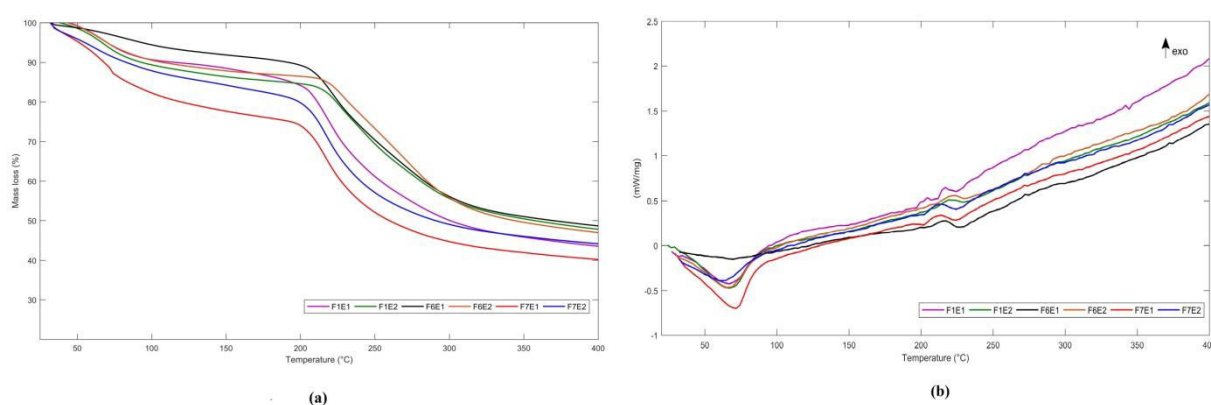


**Fig.4:** TG (a) and DSC (b) curves of selected polymer composites from alginate and babassu coconut mesocarp.

### 3.3.3 Mechanical Characterization

The results for the mechanical tests performed on the selected films in the first and second stages are presented in Table 3, where the effect of the second cross-linking performed on the mechanical behavior is statistically evident. The Tensile strength and elongation at break of the films are close to values found in the literature for alginate films (Harper et al., 2015; Bierhalz et al., 2014; Santana & Kieckbusch, 2013), and approximate values found by Maniglia et al. (2017) for babassu coconut mesocarp films. While the presence of this material decreased the tensile strength, but without compromising the Young's modulus, it follows the linear relationship regarding the presence of the plasticizer used, glycerol, with a higher value for assay F7, where there is a greater presence. This is similar to the behavior observed by Ngo et al. (2018) when studying alginate and pectin blends incorporated with ZnO nanoparticles, with the changes in stress and elongation at break being due to the formation of hydrogen bridges between the matrices used in the present work. It is noted that an addition of 1g in F1 and F7 were most satisfactory, while the agglomeration of

unsatisfactorily gelatinized starch granules that weaken the film structure was also evident, as can be seen in micrographs.

### **3.3.4 Degradation**

Table 3 shows the results of degradation, which were more stable than films of pectin and pure alginate to degradation (Lopes et al, 2017; Solak & Dyankova, 2014). In 60 days the films ranged between 63-78% in first stage and between 85-90% in the second stage. The larger loss mass in the second stage was due to fractures, as can be seen in the SEM images. These fractures provided the action of organic matter decomposing microorganisms.

### **3.3.5 Scanning Electron Microscopy**

The SEM micrographs of the surfaces and cross sections of the selected films (first stage and second stage) are shown in Figs. 5 and 6. It is evident that there is an intense formation of crystals on the surface due to the decrease in solubility caused by the presence of the babassu coconut mesocarp, a result similar to that observed by Santana and Kieckbusch (2013) when using mannitol, a low solubility plasticizing agent, in alginate films. In Figs. 5 and 6, it is observed that there was a relative decrease of crystal formation, or its greater compaction as seen in the F6 and F7 micrographs, which were washed by the second cross-linking. Arzate-Vázquez et al. (2012) note that the compaction that occurs in films characterizes them as strong films. The most compact film was F6 after the second cross-linking, Figs. 6(c) and 6(d), observing the cross section. Complementary cross-linking caused some fractures in F1, a formulation with a low proportion of the babassu coconut mesocarp. The micrograph also revealed the presence of starch granules that were not solubilized (white circles). Non-solubilized granules may cause structural nonconformity due to their non-gelatinization (Mei et al., 2016; Souza & Andrade, 2000; Hermasson & Svegmarm, 1996).

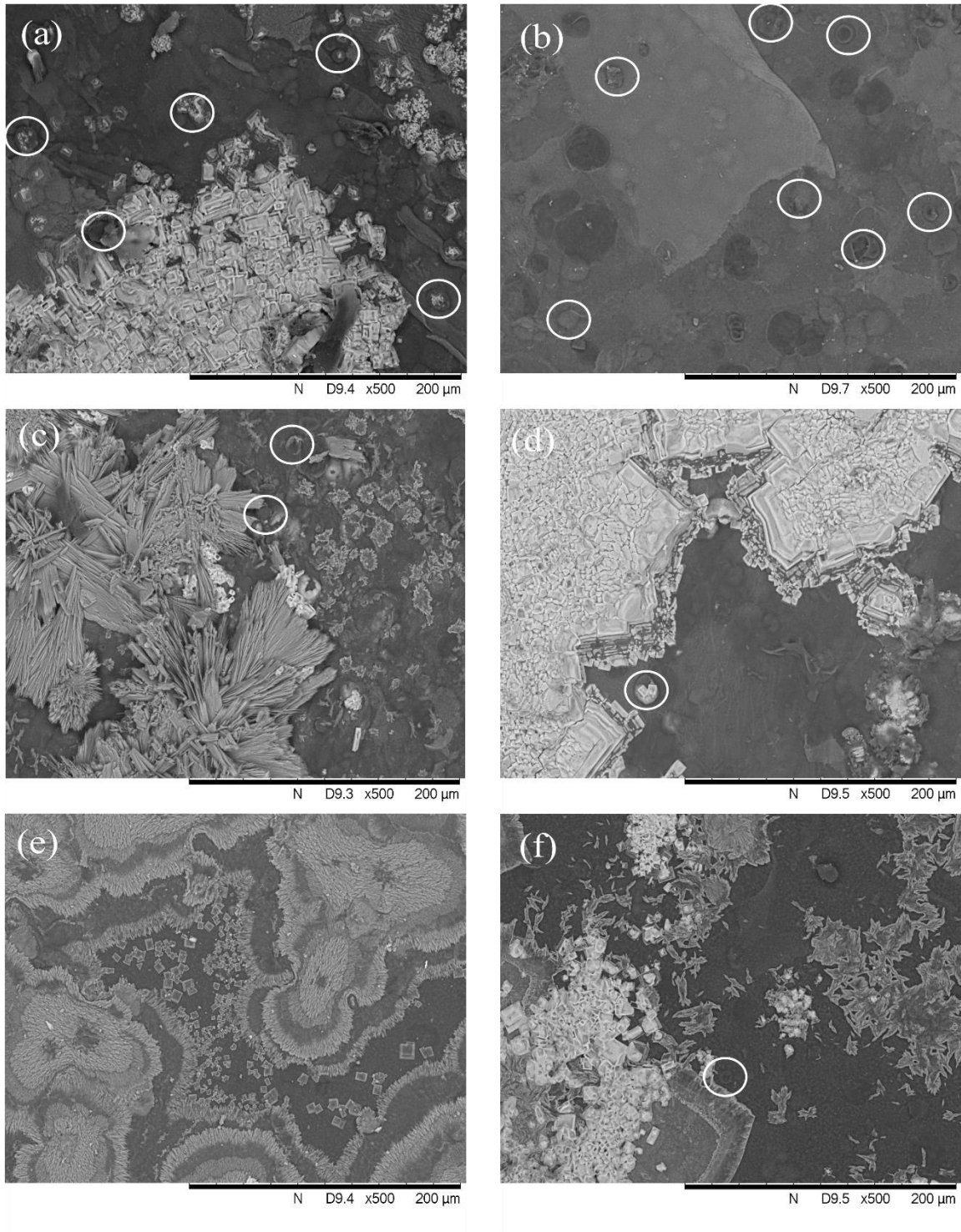


**Fig. 5:** Micrograph of the polymer composites of babassu coconut mesocarp and alginate in the first stage (left), and second stage (right), of the surface: (a,b), (c,d), (e,f), formulations films 1, 6 and 7, respectively.

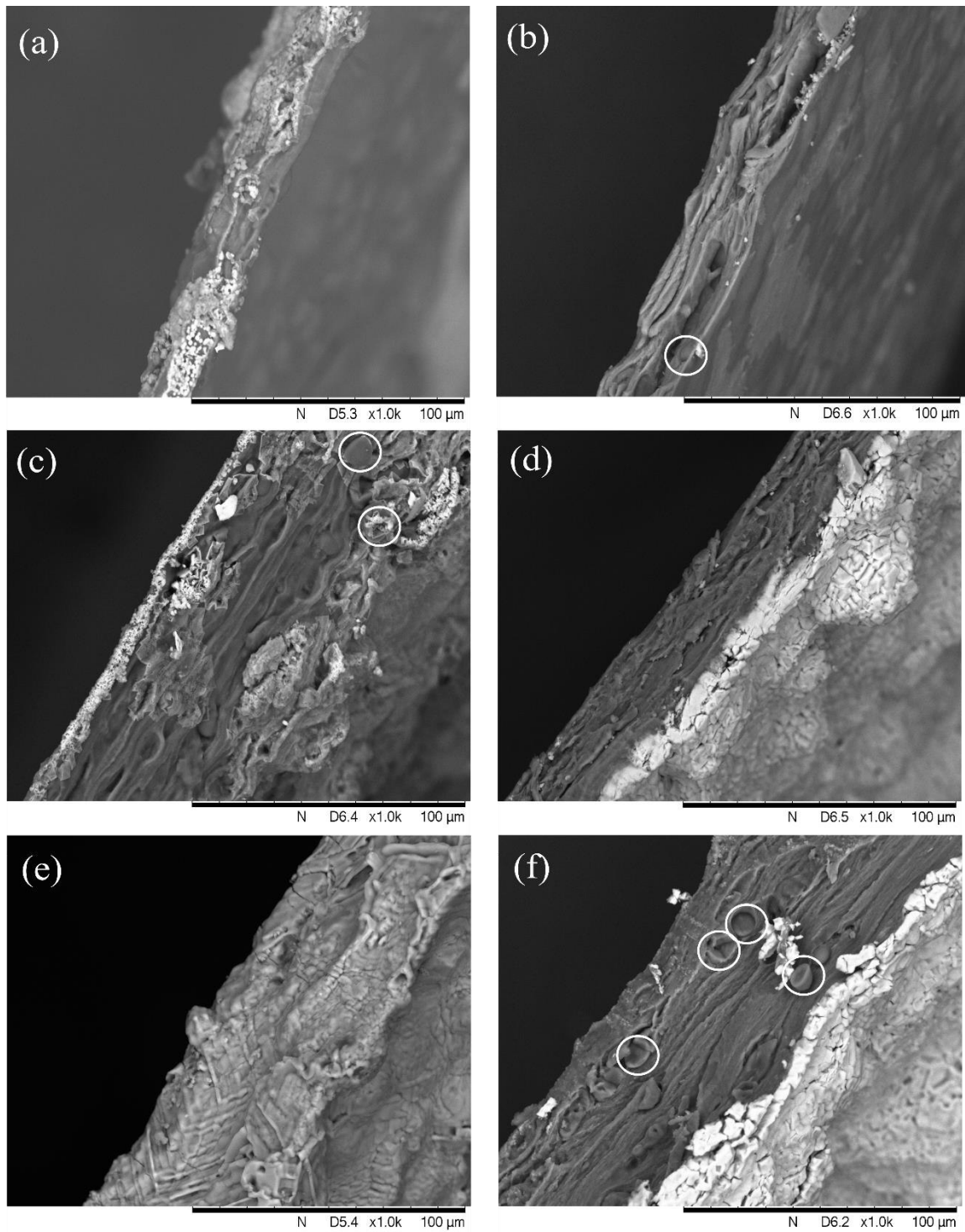


**Fig. 6:** Micrograph of the polymer composites of babassu coconut mesocarp and alginate in the first stage (left), and second stage (right), of the cross-section: (a,b), (c,d), (e,f), formulations films 1, 6 and 7, respectively.

**Table 2:** Moisture content ( $\omega$ ) and water solubility (S), thickness ( $\delta$ ) and water vapor permeability (WVP) of the babassu coconut mesocarp and alginate polymer composites in the first and second stages.

Formulation	$\omega_1$	$\omega_2$	S <sub>1</sub>	S <sub>2</sub>	$\delta_1$	$\delta_2$	WVP <sub>1</sub>	WVP <sub>2</sub>
F1	40.644±1.257 <sup>aB</sup>	21.485±2.715 <sup>cdA</sup>	18.265±1.989 <sup>bcB</sup>	9.345±0.282 <sup>cA</sup>	0.06±0.000 <sup>aB</sup>	0.040±0.000 <sup>aA</sup>	2.523±0.214 <sup>aB</sup>	1.405±0.074 <sup>dA</sup>
F2	46.491±0.913 <sup>aB</sup>	11.752±2.816 <sup>aA</sup>	22.211±1.804 <sup>cB</sup>	13.673±1.338 <sup>dA</sup>	0.08±0.006 <sup>aB</sup>	0.060±0.010 <sup>aA</sup>	3.333±0.435 <sup>aA</sup>	3.285±0.137 <sup>bcdA</sup>
F3	36.395±3.534 <sup>aB</sup>	17.982±2.802 <sup>bcA</sup>	15.981±0.939 <sup>abB</sup>	7.339±0.476 <sup>bcA</sup>	0.06±0.006 <sup>aA</sup>	0.050±0.000 <sup>aA</sup>	3.650±0.767 <sup>abB</sup>	2.095±0.732 <sup>abcA</sup>
F4	46.257±0.408 <sup>aB</sup>	20.529±2.816 <sup>bcdA</sup>	17.966±0.687 <sup>bbB</sup>	8.311±0.855 <sup>bcA</sup>	0.10±0.015 <sup>aB</sup>	0.040±0.000 <sup>aA</sup>	4.047±0.840 <sup>abB</sup>	2.020±0.257 <sup>abA</sup>
F5	39.193±3.186 <sup>aB</sup>	16.552±2.717 <sup>abA</sup>	16.594±0.950 <sup>abB</sup>	6.315±0.563 <sup>abA</sup>	0.08±0.006 <sup>aB</sup>	0.050±0.000 <sup>aA</sup>	4.090±0.390 <sup>abB</sup>	2.250±0.387 <sup>abcA</sup>
F6	36.401±1.314 <sup>aB</sup>	12.980±3.774 <sup>abA</sup>	13.693±0.968 <sup>aB</sup>	4.170±1.348 <sup>aA</sup>	0.09±0.006 <sup>aA</sup>	0.070±0.010 <sup>aA</sup>	4.305±0.401 <sup>abA</sup>	4.056±0.696 <sup>dA</sup>
F7	45.051±2.803 <sup>aB</sup>	24.313±1.633 <sup>dA</sup>	22.257±0.718 <sup>cB</sup>	13.955±0.882 <sup>dA</sup>	0.09±0.015 <sup>aB</sup>	0.045±0.005 <sup>aA</sup>	3.117±0.214 <sup>aB</sup>	1.885±0.005 <sup>abA</sup>
F8	42.551±2.079 <sup>aB</sup>	15.278±2.097 <sup>abA</sup>	22.270±2.633 <sup>cB</sup>	12.703±0.812 <sup>dA</sup>	0.09±0.023 <sup>aB</sup>	0.063±0.004 <sup>aA</sup>	3.927±1.326 <sup>abB</sup>	2.680±0.198 <sup>abcA</sup>
F9	38.081±0.563 <sup>aB</sup>	12.304±1.919 <sup>aA</sup>	16.132±1.472 <sup>abB</sup>	7.168±0.907 <sup>bcA</sup>	0.10±0.015 <sup>aB</sup>	0.065±0.005 <sup>aA</sup>	5.153±1.029 <sup>bbB</sup>	3.615±0.024 <sup>cdA</sup>

$\omega_1$  is the water content in the first stage (%);  $\omega_2$  is the water content in the second stage (%); S<sub>1</sub> is the solubility in the first stage (%); S<sub>2</sub> is the solubility in the second stage (%);  $\delta_1$  is the thickness in the first stage (mm);  $\delta_2$  is the thickness in the second stage (mm); WVP<sub>1</sub> is the water vapor permeability in the first stage [(g.mm)/(m<sup>2</sup>.day.kPa)]; WVP<sub>2</sub> is the water vapor permeability in the second stage [(g.mm)/(m<sup>2</sup>.day.kPa)]; Mean ± standard deviation; Averages with the same lowercase letter in each column indicate that there is no significant difference (p <0.05) by the Tukey test; Averages with the same uppercase letter on each line indicate that there is no significant difference (p <0.05) by the Tukey test.

**Table 3:** Tensile Strength (TS), elongation at break (e), Young's Modulus (E), and degradability (D) of the babassu coconut mesocarp and alginate polymer composites in formulations F1, F6 and F7.

Formulation	TS <sub>1</sub> (MPa)	e <sub>1</sub> (%)	E <sub>1</sub> (MPa)	TS <sub>2</sub> (MPa)	e <sub>2</sub> (%)	E <sub>2</sub> (MPa)	D <sub>1</sub> (%)	D <sub>2</sub> (%)
F1	1.446±0.132 <sup>aA</sup>	22.219±3.216 <sup>bbB</sup>	14.05±0.011 <sup>aB</sup>	6.119±0.981 <sup>baA</sup>	10.528±0.958 <sup>abA</sup>	448.33±92.222 <sup>aB</sup>	77.885±0.302 <sup>aB</sup>	85.284±0.253 <sup>caA</sup>
F6	2.980±0.175 <sup>baA</sup>	16.757±2.150 <sup>aB</sup>	30.66±0.230 <sup>bbB</sup>	3.445±0.148 <sup>aA</sup>	9.404±0.553 <sup>aA</sup>	594.793±56.529 <sup>bbB</sup>	63.537±0.080 <sup>cbB</sup>	87.195±0.062 <sup>baA</sup>
F7	3.445±1.269 <sup>caA</sup>	21.059±5.926 <sup>bbB</sup>	28.432±17.423 <sup>bbB</sup>	3.848±5.926 <sup>abA</sup>	14.274±3.327 <sup>baA</sup>	764.667±136.824 <sup>cbB</sup>	66.657±0.016 <sup>cbB</sup>	90.074±0.117 <sup>aA</sup>

Index 1: Reference to first stage films; Index 2: reference to second stage films of the; Mean ± standard deviation; Averages with the same lowercase letter in each column indicate that there is no significant difference (p <0.05) by the Tukey test; Averages with the same uppercase letter on each line indicate that there is no significant difference (p <0.05) by the Tukey test.

### 3.3.6 Time and degree of swelling

The films in the first stage were very fragile as they swelled, making the analysis procedure unfeasible. Thus, this analysis was performed only for films with complementary cross-linking. Due to a certain hygroscopic capacity of the materials used in the fabrication of composites, the swelling tests revealed a high water absorption capacity. Swelling occurs quite rapidly, with a time of approximately 10 minutes, Figure 7. Literature indicates that the degree of swelling does not vary significantly with the amount of plasticizer (Santana & Kieckbusch, 2013; Bierhalz et al., 2014), it can be inferred that the presence of higher alginate concentration led to high swelling of film formulation 7 (F7).

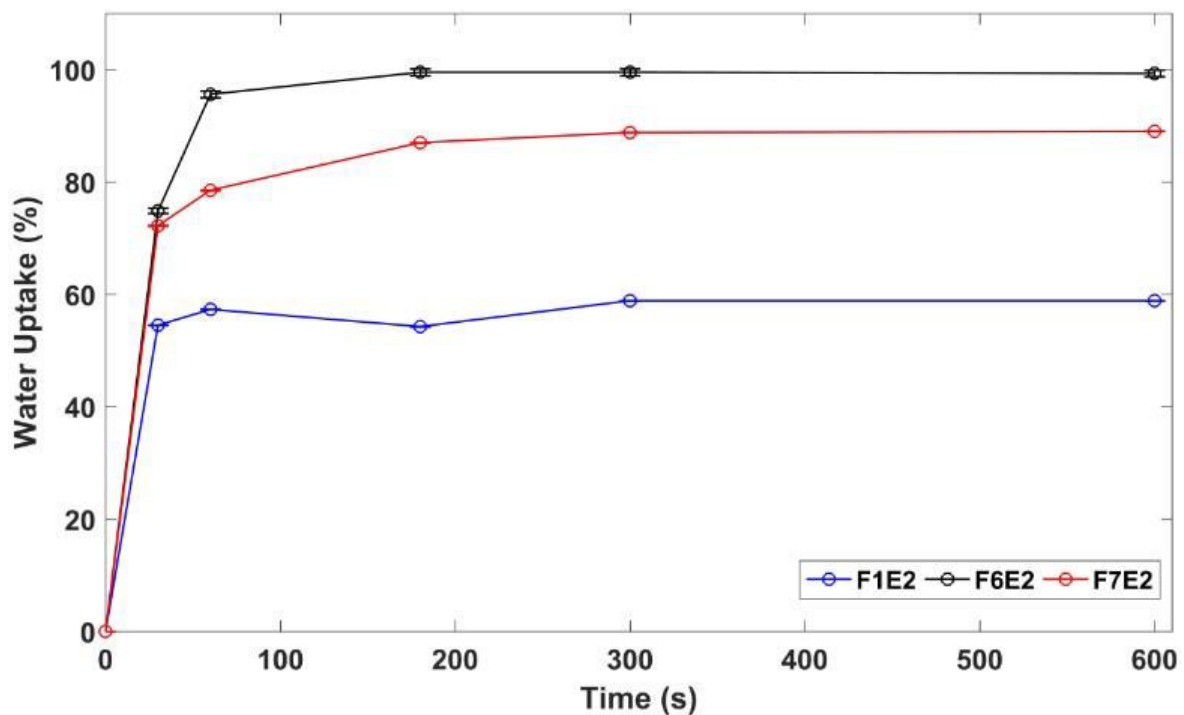


**Fig. 7:** Graphs of swelling tests of the films from second stage, samples F1, F6 and F7.

## 4. Conclusions

In general, the elaborated films were visually attractive, with uniform coloration, without ruptures and with good functional properties for both the first and second stages. However, in the second stage they were more compact with greater resistance and absence of brittle zones. The different concentrations of mesocarp, alginate and glycerol had marked influences on properties such as WVP and solubility. However, for the thickness and moisture, this influence was not accentuated. Comparing the treatments, the polymeric composites after the application of the cross-linker solution were thinner, permeable and hygroscopic, presenting statistically lower values for the second stage. From the thermal

and mechanical characterizations of the selected films (formulations 1, 6 and 7), it was noted that the highest stability was obtained for the formulation 6 film, with 3g of babassu coconut mesocarp, 7.5g of alginate and 4g glycerol. These films showed proximity to the desired properties of food packaging and curative wrapping films, supplementary tests with use of injection and extrusion equipment were carried out to evaluate the production on large scale of this product.

### **Acknowledgments**

The authors would like to thank the Bioresources Product and Process Engineering Laboratory, Materials Laboratory and the Center for Analytical Chemistry of the Federal University of Maranhão for their analysis and the Fundação de Amparo à Pesquisa e ao Desenvolvimento Científico e Tecnológico do Maranhão - FAPEMA for financial support.

### **REFERENCES**

ASTM G160, Standard practice for evaluating microbial susceptibility of nonmetallic materials by laboratory soil burial, ASTM International, West Conshohocken, 1998.

AOAC, Official Methods of Analysis AOAC International, Gaithersburg 2007.

ASTM D882-18, Standard test method for tensile properties of thin plastic sheeting, ASTM International, West Conshohocken, PA, 2012.

ASTM. Standard test methods of water vapor transmission of materials. American society for testing and materials, Philadelphia, E 96-95, 2016.

Arzate-Vázquez, I., Chanona-Pérez, J. J., Calderon-Dominguez, G, Terres-Rojas, E., Garibay-Febles, V., et al. (2012). Microstructural characterization of chitosan and alginate films by microscopy techniques and texture image analysis. *Carbohydrate Polymers*, 87, 289-299.

Barroqueiro, E. S., Barroqueiro, F. S., Pinheiro, M. T., Maciel, M. C., Silva, L. A., Lopes, A. S., et al. (2011). Evaluation of acute toxicity of babassu mesocarp in mice. *Brazilian Journal of Pharmacognosy*, 21 (4), 710-714.

Barroqueiro, E. S., Prado, D. S., Barcellos, S. T., Pereira, W. S., Silva, L. A., Maciel, M. C., et al. (2016). Immunomodulatory and Antimicrobial Activity of Babassu Mesocarp Improves the Survival in Lethal Sepsis. *Evidence-Based Complementary and Alternative Medicine*, 2016, 1-7.

Bierhalz, A. C., da Silva, M. A., & Kieckbusch, T. G. (2012). Natamycin release from alginate/pectin films for food packaging applications. *Journal of Food Engineering*, 110, 18-25.



- Bierhalz, A. C. K., Moraes, Â.M. (2017). Composite membranes of alginate and chitosan reinforced with cotton or linen fibers incorporation epidermal growth factor. *Material Science & Engineering C-Materials for Biological Applications*, 76, p. 287-294.
- Campos, J. L. A., Da Silva, T. L. L., Albuquerque, U. P., Peroni, N., Araújo, E. L. (2015). Knowledge, Use, and Management of the Babassu Palm (*Attalea speciosa* Mart. Ex Spreng) in the Araripe Region (Northeastern Brazil). *Economy Botany*, 69(3), p. 240-250.
- Carrazza, L. R., Ávila, J. C., & Da Silva, M. L. (2012). *Manual tecnológico de aproveitamento integral do fruto e da folha do babaçu*. Brasília: ISPN.
- Chaudhary, D. S., Adhikari, B. P., & Kasapis, S. (2011). Glass-transition behaviour of plasticizers starch biopolymer system - A modified Gordon-Taylor approach. *Food Hydrocolloids*, 114-121.
- Chuang, L., Panyoi, N., Shanks, R., & Kapasis, S. (2015). Effect of sodium chloride on the glass transition of condensed starch systems. *Food Chemistry*, 65-71.
- Cinelli, B. A., López, J. A., Castilho, L. R., Freire, D. M., & Castro, A. M. (2014). Granular starch hydrolysis of babassu agroindustrial residue: a bioprocess within the context of biorefinery. *Fuel*, 41-48.
- Da Silva, D. C., Lopes, I. A., Da Silva, L. J., Barros Filho, A. K., Villa-Véllez, H. A., & Santana, A. A. (2019). Physical properties of films based on pectin and babassu coconut mesocarp. *International Journal of Biological Macromolecules*, 130, 419-428.
- Da Silva, M. C., Ferreira, A. S., Vale, A. A., Santos, A. P., Silva, L. A., Pereira, P. V., et al. (2018). Antileishmanial and Immunomodulatory Effect of Babassu-Loaded PLGA Microparticles: A useful drug target to Leishmania amazonensis Infection. *Evidence-Based Complementary and Alternative Medicine*, 1-14.
- EMBRAPA. (1984). *Babaçu: programa nacional de pesquisa*. Brasília: Embrapa-DDT.
- Fishman, M. L., Coffin, D. R., Onwulata, C. I., & Konstance, R. P. (2004). Extrusion of pectin and glycerol with various combinations of orange albedo and starch. *Carbohydrate Polymers*, 57, 401-413.
- Harper, B. S., Barbut, S., Smith, A., & Marcone, M. F. (2016). Mechanical and microstructural properties of "wet" alginate and composite films containing various carbohydrates. *Food Engineering & Materials Science*, 85-92.
- Hermansson, A. -M., & Svegmarm, K. (1996). Developments in the understanding of starch functionality. *Trends in Food Science and Technology*, 345-353.
- Irissin-Mangata, J., Bauduin, G. B., & Gontard, N. (2001). New plasticizers for wheat gluten films. *European polymer journal*, 1533-1541.

- Landim, A. P., Bernardo, C. O., Martins, I. B., Francisco, M. R., Santos, M. B., & De Melo, N. R. (2016). Sustentabilidade quanto às embalagens de alimentos no Brasil. *Polímeros*, 82-98.
- Lopes, I. A., Santos Jr, J., Da Silva, D. C., Da Silva, L. J., Barros, A. K., Villa-Vélez, H. A., et al. (2017). Characterization of Pectin Biofilms with the Addition of Babassu Mesocarp and Whey Protein Concentrate. *American Journal of Materials Science*, 7 (3), 64-70.
- Mali, S., Grossmann, M. V., & Yamashit, F. (2010). Filmes de amido: produção, propriedades e potencial de utilização. *Semina: ciências agrárias*, 137-156.
- Maniglia, B. C., & Tapia-Blácido, D. R. (2016). Isolation and characterization of starch from babassu mesocarp. *Food Hydrocolloids*, 55, 47-55.
- Maniglia, B. C., Tessaro, L., Lucas, A. A., & Tapia-Blácido, D. R. (2017). Bioactive films based on babassu mesocarp flour and starch . 70, 383-391.
- MEI, L. H. (2016). *Bioplásticos biodegradáveis & biobased: definições, fontes e aplicações*. Campinas: Editora Unicamp.
- Moe, S. T. (1995). Alginates. In: A. M. Stephen, *Food polysaccharides and their applications* (pp. 289-334). New York: Marcel Dekker.
- Ngo, T. M., Dang, T. M., Tran, T. X., & Rachtanapun, P. (2018). Effects of Zinc Oxide Nanoparticles on the Properties of Pectin/Alginate Edible Films. *International Journal of Polymer Science*, 1-9.
- Nunes, M. A., Castro-Aguirre, E., Auras, R. A., Bardi, M. A., & Carvalho, L. H. (2019). Effect of Babassu Mesocarp Incorporation on the Biodegradation of PBAT/TPS Blend. *Macromolecular Symposia*, 1-5.
- Nunes, M. A., Marinho, V. A., Falcão, G. A., Canedo, E. L., Bardi, M. A., & Carvalho, L. H. (2018). Rheological, mechanical and morphological properties of poly(butylene adipate-co-terephthalate)/thermoplastic starch blends and its biocomposite with babassu mesocarp. *Polymer Testing*, 281-288.
- Parreidt, T. S., Muller, K., Schmid, M. (2018). Alginate-Based Edible Films and Coatings for Food Packaging Applications. *Foods*, 7, 170, p. 1-38.
- Paixão, L. C., Lopes, I. A., Barros Filho, A. K. D., Santana, A. A. (2019). Alginate biofilms plasticized with hydrophilic and hydrophobic plasticizers for application in food packaging. *Journal of Applied Polymer Science*, p. 1-11.
- Pielesz, A. M., & Sarna, E. (2011). Antibacterial activity and scanning electron microscopy (SEM) examination of alginate-based films and wound dressings. *Ecological Chemistry and Engineering*, 197-209.

- Santana, A. A., & Kieckbusch, T. G. (2013). Physical Evaluation of Biodegradable Films of Calcium Alginate Plasticized with Polyols. *Brazilian Journal of Chemical Engineering*, 30 (4), 835-845.
- Seixas, F. L., Turbiani, F. R., Salomão, P. G., Souza, R. P., & Gimenes, M. L. (2013). Biofilms Composed of Alginate and Pectin: Effect of Concentration of Crosslinker and Plasticizer Agents. *Chemical Engineering Transactions*, 1693-1698.
- Silva, K. S., Mauro, M. A., Gonçalves, M. P., & Rocha, C. M. (2016). Synergistic interaction of locust bean gum with whey proteins: Effect on physicochemical and microstructural properties of whey protein-based films. *Food Hydrocolloids*, 179-188.
- Silva, M. A., Bierhalz, A. C., & Kieckbusch, T. G. (2009). Alginate and pectin composite films crosslinked with Ca<sup>2+</sup> ions: Effect of the plasticizer concentration. *Carbohydrate Polymers*, 736-742.
- Solak, A. O., Dyankova, S. M. (2014) Composite films from Sodium Alginate and High Methoxul Pectin – Physicochemical Properties and Biodegradation in Soil. *Ecologia Balkanica*, 6, p. 25-34.
- Souza, R. C., & Andrade, C. T. (2000). Investigação dos Processos de Gelatinização e Extrusão de Amido de Milho. *Polímeros: Ciência e Tecnologia*, 24-30.
- Souza, M. H. S. L., Monteiro, C. A., Figueredo, P. M. S., Nascimento, F. R. F., Guerra, R. N. M. (2011). Ethnopharmacological use of babassu (*Orbignya phalerata* Mart) in communities of babassu net breakers in Maranhão, Brazil. *Journal of Ethnopharmacology*, 133, p. 1-5.
- Tan, Z., Yi, Y., Wang, H., Zhou, W., Yang, Y., & Wang, C. (2016). Physical and Degradable Properties of Mulching Films Prepared from Natural Fibers and Biodegradable Polymers. *Applied Sciences*, 1-11.
- Teixeira, P. R., Teixeira, A. S., Farias, E. A., Da Silva, D. A., Nunes, L. C., Leite, C. M., et al. (2018). Chemically modified babassu coconut (*Orbignya* sp.) biopolymer: characterization and development of a thin film for its application in electrochemical sensors. *Journal of Polymer Research*, 25:127.
- Xiao, Q., Gu, X., & Tan, S. (2014). Drying process of sodium alginate films studied by two-dimensional correlation ATR-FTIR spectroscopy. *Food Chemistry*, 179-184

## CONCLUSÃO GERAL

Diante das possibilidades de materiais poliméricos biodegradáveis e a possibilidade do seu uso na substituição dos materiais poliméricos sintéticos nos mais diversos utensílios, o presente trabalho desenvolveu diferentes compósitos com o uso de reforço de mesocarpo do coco babaçu. A aplicação deste subproduto agrícola em diferentes matrizes poliméricas (concentrado proteico de soro do leite, pectina e alginato) mostram a possibilidade de incorporar esta matriz na elaboração de filmes.

A utilização da metodologia de *casting*, uma vez que possui bons resultados em laboratório, podendo ser usado como base para elaboração em larga escala, utilizando processos de extrusão, mostrou-se eficaz na elaboração dos biocompósitos. Percebe-se também que a utilização do glicerol, usado para “plastificar” o material, foi bem sucedida: as análises de infravermelho e de resistência mecânica evidenciam potencial interação do glicerol com os diferentes componentes dos biocompósitos.

A utilização de agentes reticulantes, principalmente com a matriz de alginato, evidenciou a propriedade de se executar o *crosslinking*, onde a utilização de mais de um estágio de *crosslinking* propiciou ao material o melhoramento das principais propriedades funcionais. Os efeitos sinérgicos da utilização do glicerol, agente plastificante, e cloreto de cálcio, agente reticulante, na elaboração do material foram abordados, de forma que as propriedades fossem mais próximas de polímeros sintéticos. Os resultados obtidos foram próximos e promissores, de forma que as principais propriedades físicas funcionais, como solubilidade e umidade foram minimizadas sem se perdesse as propriedades físicas e microestruturais dos compósitos.

A utilização do mesocarpo do coco babaçu sem tratamentos avançados para purificação do amido (presente em grande quantidade no mesocarpo do coco babaçu), mostra a possibilidade do aproveitamento das propriedades bioativas e da porcentagem de fibras presentes no mesocarpo, evidenciando subproduto como uma alternativa para reforço em biopolímeros. A utilização, entretanto, de granulometria controlada é necessária para melhores propriedades.

Diante do exposto, ao se determinar a influência das matrizes naturais e sua mistura com o mesocarpo de coco babaçu, foi possível perceber que estas interagem de maneira direta devido às suas características químicas similares (são ricas em macromoléculas de alta solubilidade em água). Desta forma, as formulações determinam as concentrações de cada componente que garantem as melhores propriedades do material desejado.

Em última análise, tendo em vista os benefícios ambientais e sociais, estes compósitos podem ser alternativas, *a priori* em perspectiva regional, para elaboração de utensílios para embalagens e sacolas, entre outros. Sendo assim, os estudos preliminares deste trabalho podem servir como base para futuros trabalhos e aplicações.

### **SUGESTÕES PARA TRABALHOS FUTUROS**

- Testes e avaliação de injeção e extrusão do material estudado, produção de *pellets* e fios;
- Elaboração de protótipos de sacolas, embalagens e utensílios utilizando as formulações selecionadas;
- Estudo da incorporação de fibras vegetais nos compósitos a fim de se aperfeiçoar as propriedades físicas e químicas;
- Analisar a concentração elementar do cálcio na segunda reticulação aplicada, com a finalidade de avaliar a incorporação deste elemento nos filmes;
- Avaliar os custos de material e estudar as formulações via custo e economia;
- Aplicação do material como embalagem bioativa e *wound dressing*, tendo em vista as propriedades curativas do mesocarpo do coco babaçu;
- Analisar os filmes biopoliméricos quanto ao cultivo de diferentes microorganismos;
- Desenvolver arranjos e estruturas tridimensionais através das tecnologias de impressão 3D com os biopolímeros desenvolvidos.